

PLANT ROOT CONTRIBUTIONS TO THE CARBON BALANCE OF A CHANGING
AGRICULTURAL MIDWEST

BY

CHRISTOPHER KYLE BLACK

DISSERTATION

Submitted in partial fulfillment of the requirements
for the degree of Doctor of Philosophy in Plant Biology
in the Graduate College of the
University of Illinois at Urbana-Champaign, 2016

Urbana, Illinois

Doctoral Committee:

Professor Evan H. DeLucia, Chair
Associate Professor Carl J. Bernacchi
Assistant Professor Sarah C. Davis, Ohio University
Associate Professor Andrew D. B. Leakey

Abstract

The long-term carbon balance of the agricultural Midwestern United States will depend on the interactions between climate, land use decisions, plant biology, and biogeochemistry. In agricultural systems, C storage is fully determined by belowground pools, so it is vital to understand the links between root placement and C status under a variety of potential future conditions and land use types. I considered three such links: the long-term trajectory of soil C in a conventional maize-soybean rotation subjected to climate change, the potentially major increase in root C inputs associated with a change from row crops to high-yielding perennial grasses (*Miscanthus × giganteus* and *Panicum virgatum*), and the taxonomic partitioning of vertical niche space in a restored prairie.

To determine the effect of climate change on soil C in conventional row crop agriculture, I measured root and soil respiration under soybeans and maize grown under elevated temperature (ambient + ~2 °C) and elevated CO₂ (+200 ppm) for three years, then used a process-based ecosystem model (DayCent) to extend these observations and infer long-term changes in soil C. Heating and CO₂ both increased microbial respiration by ~20%, and heating reduced root respiration by ~25%. Particulate organic matter was lower in elevated CO₂ plots, possibly indicating a CO₂ priming effect on the loss of old soil carbon. DayCent results agreed with heated-plot observations but did not resolve the speculated CO₂ priming effect, because the model has no mechanism to simulate priming. Over the next several decades, I predict a substantial loss of C from agricultural soils.

To clarify differences in root architecture between several potential biofuel crops, I collected minirhizotron images from 0-100 cm depth over five growing seasons from a maize-maize-soybean row crop rotation and from three perennial grasses. I developed a Bayesian

statistical model that accounts for near-surface underdetection effects and correctly handles the frequent zero counts typical of minirhizotron data. The model performed well against direct measurements from deep cores and allowed improved inferences about the amount of root allocated to each soil layer and how it changes through time. Mature perennial crops showed little change in relative allocation through time, but total root volume of perennial grasses increased dramatically from 2010 to 2014 and showed little change during a historic drought in 2012, implying that these large, deep root systems confer drought tolerance. By growing exceptionally large, fine, highly-dispersed root systems that sent substantial amounts of C into very deep soil, land use conversion from row crops to perennial grass biofuels is likely to create a large and persistent C sink.

To learn how species arrange themselves in space within complex communities and infer their roles in C cycling, I used a DNA metabarcoding approach to identify the *ITS2* sequences of taxa present in mixed root samples from varying depths (0-10, 10-30, 30-50, 50-75, 75-100 cm) in a restored prairie and looked for evidence of taxonomic partitioning. Spatial patterning was strongest between functional groups, with the prevalence of grasses increasing and of forbs decreasing with depth. Pairs of taxa with one from Asteraceae and one from Poaceae tended to co-occur with each other less often than expected by chance (spatial segregation), while most other pairs of taxa were found to co-occur randomly or positively, indicating that there is little spatial partitioning at this site other than the depth of grass roots. This may indicate that grass roots are disproportionately important for deep-soil functions that affect the resilience of the whole ecosystem, such as water uptake, N leaching prevention, and C storage.

Overall, this research highlights that business as usual will probably not be a tenable response to climate change and that a shift from row cropping toward perennial grass biofuel

systems, either in the form of high-yield monocultures or as low-input high-diversity systems, is likely to promote C storage. However, the time horizons required for significant accumulation are long (decades to generations) and policies intended to promote C storage will only be effective if they provide incentives structured for long-term stability.

Acknowledgements

If I spoke to you between 2009 and 2016, you helped me finish this project; either by letting me talk carbon at you or by forcing me to take a break from talking about carbon. Thank you all!

I am *especially* grateful for consistent, dedicated help from:

My advisor, Evan DeLucia, and my committee: Sarah Davis, Carl Bernacchi, Andrew Leakey, and Mark David, for advice, encouragement, and telling me when I was wrong.

Coauthors Tara Hudiburg, Michael Masters, David LeBauer, Krista Anderson-Teixeira, Scott Woolbright, Taylor Pederson, and Christopher Sligar, for their contributions at every stage from experimental design through tedious lab/fieldwork to copyediting.

The IGB and Plant Biology staff, especially Melinda LaBorg, Rayme Dorsey, Lisa Boise, Connie Wilder, and Jana Lenz. If there is a single deadline I didn't miss on my way to the degree, it is to their credit rather than mine.

The Plant Biology Association of Graduate Students and the DeLucia lab, for fellowship, celebration, commiseration, and for watering my desk plants while I was gone for months.

Programming and statistics mentors Michael Dietze, Jenny Bryan, Charlie Loyd, Nick Blanchard-Wright, Sam Kimbrel, Baptiste Auguié, and an exceptionally helpful user of the Freenode #r channel who I know only as "MrFlick." If this crew could teach me Git and vector math, they can teach anyone anything.

My wife, Laurel Brehm, for leading the way. It's official now: You will *always* have more degrees than me.

Table of Contents

CHAPTER 1: Introduction.....	1
CHAPTER 2: Elevated CO ₂ and temperature increase soil C losses from a soybean-maize ecosystem.....	11
CHAPTER 3: Root volume distribution of maturing perennial grasses revealed by correcting for minirhizotron surface effects.....	58
CHAPTER 4: Molecular analysis shows taxonomic partitioning of root placement by depth in a prairie plant community.....	98
CHAPTER 5: Conclusion.....	130

Chapter 1

Introduction

Earth's climate is changing because of increases in atmospheric CO₂ caused by human fossil fuel use. In the Midwestern United States, temperatures are forecast to increase 2-4 °C from 20th-century averages and [CO₂] to exceed 500 ppm by the mid-21st century (Romero-Lankao et al. 2014, Melillo et al. 2016). These changes will have profound effects on the ecology and biogeochemistry of all ecosystems, and therefore on the policies and land use decisions needed to manage them effectively. Land use decisions in turn change ecosystem C storage and will therefore feed back to global climate; these feedbacks may be stabilizing if a new land use stores more C or destabilizing if it releases C (Anderson-Teixeira and DeLucia 2011). Therefore when considering possible land-use scenarios, quantifying their C storage potential is fundamental to predicting climate responses and is an essential step toward choosing policies that promote positive climate outcomes.

The dominant ecosystems of the Midwest are agricultural, and are currently managed almost exclusively for the production of maize and soybean, generally grown in rotation. In 2016 a total of 71.3 million Ha were planted to maize and soybean (NASS 2016), making it the largest ecosystem type in the continental US by area. Since their aboveground biomass is removed or tilled in each year, C storage in these ecosystems consists exclusively of the belowground C pool. A large proportion of new C inputs come from root and root-exudate C and the overall annual ecosystem C balance depends greatly on tillage decisions (Allmaras et al. 2004, Bernacchi et al. 2005). Therefore, understanding the C storage potential of agroecosystems is primarily a question of understanding root and soil C cycling.

The largest current use for US-produced maize (~40% of total production; NASS 2016) is as a feedstock for the production of ethanol. It has been suggested that changing some of this acreage to produce cellulosic fuel crops could potentially have climate and economic benefits. In general, cellulosic crops that take a “land sparing” approach (Anderson-Teixeira et al. 2012) by maximizing ethanol production on a small number of acres appear most likely to be successful in current economic conditions (Heaton et al. 2008, Davis et al. 2012, Hudiburg et al. 2016), while lower-productivity but lower-input systems such as prairie restorations may still have considerable benefits if other ecosystem services, such as biodiversity and resilience to unpredictable climates, are considered (Fornara and Tilman 2009, Gelfand et al. 2013). However, considerable uncertainty remains about the accumulation rate and turnover time of soil C in both high- and low-input biofuel crops (Anderson-Teixeira et al. 2013, Agostini et al. 2015, Bach and Hofmockel 2016).

The central aim of my dissertation research was to quantify how the mass, placement, and chemical & taxonomic makeup of roots will affect the trajectory of belowground C storage in the warmer, higher CO₂ Midwest of the coming decades. Within this overarching framework, I focused on three land-use scenarios that can be characterized as conventional tillage, high-yield perennial grasses, and low-input restored prairie. Because these scenarios differ greatly in their depth of previous study, the outstanding questions about belowground C cycling differ in each system. This means that in each system I collected very different measurements, not all of which can immediately be converted into units of carbon. But in each case I have attempted to assess what my results mean for the long-term C status of the system.

Scenario 1: Maize-soybean rotation

I began with a business-as-usual scenario, where the Midwestern United States continues to be mostly managed as a conventional maize-soybean rotation and farmers do their best to maintain maximum yields in an increasingly warm and high-CO₂ environment. In this scenario the responses of crop roots are relatively well-studied: Elevated CO₂ increases soybean plant size, including the root system (Ainsworth and Long 2005, Ruiz-Vera et al. 2013, Gray et al. 2016), and appears to have little effect on maize plant size (Leakey et al. 2006, Ruiz-Vera et al. 2015). It is important to note that from an agronomic perspective, these increases in biomass appear unlikely to translate into reliable yield increases (Ruiz-Vera et al. 2013, 2015, Gray et al. 2016), but from a carbon cycling perspective it is likely that maize-soybean ecosystems will have higher C inputs to the soil in the future. Therefore in this chapter I focused on the question of outputs: How do elevated temperature and CO₂ affect the rate of C loss from the soil? By measuring soil CO₂ flux for three years, partitioning it into root-derived and microbe-derived components, and comparing the results against the predictions of a 100-year in silico experiment using an ecosystem biogeochemistry model (Parton et al. 1998), I found that elevated temperature increases the microbial breakdown of soil organic matter and that increases in biomass input from elevated CO₂ appear to prime additional increases in respiration, suggesting that the long-term result of the business as usual scenario will be substantial losses of soil C.

Scenario 2: High-yield biofuels

Next, I asked whether some of the predicted soil C losses can be avoided by changing management strategies. High-yielding perennial grasses have large root systems and reduced disturbance cycles and have been proposed as a promising biofuel feedstock that may also

increase soil C storage (Agostini et al. 2015). However, the stability of this C may depend greatly on the timing of its arrival and its physical placement in the soil profile (De Deyn et al. 2008). To explore root C inputs in more depth, improved nondestructive methods of root monitoring are needed (Rewald et al. 2012, Topp et al. 2016). I developed and calibrated a Bayesian statistical model written in Stan (Stan Development Team 2016) to estimate the root volume of a full soil profile from minirhizotron images, and combined it with results from direct sampling to show that perennial monocultures of switchgrass and *Miscanthus* can have root systems comparable in size to native prairies, and importantly that they store much of this mass in the deepest soil layers where it may be highly resistant to decomposition. This suggests that these root carbon inputs can be maintained as soil carbon for longer than if they were sent to shallower soil.

Scenario 3: Low-input high-diversity biofuels

Finally, I turned to a multispecies grassland more like the native vegetation of our region of the Midwest. As an ethanol crop, restored prairies produce far less biomass per acre than high-yielding monocultures, and therefore they would require substantially more land diverted from food production (Heaton et al. 2008), making their widespread adoption seem unlikely at present. However, as the biome that literally created the fertility of the Corn Belt, the ability of prairies to store soil C over the long term is indisputable (David et al. 2009), and their adoption could accelerate if climate policy shifts to increase attention to other management goals such as yield stability in extreme conditions, supporting trophic diversity, and preserving locally adapted species (Fargione et al. 2009). Compared to the monocultures of the other two scenarios, my challenge in quantifying root inputs to this complex community mixture was very basic: “Here

are some roots, but which species grew them?" I used DNA metabarcoding to disentangle the species in the root mixture and asked whether there is any spatial structure to the root stand: How do the species partition the niche space, and how does that affect the potential for C storage? I found that grasses increased in prevalence deeper in the soil profile, implying that deep-soil C inputs are likely also enriched in grass roots. Since grasses tend to have lower turnover than forb roots, and since deep soil layers have the highest chance of long-term C storage, this combination suggests that deep-soil C storage under prairies could be greater and more stable than suggested by shallow sampling.

Scaling up: Exploiting computation to match small samples to big questions

In addition to their link of arising from an interest in soil C, these projects also share a common methodological theme: In each case the scale of the inference I wanted to make was poorly matched to the scale of the available measurement methods. Quantifying soil C contents or root mass is easy for any given sample, but obtaining each sample is laborious and usually destructive, and belowground systems are characterized by extreme heterogeneity on all scales. This means that questions about changes in belowground C across time or space are inherently difficult, often to the point of impracticality, to answer by direct measurement alone. Therefore each of the following chapters includes a substantial computational component. My approach was to collect what direct measurements were available, then use models to synthesize the available information to match the scale of the question.

The model is different for each question: In chapter 2, I scaled root and microbial respiration from instantaneous flux rates to century-scale changes in pool size by using a well-tested and mechanistically validated simulation of ecosystem biogeochemical processes. In

chapter 3, I used a novel Bayesian statistical model to correct biases in image-based estimates of root distribution, therefore bringing an indirect measurement method into closer agreement with more laborious direct observations. Finally, in chapter 4, I applied bioinformatic tools from the rapidly emerging field of environmental metagenomics to filter noisy, mixed-sample DNA sequences into estimates of root identity and to attribute spatially partitioned niches to their taxonomic groups.

All of these computational analyses used different sets of programming tools, but a critical common theme is that the assumptions I made while programming them are *at least* as important for the quality of my inferences as are the methods I used for my direct measurements. However, unlike collecting soil cores, it is easy to redo computations! To that end, all of the code and data for these chapters are freely available online at my public code repository at <https://github.com/infotroph/> and also at locations listed in each chapter. I encourage anyone to reproduce my analyses, test my assumptions for themselves, or alter the code for their own purposes. If you find errors, please tell me.

References

- Agostini, F., A. S. Gregory, and G. M. Richter. 2015. Carbon sequestration by perennial energy crops: is the jury still out? *BioEnergy Research* 8:1057–1080.
- Ainsworth, E. A., and S. P. Long. 2005. What have we learned from 15 years of free-air CO₂ enrichment (FACE)? A meta-analytic review of the responses of photosynthesis, canopy properties and plant production to rising CO₂. *New Phytologist* 165:351–372.

- Allmaras, R. R., D. R. Linden, and C. E. Clapp. 2004. Corn-residue transformations into root and soil carbon as related to nitrogen, tillage, and stover management. *Soil Science Society of America Journal* 68:1366–1375.
- Anderson-Teixeira, K. J., and E. H. DeLucia. 2011. The greenhouse gas value of ecosystems. *Global Change Biology* 17:425–438.
- Anderson-Teixeira, K. J., B. D. Duval, S. P. Long, and E. H. DeLucia. 2012. Biofuels on the landscape: Is “land sharing” preferable to “land sparing”? *Ecological Applications* 22:2035–2048.
- Anderson-Teixeira, K. J., M. D. Masters, C. K. Black, M. Zeri, M. Z. Hussain, C. J. Bernacchi, and E. H. DeLucia. 2013. Altered belowground carbon cycling following land-use change to perennial bioenergy crops. *Ecosystems* 16:508–520.
- Bach, E. M., and K. S. Hofmockel. 2016. A time for every season: soil aggregate turnover stimulates decomposition and reduces carbon loss in grasslands managed for bioenergy. *Global Change Biology Bioenergy* 8:588–599.
- Bernacchi, C. J., S. E. Hollinger, and T. Meyers. 2005. The conversion of the corn/soybean ecosystem to no-till agriculture may result in a carbon sink. *Global Change Biology* 11:1867–1872.
- David, M. B., G. F. McIsaac, R. G. Darmody, and R. A. Omonode. 2009. Long-term changes in mollisol organic carbon and nitrogen. *Journal of Environmental Quality* 38:200–211.
- Davis, S. C., W. J. Parton, S. J. Del Grosso, C. Keough, E. Marx, P. R. Adler, and E. H. DeLucia. 2012. Impact of second-generation biofuel agriculture on greenhouse-gas emissions in the corn-growing regions of the US. *Frontiers in Ecology and the Environment* 10:69–74.

- De Deyn, G. B., J. H. C. Cornelissen, and R. D. Bardgett. 2008. Plant functional traits and soil carbon sequestration in contrasting biomes. *Ecology Letters* 11:516–531.
- Fargione, J. E., T. R. Cooper, D. J. Flaspohler, J. Hill, C. Lehman, T. McCoy, S. McLeod, E. J. Nelson, K. S. Oberhauser, and D. Tilman. 2009. Bioenergy and wildlife: Threats and opportunities for grassland conservation. *BioScience* 59:767–777.
- Fornara, D. A., and D. Tilman. 2009. Ecological mechanisms associated with the positive diversity-productivity relationship in an N-limited grassland. *Ecology* 90:408–418.
- Gelfand, I., R. Sahajpal, X. Zhang, R. C. Izaurralde, K. L. Gross, and G. P. Robertson. 2013. Sustainable bioenergy production from marginal lands in the US Midwest. *Nature* 493:514–517.
- Gray, S. B., O. Dermody, S. P. Klein, A. M. Locke, J. M. McGrath, R. E. Paul, D. M. Rosenthal, U. M. Ruiz-Vera, M. H. Siebers, R. Strellner, E. A. Ainsworth, C. J. Bernacchi, S. P. Long, D. R. Ort, and A. D. B. Leakey. 2016. Intensifying drought eliminates the expected benefits of elevated carbon dioxide for soybean. *Nature Plants* 2:16132.
- Heaton, E. A., F. G. Dohleman, and S. P. Long. 2008. Meeting US biofuel goals with less land: the potential of Miscanthus. *Global Change Biology* 14:2000–2014.
- Hudiburg, T. W., W. Wang, M. Khanna, S. P. Long, P. Dwivedi, W. J. Parton, M. Hartman, and E. H. DeLucia. 2016. Impacts of a 32-billion-gallon bioenergy landscape on land and fossil fuel use in the US. *Nature Energy* 1:15005.
- Leakey, A. D. B., M. Uribelarrea, E. A. Ainsworth, S. L. Naidu, A. Rogers, D. R. Ort, and S. P. Long. 2006. Photosynthesis, productivity, and yield of maize are not affected by open-air elevation of CO₂ concentration in the absence of drought. *Plant Physiology* 140:779–790.

- Melillo, J. M., T. Richmond, and G. W. Yohe, editors. 2016. Climate change impacts in the United States: The third National Climate Assessment. Page 814. U.S. Global Change Research Program; U.S. Government Printing Office.
- NASS. 2016. Census of Agriculture Quick Stats 2.0. http://www.nass.usda.gov/Quick_Stats/.
- Parton, W. J., M. D. Hartman, D. S. Ojima, and D. S. Schimel. 1998. DAYCENT and its land surface submodel: description and testing. *Global and Planetary Change* 19:35–48.
- Rewald, B., C. Meinen, M. Trockenbrodt, J. E. Ephrath, and S. Rachmilevitch. 2012. Root taxa identification in plant mixtures – current techniques and future challenges. *Plant and Soil* 359:165–182.
- Romero-Lankao, P., J. B. Smith, D. J. Davidson, N. S. Diffenbaugh, P. L. Kinney, P. Kirshen, P. Kovacs, and L. Villers-Ruiz. 2014. North America. Pages 1439–1498 in V. R. Barros, C. B. Field, D. J. Dokken, M. D. Mastrandrea, K. J. Mach, T. E. Bilir, M. Chatterjee, K. L. Ebi, Y. O. Estrada, R. C. Genova, B. Girma, E. S. Kissel, A. N. Levy, S. MacCracken, P. R. Mastrandrea, and L. L. White, editors. *Climate change 2014: Impacts, adaptation, and vulnerability. Part B: Regional aspects. Contribution of working group II to the fifth assessment report of the Intergovernmental Panel on Climate Change*. Cambridge University Press, Cambridge, United Kingdom; New York, NY, USA.
- Ruiz-Vera, U. M., M. H. Siebers, D. W. Drag, D. R. Ort, and C. J. Bernacchi. 2015. Canopy warming caused photosynthetic acclimation and reduced seed yield in maize grown at ambient and elevated [CO₂]. *Global Change Biology* 21:4237–4249.
- Ruiz-Vera, U. M., M. Siebers, S. B. Gray, D. W. Drag, D. M. Rosenthal, B. A. Kimball, D. R. Ort, and C. J. Bernacchi. 2013. Global warming can negate the expected CO₂ stimulation

in photosynthesis and productivity for soybean grown in the Midwest United States. *Plant Physiology* 162:410–423.

Stan Development Team. 2016. Stan Modeling Language Users Guide and Reference Manual, version 2.12.0. <http://mc-stan.org>.

Topp, C. N., A. L. Bray, N. A. Ellis, and Z. Liu. 2016. How can we harness quantitative genetic variation in crop root systems for agricultural improvement? *Journal of Integrative Plant Biology* 58:213–225.

Chapter 2

Elevated CO₂ and temperature increase soil C losses from a soybean-maize ecosystem¹

Abstract

Warming temperatures and increasing CO₂ are likely to have large effects on the amount of carbon stored in soil, but predictions of these effects are poorly constrained. We elevated temperature (canopy: +2.8 °C; soil growing season: +1.8 °C; soil fallow: +2.3 °C) for three years within the 9th-11th years of an elevated CO₂ (+200 ppm) experiment on a maize-soybean agroecosystem, measured respiration by roots and soil microbes, then used a process-based ecosystem model (DayCent) to simulate the decadal effects of warming and CO₂ enrichment on soil C. Both heating and elevated CO₂ increased respiration from soil microbes by ~20%, but heating reduced respiration from roots and rhizosphere by ~25%. The effects were additive, with no heat x CO₂ interactions. Particulate organic matter and total soil C declined over time in all treatments and were lower in elevated CO₂ plots than in ambient plots, but did not differ between heat treatments. We speculate that these declines indicate a priming effect, with increased C inputs under elevated CO₂ fueling a loss of old soil carbon. Model simulations of heated plots agreed with our observations and predicted loss of ~15% of soil organic C after 100 years of heating, but simulations of elevated CO₂ failed to predict the observed C losses and instead predicted a ~4% gain in soil organic C under any heating conditions. Despite model uncertainty,

¹ Reprinted with permission from: Black, C. K., Davis, S. C., Hudiburg, T. W., Bernacchi, C. J. and DeLucia, E. H. 2016. Elevated CO₂ and temperature increase soil C losses from a soybean–maize ecosystem. *Global Change Biology*. doi: 10.1111/gcb.13378

our empirical results suggest that combined, elevated CO₂ and temperature will lead to long term declines in the amount of carbon stored in agricultural soils.

Introduction

Human activity, primarily fossil fuel burning, is increasing atmospheric [CO₂] and raising global mean temperature (Hartmann et al. 2013). These changes are likely to have direct and indirect effects on storage of soil organic carbon (SOC), but estimates of the direction and magnitude of these effects are poorly constrained (Dieleman et al. 2012, Lu et al. 2013). Soils worldwide store over two orders of magnitude more C than annual anthropogenic emissions (\approx 1500 Pg C in the top 1 m; Eswaran et al. 1993), so even small changes in soil C storage in response to climate change could produce large feedbacks to the global C cycle. This may be especially true of the SOC-rich former prairie soils of the agriculturally managed Midwestern United States, where annual tillage, infrequent water limitation, regular fertilization, and frequent pulses of highly labile C from crop residues provide ideal conditions for temperature-controlled microbial activity (Tisdall and Oades 1980).

Changes in soil C are difficult to detect on short timescales because some pools turn over slowly, with mean residence times of hundreds of years. Although it is conceptually useful to identify the faster-cycling subpools of soil C, we lack experimental methods to measure them directly (Schmidt et al. 2011). Instead, changes in the rate of CO₂ fluxes from soil can be used as a proxy for changes in the soil C cycle by partitioning total CO₂ flux (R_{tot}) into components attributed to “autotrophic” respiration (R_{aut}) from plant roots and rhizosphere organisms, or to “heterotrophic” respiration (R_{het}) from soil microbes in the process of breaking down soil organic matter (SOM). Because R_{het} is the primary avenue for loss of soil C, any change in R_{het} indicates

a change in the rate of soil C loss. R_{het} is strongly controlled by soil temperature and moisture and therefore expected to shift under future climate conditions (Davidson and Janssens 2006, Subke and Bahn 2010, Conant et al. 2011, Bradford 2013). In contrast, changes in R_{aut} are indirectly linked to the rate of C *input* from roots, so a unit change in R_{tot} could indicate either increasing or decreasing soil C. Therefore correct partitioning of fluxes is essential to their use as a proxy for changes in pool size (Kuzyakov and Larionova 2005).

Previous soil heating experiments have generally shown short-term increases in R_{tot} (Rustad et al. 2001, Wu et al. 2011), except when heating exacerbated soil water limitations (Schindlbacher et al. 2012, Wall et al. 2013, Suseela and Dukes 2013, Pendall et al. 2013, Wang et al. 2014). This heating effect often diminishes after a few years of treatment. Whether these responses will persist over the long term under climate change depends on whether a particular soil's R_{het} response is modulated by availability of nutrients or C substrates (Luo et al. 2001, Chevallier et al. 2015) or by physiological adaptation of the microbial community (Allison et al. 2010, Bradford 2013). In addition, few of these studies were able to separate soil respiration into its autotrophic and heterotrophic components. Since R_{het} is strongly controlled by thermal kinetics while R_{aut} responds to a wide variety of non-thermal factors, it has been widely assumed that temperature-associated increases in R_{tot} are driven by increasing R_{het} , but support for this assumption is equivocal (Hartley et al. 2007, Bond-Lamberty and Thomson 2010, Suseela and Dukes 2013, Wang et al. 2014).

Previous CO₂ enrichment experiments have generally shown sustained increases in R_{tot} (King et al. 2004, Bernhardt et al. 2006, Pregitzer et al. 2006, Peralta and Wander 2008, Carrillo et al. 2011, Drake et al. 2011, Adair et al. 2011, Keidel et al. 2015), but there are few reported results from field experiments that manipulate both heat and CO₂ simultaneously. Of those that

are reported (Carrillo et al. 2011, Pendall et al. 2011, 2013, Selsted et al. 2012), the observed responses seem to be mostly mediated by water availability, with heat increasing R_{tot} when moisture is available and reducing it when heating produces drier soil. Elevated CO₂ mediates these effects by ameliorating soil water stress through increased plant water use efficiency, but the strength and predictability of this effect seems to vary widely both within and between experiments.

The objective of this study was to measure the root- and SOM-derived components of soil respiration in an intact maize-soybean ecosystem subjected to mid-21st century temperature (+3.5 °C) and CO₂ (585 ppm) conditions under fully open-air conditions at SoyFACE (Urbana IL, USA). We then used a process-based biogeochemical model (DayCent; Parton et al. 1998) to predict the long-term effects of these respiratory responses on soil C storage. We predicted that elevated temperature would increase the activity of soil heterotrophs, leading to increased respiration in root-free soil and long-term losses of C from the most labile pools of SOM. We further predicted that elevated CO₂ would increase plant biomass above and belowground, leading to higher C inputs that would at least partially ameliorate the long-term effect of heat on soil C, and therefore that the long-term fate of soil C at our site would depend on the strength of the interaction between heat and CO₂ effects.

Materials and methods

Site description

Measurements were made at the *Soybean Free-Air Concentration Enrichment* (SoyFACE) experiment (40.04N, 88.23W; elev. 215 m; soyface.igb.illinois.edu), a 32-Ha experimental site near Urbana IL, USA. The site is flat, tile-drained, and has been cultivated for over 100 years.

Soils are deep and highly productive, mapped as Flanagan silt loam (fine, smectitic, mesic Aquic Argiudoll) and Drummer silty clay loam (fine-silty, mixed, superactive, mesic Typic Endoaquoll). The mean annual temperature is 11 °C, with monthly mean temperatures ranging from -3 °C in January to 24 °C in July, and annual precipitation is ~1 m, with approximately half falling during the May-September growing season (Angel 2010a).

The site was managed in a two-year rotation, with maize (*Zea mays* cv 34B43) and soybean (*Glycine max* cv 93B15) alternating between the eastern and western halves of the site. Maize was fertilized with 202 kg N Ha⁻¹ yr⁻¹ and soybean was not fertilized. The soil was typically chisel plowed each spring before planting, and in the fall after maize harvest but not after soybean. Measurements were taken from 2009-2011 in the west half of the site, where the crop rotation cycle for these years was soybean-maize-soybean. Management of these crops was consistent with previously reported practices at the site (Leakey et al. 2004, Morgan et al. 2005), with the exception that no fall tillage was done after the 2010 maize crop so that the heating equipment could be kept in operation overwinter.

Elevated CO₂ and temperature treatments

The field was divided into four experimental blocks, each containing two 20-m octagonal rings spaced 100 m apart to avoid cross-contamination by fumigation gases. One ring in each block was maintained at ambient atmospheric conditions (approximately 390 ppm CO₂), while the other was fumigated to a target of 585 ppm CO₂ using *Free Air Concentration Enrichment* (FACE) technology (Miglietta et al. 2001). Elevated CO₂ was maintained from dawn until dusk throughout the growing season. The high-CO₂ rings in the study area have been fumigated every growing season since 2001.

Starting in 2009, each ring was further split by imposing an elevated temperature treatment. One 3-m hexagonal subplot of each ring was equipped with overhead infrared heaters as in Kimball (2005). The heaters were adjusted throughout the growing season to stay 1.4 m above the canopy and were controlled by infrared radiometers to maintain a difference of 3.5 °C between the canopy-top temperature of heated and unheated plots. When rain was falling and when soil temperature was \leq 5 °C, heating was ineffective and heater output was therefore reduced to a minimum. The heating system operated continuously between June 2009 and September 2011 except during planting when all equipment was removed to allow field tillage, during harvest when power cables were removed to allow harvester traffic, and during a two-week period in January 2010 when the equipment was rebuilt to repair damage from rodents. Further details on the heating treatment are reported in (Ruiz-Vera et al. 2013, 2015, Rosenthal et al. 2014).

Measurement of soil properties and CO₂ efflux

CO₂ efflux from soil was measured at three locations in each plot using 20-cm diameter collars made from PVC pipe. At each location, one collar was inserted 3 cm into the soil to capture total soil respiration (R_{tot}), and a second collar was inserted 25 cm to capture respiration by soil heterotrophs (R_{het}) by excluding roots and rhizosphere: The top 30 cm of soil contain at least 70% of soybean and 60% of maize root mass (Mayaki et al. 1976, Anderson-Teixeira et al. 2013), so this root-exclusion collar acts as a small trenched plot (Vogel and Valentine 2005). Collars were installed at crop emergence time each spring and left in place all year, then removed for field tillage just before the next year's planting. This annual reinstallation also eliminated several major limitations that apply to root-exclusion methods in untilled systems: it removed any accumulated difference in C or nutrient availability from previous years of root

exclusion, and there was no need to correct for decomposition of roots severed during installation (Hanson et al. 2000) because root biomass at installation was near zero. Respiration by roots and rhizosphere (R_{aut}) was calculated for each location as the difference between R_{tot} and R_{het} .

CO_2 efflux rates were measured using an infrared gas analyzer (LI-8100; Li-Cor, Lincoln NE USA) fitted with a 20-cm static chamber (Li-Cor 8100-103) that rested on top of the soil collar. For each observation, the chamber was closed for two minutes while $[\text{CO}_2]$ was logged every second. Linear regressions on static-chamber observations underestimate the initial flux rate (Healy et al. 1996), so flux rates were computed in software by the LI-8100, which fit a saturating exponential curve of the form:

$$C_t = C_\infty + (C_0 - C_\infty)e^{-a(t-t_0)};$$

where C_0 is $[\text{CO}_2]$ at the moment the chamber closed, t is time, and a and C_∞ are fitted parameters representing curvature and $[\text{CO}_2]$ at the asymptote, respectively. Evaluating the derivative of C_t at $t = 0$ then gives the instantaneous initial slope $a(C_\infty - C_0)$, which was scaled by the volume of the soil chamber to give CO_2 flux rate at the moment the chamber closed.

Using exponential rather than linear fits is especially important in a FACE setting, because it allows a further correction for initial chamber conditions: Respiration was measured while fumigation was active. Pure CO_2 is released from the upwind side of the ring and mixes to the target concentration as it is blown across the plot (Miglietta et al. 2001), meaning that in elevated- CO_2 plots the flux chamber would sometimes close on a transient high- $[\text{CO}_2]$ air mass (up to 2000 ppm). In these cases the CO_2 concentration gradient from soil to chamber air, and thus the rate of diffusion across the soil surface, was small. This meant that for these readings the fitted flux rate ‘at the moment the chamber closed’ was much smaller than the true equilibrium

rate. We corrected this bias using a method recommended by Li-Cor Inc. that re-evaluates the previously fit $[CO_2]$ curve to find the equilibrium flux $a(C_\infty - C_{target})$, where a and C_∞ are taken from the previous curve fit and C_{target} is the daily average $[CO_2]$ in that ring (585 PPM for fumigated rings, 370-400 PPM for unfumigated rings).

Soil temperatures were measured simultaneously with each respiration measurement using a thermocouple probe inserted to 5 cm depth. Soil volumetric water content was measured from 5 to 105 cm depth 2-3 times each week using a capacitance probe and is reported elsewhere (Rosenthal et al. 2014, Ruiz-Vera et al. 2015).

Particulate organic matter (POM), which consists of fragmented but undecomposed plant matter and is used as a proxy for the abundance of labile soil C, was measured using a procedure modified from Marriott & Wander (2006). Briefly, air-dried soil was sieved to 2 mm and a 10-g sample was weighed into a 30-mL plastic bottle. The mouth of the bottle was covered with a 53- μm nylon mesh to retain POM and sand while allowing silt and clay particles to escape. The bottle was submerged in 5% sodium hexametaphosphate (HMP) and shaken for one hour, then the HMP and suspended fines $<53\ \mu m$ were removed, replaced with deionized water, and shaking was repeated until no further fine material was extracted. The remaining POM + sand was transferred to a pouch of 53- μm mesh, rinsed with DI water, dried at 30 °C, and weighed. Samples were then ground in a ball mill (Geno Grinder 2010; BT&C, Lebanon New Jersey, USA) and combusted to determine C content using an elemental analyzer (Costech ECS4010; Costech Analytical Technologies, Valencia, California, USA).

Statistical analysis

Analysis of variance for soil respiration was performed in a complete-block design using CO_2 as a whole-plot fixed effect and heat as a split-plot fixed effect nested within CO_2 . Blocks

were treated as random, and autocorrelation within plots from repeated measurement through the season was estimated as a first-order autoregressive function. R_{tot} , R_{het} , and R_{aut} fluxes for each season were analyzed separately as mixed-effects linear models with repeated measures using the nlme and lsmeans packages in R 3.2.4 (Lenth 2016, Pinheiro et al. 2016, R Core Team 2016). The date of each survey event was included as a categorical variable to account for within-season changes. Although most of the temporal variation is likely to be driven by weather and crop growth phase, the Day effect was treated as a catchall term and no explicit temperature or moisture covariates were included in the model. Because repeated measurements within the same plot are pseudo-replicates, the three flux measurements from each plot were averaged, giving n=4 observations per treatment in each day. Because experiments with few replicates have low power to detect small differences, we set a significance threshold of $p \leq 0.1$ to minimize the chance of false negative conclusions (Filion et al. 2000). Full statistical output and data-processing scripts are available in the data package for this manuscript (Black et al. 2016).

Modeling of soil respiration and soil organic carbon

Because a three-year heating experiment is likely too short to detect changes in SOC, we performed an *in silico* experiment using a process-based ecosystem model (DayCent; Parton et al. 1998) to simulate the effects of a 100-year global change manipulation and better understand the long-term effects of elevated CO₂ and temperature on soil carbon dynamics. DayCent has been widely used to model soil C, N, P and S dynamics and trace gas fluxes. It has been particularly well-validated for crop and grassland systems, and is straightforward to modify for predicted future conditions, making it ideal for simulations of the future ecosystem effects of climate and/or land-use changes (Davis et al. 2010, 2012, Hartman et al. 2011). DayCent model development has been closely tied to previous global change experiments and its input

parameters are designed for easy calibration against experimentally measured responses (Parton et al. 2007, Frey et al. 2013).

To predict the medium- and long-term effects of ongoing ecosystem warming and elevated CO₂ on soil carbon cycling, we performed a three-part set of DayCent simulations to simulate the historic development of the SoyFACE site from native prairie into a maize-soy rotation, extended this simulation through the 21st century, then ran the model four times using all factorial combinations of elevated CO₂ and heat.

To calibrate the size and turnover rates of soil C pools, the model was first run to equilibrium by simulating a native tallgrass prairie at pre-industrial [CO₂] of 294 PPM. Each simulation lasted 3867 years and looped over a weather file made by randomly ordering the years of an 1889-2009 temperature and precipitation record for Urbana, Illinois (Angel 2010b). Vegetation for the spin-up period used prairie grass parameters provided by Hudiburg et al. (2015), with autumn burning every 5th year and low-intensity grazing by bison (10% of foliage removed 3 times per growing season). Soil parameters were based on bulk densities and organic matter contents of undisturbed Illinois prairie remnants (David et al. 2009), and on physical properties of the Flanagan and Drummer soil series (NRCS 2012). To match the high-moisture conditions predominant in Central Illinois before the introduction of artificial drainage, a standing water table was simulated from January through May. Soil organic matter turnover times were adjusted to produce steady-state (<1% change per decade in last 100 yr) SOM C and N of 10450 and 760 g m⁻², respectively, in the top 20 cm (Figure 2.S1). These totals are comparable to those measured in tallgrass prairie remnants on deep, mesic soils throughout the Midwest (Aref and Wander 1998, Kucharik et al. 2006, Matamala et al. 2008, David et al. 2009, Jelinski and Kucharik 2009, Brye and Riley 2009) and were achieved using turnover rates for the

active, intermediate, and slow soil C pools of 11, 0.1, and 0.002 yr^{-1} , giving residence times of 33 days, 10 years and 500 years, respectively.

Annual row crops were simulated beginning in 1868, the year our site was first recorded as occupied by European settlers. To simulate the change from an untilled, seasonally wet prairie to a tile-drained, annually-tilled crop system, we ceased simulating a standing water table, increased the maximum decomposition rate of intermediate- and slow-turnover organic matter, and reduced leaching rates for N and OM (Table 2.S1). Additionally, we reduced the rate of nonsymbiotic soil N fixation and the fraction of mineralized N lost to nitrification to better match conditions observed in row crop systems (Table 2.S1). Site-specific parameters were based on soil conditions measured at the site (Peralta and Wander 2008, C. Black, unpublished data; J. Jastrow, unpublished data; Moran and Jastrow 2010), soil moisture measured at the site (S. B. Gray, unpublished data; Rosenthal et al. 2014, Ruiz-Vera et al. 2015), and historical weather data from the Illinois State Water Survey (Angel 2010b). Atmospheric $[\text{CO}_2]$ was increased linearly to match the rise in industrial fossil fuel burning, from 294 ppm in 1868 to 370 ppm in 2000. Crop-specific parameters for maize and soybeans were developed by Hudiburg et al. (2015) to match the rate and physiological mechanisms of 20th-century crop genetic improvements: maize yield gains have come mostly from increases in planting density and photosynthetic capacity (Duvick 2005), so we simulated an increase in the maximum daily biomass production rate, with minor adjustments to other parameters (Table 2.S3). In contrast, soybean yield increases have come mostly from improved yield partitioning at constant plant size (Koester et al. 2014), so our soybean parameters were constant except that we increased the maximum harvest index in 1950 and 1980.

The management history of the site before 1980 was inferred from records of crop acreage and fertilizer usage for Champaign County retrieved from the National Agricultural Statistics Service (NASS 2011). Site management since 1980 is well described (Moran and Jastrow 2010) and was simulated accordingly (Table 2.S2). Briefly, management progressed from low-yielding mixed maize/oat/pasture in 1869 through increasingly intensive cropping and fertilization to a maize-soybean-oat rotation by 1935 and a maize-soybean rotation by 1950, with fertilization rates and cultivar parameters adjusted each decade to match NASS records. Beginning in 1970 we changed cultivation from moldboard plow every spring and fall to chisel plowing each spring and in fall after maize only, and fertilization rates were held steady at 157 kg N Ha⁻¹. This management schedule was continued though 1999, then concluded in 2000 with one year of winter wheat (Moran and Jastrow 2010).

To simulate the SoyFACE climate change manipulations, we extended the 20th-century simulation for the years 2001-2109 using the actual 2001-2011 planting and harvest dates of the SoyFACE experimental field. Weather data for 2001-2011 was retrieved from DAYMET (Thornton et al. 2014) and the model was run four times: a control run with actual weather conditions and [CO₂] set to 370 ppm (ambient conditions at the initiation of the SoyFACE experiment), a CO₂-only run with [CO₂] increased by 200 ppm to 570 ppm as a step change in 2001, a heat-only run with daily maximum and minimum temperatures increased 3.5 °C as a step change in 2009, and a heat+CO₂ run with both temperature and CO₂ increased. Note that we did not simulate any further increase in [CO₂] after the step change, so for all model-data comparisons we treated values modeled at 370 or 570 ppm as equivalent to field values observed in 2009-2011 at ~390 or 585 ppm.

Our model calibration strategy was to use the performance of our spin-up and historic hindcast scenarios as indicators of correct parameter calibration, then run the climate change scenarios with no further changes in model tuning. To the extent that model hindcasts do match known conditions, we gain confidence that model predictions for the future are reasonable. To evaluate model performance in more detail, we compared modeled soil temperature, moisture, and respiration rates against our 2009-2011 field observations. We also compared modeled aboveground biomass and grain yields for 2001-2008 against detailed phenological measurements from SoyFACE, using a database compiled by Twine et al (2013). All model parameters and analysis scripts are available online (Supplement 2.S1; Black et al. 2016).

Results

Temperature and CO₂ manipulation

Infrared heating produced a mean temperature increase of approximately 3.1, 2.7, and 2.6 °C at the top of the canopy in 2009, 2010, and 2011, respectively, and CO₂ fumigation consistently maintained ~585 ppm CO₂ during daylight hours (Ruiz-Vera et al. 2013, 2015). Soil temperature at 5-cm depth was increased by 1.8 ± 0.2 °C (mean \pm standard error of daily differences) during the growing seasons (Figure 2.1). During fallow seasons, heater output was intermittently reduced during extreme cold snaps (less than 16% of total time) but soil temperature for the whole season was still increased by 2.3 ± 0.1 °C (Figure 2.1). There was no consistent difference in soil temperature between eCO₂ and unfumigated plots given the same heat treatment.

Soil respiration

Overall, heating caused a consistent and large increase in R_{het} but reduced R_{aut} by a similar degree, producing no appreciable net effect of heating on R_{tot} , while eCO₂ increased R_{het} and affected R_{aut} differently each year, with the net effect of a small stimulation in R_{tot} from eCO₂. Averaged across the entire experiment, R_{het} was higher than control by 16, 12, and 48% in the eCO₂, heat, and heat+CO₂ treatments, respectively. R_{aut} was slightly (3%) higher in eCO₂ and lower in heated plots by 21% (heat) and 31% (heat+eCO₂). R_{tot} was higher in eCO₂ treatments by 11% (unheated eCO₂) and 13% (heated eCO₂) but 3% lower in the heated ambient CO₂ treatment (Figure 2.2).

Separate mixed-model analyses of respiration from each season (Table 2.1) showed that under soybeans in 2009, R_{tot} was unchanged while R_{het} increased and R_{aut} decreased in both heat and eCO₂ treatments. Under maize in 2010, CO₂ increased R_{tot} , heat increased R_{het} , and there were no differences in R_{aut} between treatments. Under soybeans in 2011, there were no differences in R_{tot} between treatments while R_{het} was higher and R_{aut} was lower in heated plots. R_{het} also showed a three-way interaction between Heat, CO₂, and Day, with higher R_{het} from heated eCO₂ plots on June 24 and July 18 but no statistical difference between treatments on the other days of the season (Figure 2.3). During the fallow period following soybeans (winter 2009-2010), R_{aut} and R_{tot} did not differ between treatments while R_{het} was higher in eCO₂ plots and had an interactive effect with heat and day, with a trend ($p < 0.12$) for higher R_{het} from heated plots on October 7 and December 31, lower R_{het} from heated plots on December 10, and no statistical difference on the other days. During the fallow period following maize (winter 2010-2011), no component of soil respiration (R_{tot} , R_{het} , R_{aut}) differed between treatments. The main effect of

Day was significant in all treatments every season, while the heat by CO₂ and CO₂ by Day interactions were never significant.

Particulate organic matter

POM-C declined from the beginning to the end of the experiment (2009 > all other harvests; Tukey HSD p < 0.01; Figure 2.4) and was approximately 14% lower in eCO₂ plots than in ambient plots (ANOVA F=7.69, p < 0.01; Figure 2.4), but showed no statistically resolvable difference between heated and unheated plots (ANOVA F=0.29, p > 0.5). Averaged across all treatments, the top 30 cm of soil contained 588 ± 41 g POM C m⁻² (mean ± SE) in Spring 2009, 439 ± 21 in Spring 2010, 444 ± 25 in Spring 2011, and 457 ± 22 in Fall 2011.

DayCent model

DayCent simulations of 20th-century grain yields of maize and soybeans agreed well with historic crop yields from Champaign County and captured about half of the observed year-to-year variation in yield (Figure 2.S2 & Figure 2.S3; root-mean-square error = 82.6 g C m⁻², RMSE/mean = 0.53). Modeled total C and N in soil organic matter at the end of the historic agriculture scenario were both very near the values measured at SoyFACE (Figure 2.S1). During the 2001-2008 CO₂ simulation, the temporal dynamics of modeled aboveground biomass within each season matched well with values observed at SoyFACE in those years (Figure 2.S4). Observed soybean grain yields at the site averaged 191 ± 30 g C m⁻² in ambient plots and 212 ± 39 in eCO₂ plots (Twine et al. 2013); modeled yields for the same years were 194 ± 65 and 254 ± 75 g C m⁻², respectively. Observed maize yields averaged 423 ± 15 g C m⁻² in ambient plots and 412 ± 44 in eCO₂ plots (Leakey et al. 2006, Markelz et al. 2011, Ruiz-Vera et al. 2015); modeled yields for the same years were 432 ± 38 and 460 ± 22 g C m⁻², respectively.

Modeled effects on soil temperatures were somewhat higher than the observed differences, with heated model runs 4.1 ± 0.6 °C (mean \pm sd) warmer than unheated runs at 5-cm depth during the growing season, while observed differences were less than 2 °C. Additionally, modeled soil temperature differences dropped to 3.5 °C before planting and after harvest, while observed differences were larger than during the growing season (~2.5 °C; Figure 2.1). Modeled temperatures in elevated CO₂ model runs were 0.5 ± 0.4 °C lower than those in ambient runs, but no consistent differences were observed in the field (Figure 2.1).

Compared to the values observed in the field, DayCent captured the seasonal variation and relative timing in all components of soil respiration, matched its magnitude well for R_{het}, and consistently underpredicted R_{aut}, producing a smaller overall under prediction of R_{tot} (Figure 2.S5).

When the simulation was extended to 100 years of heating and elevated [CO₂], DayCent predicted that CO₂ would increase all soil C pools, producing an increase of about ~4% in total SOM C (Figure 2.5). In contrast, heating was predicted to produce a rapid drop in all pools that overwhelmed the increased C inputs from eCO₂, producing a loss from heated runs, relative to the control scenario, of 15% of total soil C in the top 20 cm by 2109 (Figure 2.5).

Discussion

Experimental manipulation of CO₂ and temperature conditions similar to those expected for the mid-21st century increased respiration from soil microbes, likely indicating a drawdown of both labile and protected soil C. This effect would not have been detectable without partitioning respiration into its root and microbial components, and it was not offset by the observed positive effect of CO₂ on plant productivity. Instead, CO₂ increased respiration and

reduced POM C, and we saw no evidence of interactions between heat and CO₂ responses, leading us to speculate that eCO₂ primed long-term losses of SOC. Our model results adequately captured the effects of temperature and the additive effect of the temperature and CO₂ responses, but did not reproduce a CO₂ priming effect, so actual soil C losses may exceed our model-predicted value of 15% in 100 years.

Our results support the prediction that elevated temperature would increase the activity of soil heterotrophs and that this increased respiration would lead to long-term losses of soil C. Three years of heating produced strong and persistent increases in R_{het} (Figure 2.2; Table 2.1) and our model results are consistent with these increases leading to losses of C from all soil pools (Figure 2.5). Because heating reduced R_{aut} simultaneously with increasing R_{het}, there was no change in total soil respiration with heat (Figure 2.2; Table 2.1). This result contrasts with many previous studies (reviewed in Rustad et al. 2001, Wang et al. 2014) where R_{tot} increased under heating except under water limitation, but this discrepancy is explained by partitioning fluxes into their autotrophic and heterotrophic components.

Consistent with recent meta-analyses (Dieleman et al. 2012, Wang et al. 2014), we found that R_{het} responded reliably to increased temperature even when opposing changes in R_{aut} masked its effect on R_{tot}. This highlights the importance of separating soil CO₂ fluxes in global change experiments into their root and microbial components. We speculate that this masking may also occur at other sites where R_{tot} was measured without partitioning and found unresponsive to heat, especially those in grasslands and crops where root activity seems less responsive to eCO₂ than in forest systems (Wang et al. 2014).

Our results did not support the prediction that elevated CO₂ would increase plant biomass above and belowground, leading to higher C inputs that would at least partially ameliorate the

long-term effect of heat on soil C. Although aboveground plant biomass was higher in eCO₂ plots during soybean years, heating largely negated this difference (Ruiz-Vera et al. 2013) and there was little difference in root mass (S. B. Gray, in prep). R_{het} increased more in heat+eCO₂ plots than in plots given heat alone, indicating increased respiratory losses. Meanwhile R_{aut}, a probable correlate of C inputs from root exudation and turnover, was lower in eCO₂ plots in 2009 and showed no detectable change in other years, and the change in R_{aut} between heat and heat+eCO₂ plots was similar to that between unheated control and eCO₂ plots. One possible explanation for these findings is that the extra C inputs from eCO₂ were priming the breakdown of existing soil C, as seen previously at this and other FACE sites across widely differing ecosystem types (Peralta and Wander 2008, Moran and Jastrow 2010, Carrillo et al. 2011, Drake et al. 2011, Hopkins et al. 2014, Fang et al. 2015), rather than offsetting the effect of heat.

The priming hypothesis also is consistent with our observation that POM-C declined from 2009 to 2011 and was lower in eCO₂ plots than in unfumigated plots (Figure 2.4). The lack of an increase in POM-C with eCO₂ at this site was noted previously and attributed to priming by Peralta *et al.* (2008) after 3 years of fumigation, but it is worth noting that in year 3 the difference in POM-C between treatments was not yet significant. Given that the CO₂ priming effect required most of a decade to become statistically resolvable, it is perhaps not surprising that 3 years of heating did not produce a detectable change in POM-C.

Compared to other experiments that have examined the simultaneous effects of heating and eCO₂ on soil C dynamics, SoyFACE is notable for showing no obvious heat × CO₂ interactions. Although unheated FACE experiments have commonly showed direct effects of eCO₂ on soil respiration (Pendall et al. 2003, Pregitzer et al. 2008, Drake et al. 2011, Adair et al. 2011, Lam et al. 2014), many heat × CO₂ experiments are dominated by indirect effects

(Dieleman et al. 2012), which seem to be mediated by the joint effects of CO₂ and heating on soil water availability (Wan et al. 2007, Pendall et al. 2011, 2013, Selsted et al. 2012). Our site, by contrast, showed no significant heat × CO₂ interactions, perhaps because the site is only rarely dry enough to limit respiration. Water content was consistently higher in eCO₂ plots and was lower in heated plots in 2009 and on some days in 2010, but volumetric water content never dropped below 20% and the differences in soil water were not significant in 2011, the driest summer of the study (Rosenthal et al. 2014, Ruiz-Vera et al. 2015). Thus the effects of water availability on R_{het} appear to be additive to the heat effect, not a driving mechanism.

The observed changes in R_{aut} may be caused by differences in root distribution. We have no evidence of changes in total root biomass, however minirhizotron observations from maize in 2010 suggest that elevated CO₂ affected the depth distribution of roots, with greater root length in shallow soils and lower root length in deeper soils, but the effects depended on temperature treatment (S. B. Gray, in prep). In 2009 soybeans in heated plots appeared to use deeper soil water (Rosenthal et al. 2014), possibly indicating a shift of roots toward deeper soil that would have reduced the amount of root-respired C reaching the surface, thus contributing to the reduction in R_{aut} from soybeans we observed that year.

The empirical results from this study are reinforced by forward extrapolations from a process based model which indicates that heat, either singly or combined with increased CO₂, will drive long-term losses in SOC from agricultural soils, adding to losses in SOC caused by aggressive tillage practices. This result is consistent with previous models of CO₂ × warming experiments in predicting a net loss of soil C under global warming (Parton et al. 2007).

Given the difficulty of inferring SOC changes from short-term direct measurements and the number of known processes that DayCent integrates, we posit that these model results

provide our best available prediction of the *direction* of future SOC trajectories in a warming climate, and that they place a lower bound on the *magnitude* of future losses as CO₂ increases. However, our modelling approach was unable to test the hypothesis of a priming effect of eCO₂ on soil C breakdown, because DayCent's SOC model has an explicitly specified turnover time for each pool. Turnover can be manually increased to simulate priming (Cheng et al. 2013), but this requires a known degree of increase. Our observation that POM-C declined under elevated CO₂ gives an indirect indication that turnover rates have increased, but is not sufficient to constrain the magnitude of the increase, especially in slower-cycling C pools. Instead, increasing model C inputs through CO₂ fertilization lead to an increase in modeled SOM with no decrease in fast C pools that would match our observed drop in POM-C. Therefore our model results probably underestimate the extent of soil C losses under elevated CO₂. To produce more accurate long-term predictions of SOC dynamics under systems with active priming, models with explicit microbial processes may be needed (Wieder et al. 2013).

Elevated CO₂ and temperature, both singly and in combination, appear to accelerate the loss of soil C from agricultural ecosystems, through probably distinct and potentially additive pathways. Simple measurements of whole-soil respiration were not sufficient to detect these changes, so future experimental work should routinely include partitioning of soil respiration into plant-derived and SOM-derived components. Robust predictions of CO₂ priming effects will require updated ecosystem models that contain explicit microbial dynamics.

Acknowledgements

Thank you to Michael Masters, Nicholas DeLucia, Ahbisheik Pal, and Micah Sweeney for assistance with data collection; Michael Masters and Corey Mitchell for soil C analyses;

David Drag and Kannan Puthuval for maintaining the experimental site; Sharon Gray, Matthew Siebers, Andrew Leakey, and Eva Joo for sharing calibration data; and Robert Paul, Benjamin Duval, and Cindy Keogh for valuable advice about DayCent.

Portions of this research were funded by the US Department of Energy's National Institute for Climatic Change Research.

References

- Adair, E. C., P. B. Reich, J. J. Trost, and S. E. Hobbie. 2011. Elevated CO₂ stimulates grassland soil respiration by increasing carbon inputs rather than by enhancing soil moisture. *Global Change Biology* 17:3546–3563.
- Allison, S. D., M. D. Wallenstein, and M. A. Bradford. 2010. Soil-carbon response to warming dependent on microbial physiology. *Nature Geoscience* 3:336–340.
- Anderson-Teixeira, K. J., M. D. Masters, C. K. Black, M. Zeri, M. Z. Hussain, C. J. Bernacchi, and E. H. DeLucia. 2013. Altered belowground carbon cycling following land-use change to perennial bioenergy crops. *Ecosystems* 16:508–520.
- Angel, J. 2010a. Official 1981-2010 Climate Normals. Illinois State Climatologist Office, Illinois State Water Survey.
<http://www.isws.illinois.edu/atmos/statecli/newnormals/normal.USC00118740.txt>.
- Angel, J. 2010b. Climate Observations for Champaign-Urbana, IL. Illinois State Climatologist Office, Illinois State Water Survey.
<http://www.isws.illinois.edu/atmos/statecli/cuweather/index.htm>.

- Aref, S., and M. Wander. 1998. Long-term trends of corn yield and soil organic matter in different crop sequences and soil fertility treatments on the morrow plots. *Advances in Agronomy* 62:153–197.
- Bernhardt, E. S., J. J. Barber, J. S. Pippen, L. Taneva, J. A. Andrews, and W. H. Schlesinger. 2006. Long-term effects of free air CO₂ enrichment (FACE) on soil respiration. *Biogeochemistry* 77:91–116.
- Black, C. K., S. C. Davis, T. W. Hudiburg, C. J. Bernacchi, and E. H. DeLucia. 2016. Data from: Elevated CO₂ and temperature increase soil C losses from a soybean-maize ecosystem. Dryad Digital Repository. <http://dx.doi.org/10.5061/dryad.bn7j3>.
- Bond-Lamberty, B., and A. Thomson. 2010. Temperature-associated increases in the global soil respiration record. *Nature* 464:579–582.
- Bradford, M. A. 2013. Thermal adaptation of decomposer communities in warming soils. *Frontiers in Microbiology* 4:1–16.
- Brye, K. R., and T. L. Riley. 2009. Soil and plant property differences across a chronosequence of humid-temperate tallgrass prairie restorations. *Soil Science* 174:346–357.
- Carrillo, Y., E. G. Pendall, F. A. Dijkstra, J. A. Morgan, and J. M. Newcomb. 2011. Response of soil organic matter pools to elevated CO₂ and warming in a semi-arid grassland. *Plant and Soil* 347:339–350.
- Cheng, W. X., W. J. Parton, M. A. Gonzalez-Meler, R. P. Phillips, S. Asao, G. G. McNickle, E. Brzostek, and J. D. Jastrow. 2013. Synthesis and modeling perspectives of rhizosphere priming. *New Phytologist* 201:31–44.
- Chevallier, T., K. Hmaidi, E. Kouakoua, M. Bernoux, T. Gallali, J. Toucet, C. Jolivet, P. Deleporte, and B. G. Barthès. 2015. Physical protection of soil carbon in

macroaggregates does not reduce the temperature dependence of soil CO₂ emissions.

Journal of Plant Nutrition and Soil Science 178:592–600.

Conant, R. T., M. G. Ryan, G. I. Ågren, H. E. Birge, E. A. Davidson, P. E. Eliasson, S. E. Evans, S. D. Frey, C. P. Giardina, F. M. Hopkins, R. Hyvönen, M. U. F. Kirschbaum, J. M. Lavallee, J. Leifeld, W. J. Parton, J. Megan Steinweg, M. D. Wallenstein, J. Å. Martin Wetterstedt, and M. A. Bradford. 2011. Temperature and soil organic matter decomposition rates – synthesis of current knowledge and a way forward. Global Change Biology 17:3392–3404.

David, M. B., G. F. McIsaac, R. G. Darmody, and R. A. Omonode. 2009. Long-term changes in mollisol organic carbon and nitrogen. Journal of Environmental Quality 38:200–211.

Davidson, E. A., and I. A. Janssens. 2006. Temperature sensitivity of soil carbon decomposition and feedbacks to climate change. Nature 440:165–173.

Davis, S. C., W. J. Parton, S. J. Del Grosso, C. Keough, E. Marx, P. R. Adler, and E. H. DeLucia. 2012. Impact of second-generation biofuel agriculture on greenhouse-gas emissions in the corn-growing regions of the US. Frontiers in Ecology and the Environment 10:69–74.

Davis, S. C., W. J. Parton, F. G. Dohleman, C. M. Smith, S. J. Del Grosso, A. D. Kent, and E. H. DeLucia. 2010. Comparative biogeochemical cycles of bioenergy crops reveal nitrogen-fixation and low greenhouse gas emissions in a *Miscanthus × giganteus* agro-ecosystem. Ecosystems 13:144–156.

Dieleman, W. I. J., S. Vicca, F. A. Dijkstra, F. Hagedorn, M. J. Hovenden, K. S. Larsen, J. A. Morgan, A. Volder, C. Beier, J. S. Dukes, J. King, S. Leuzinger, S. Linder, Y. Luo, R. Oren, P. De Angelis, D. T. Tingey, M. R. Hoosbeek, and I. A. Janssens. 2012. Simple

additive effects are rare: a quantitative review of plant biomass and soil process responses to combined manipulations of CO₂ and temperature. *Global Change Biology* 18:2681–2693.

Drake, J. E., A. Gallet-Budynek, K. S. Hofmockel, E. S. Bernhardt, S. A. Billings, R. B. Jackson, K. S. Johnsen, J. Lichter, H. R. McCarthy, M. L. McCormack, D. J. P. Moore, R. Oren, S. Palmroth, R. P. Phillips, J. S. Pippen, S. G. Pritchard, K. K. Treseder, W. H. Schlesinger, E. H. DeLucia, and A. C. Finzi. 2011. Increases in the flux of carbon belowground stimulate nitrogen uptake and sustain the long-term enhancement of forest productivity under elevated CO₂. *Ecology Letters* 14:349–357.

Duvick, D. N. 2005. The contribution of breeding to yield advances in maize (*Zea mays* L.). *Advances in Agronomy* 86:83–145.

Eswaran, H., E. Van Den Berg, and P. Reich. 1993. Organic carbon in soils of the world. *Soil Science Society of America Journal* 57:192–194.

Fang, H., S. Cheng, E. Lin, G. Yu, S. Niu, Y. Wang, M. Xu, X. Dang, L. Li, and L. Wang. 2015. Elevated atmospheric carbon dioxide concentration stimulates soil microbial activity and impacts water-extractable organic carbon in an agricultural soil. *Biogeochemistry* 122:253–267.

Filion, M., P. Dutilleul, and C. Potvin. 2000. Optimum experimental design for Free-Air Carbon dioxide Enrichment (FACE) studies. *Global Change Biology* 6:843–854.

Frey, S. D., J. Lee, J. M. Melillo, and J. Six. 2013. The temperature response of soil microbial efficiency and its feedback to climate. *Nature Climate Change* 3:395–398.

- Hanson, P. J., N. T. Edwards, C. T. Garten, and J. A. Andrews. 2000. Separating root and soil microbial contributions to soil respiration: A review of methods and observations. *Biogeochemistry* 48:115–146.
- Hartley, I. P., A. Heinemeyer, S. P. Evans, and P. Ineson. 2007. The effect of soil warming on bulk soil vs. rhizosphere respiration. *Global Change Biology* 13:2654–2667.
- Hartman, M. D., E. R. Merchant, W. J. Parton, M. P. Gutmann, S. M. Lutz, and S. A. Williams. 2011. Impact of historical land-use changes on greenhouse gas exchange in the U.S. Great Plains, 1883–2003. *Ecological Applications* 21:1105–1119.
- Hartmann, D., A. M. G. Klein Tank, M. Rusticucci, L. V. Alexander, S. Brönnimann, Y. A.-R. Charabi, F. J. Dentener, E. J. Dlugokencky, D. R. Easterling, A. Kaplan, B. J. Soden, P. W. Thorne, M. Wild, and P. Zhai. 2013. Observations: Atmosphere and Surface. Pages 159–254 in Intergovernmental Panel on Climate Change, editor. *Climate change 2013 : The physical science basis : Working group I contribution to the fifth assessment report of the intergovernmental panel on climate change*. Cambridge University Press, Cambridge.
- Healy, R. W., R. G. Striegl, T. F. Russell, G. L. Hutchinson, and G. P. Livingston. 1996. Numerical evaluation of static-chamber measurements of soil—atmosphere gas exchange: identification of physical processes. *Soil Science Society of America Journal* 60:740–747.
- Hopkins, F. M., T. R. Filley, G. Gleixner, M. Lange, S. M. Top, and S. E. Trumbore. 2014. Increased belowground carbon inputs and warming promote loss of soil organic carbon through complementary microbial responses. *Soil Biology and Biochemistry* 76:57–69.

- Hudiburg, T. W., S. C. Davis, W. J. Parton, and E. H. DeLucia. 2015. Bioenergy crop greenhouse gas mitigation potential under a range of management practices. *Global Change Biology Bioenergy* 7:366–374.
- Jelinski, N. A., and C. J. Kucharik. 2009. Land-use effects on soil carbon and nitrogen on a U.S. Midwestern floodplain. *Soil Science Society of America Journal* 73:217–225.
- Keidel, L., C. Kammann, L. Grünhage, G. Moser, and C. Müller. 2015. Positive feedback of elevated CO₂ on soil respiration in late autumn and winter. *Biogeosciences* 12:1257–1269.
- Kimball, B. A. 2005. Theory and performance of an infrared heater for warming ecosystems. *Global Change Biology* 11:2041–2056.
- King, J. S., P. J. Hanson, E. Bernhardt, P. deAngelis, R. J. Norby, and K. S. Pregitzer. 2004. A multiyear synthesis of soil respiration responses to elevated atmospheric CO₂ from four forest FACE experiments. *Global Change Biology* 10:1027–1042.
- Koester, R. P., J. A. Skoneczka, T. R. Cary, B. W. Diers, and E. A. Ainsworth. 2014. Historical gains in soybean (*Glycine max* Merr.) seed yield are driven by linear increases in light interception, energy conversion, and partitioning efficiencies. *Journal of Experimental Botany* 65:3311–3321.
- Kucharik, C. J., N. J. Fayram, and K. N. Cahill. 2006. A paired study of prairie carbon stocks, fluxes, and phenology: comparing the world's oldest prairie restoration with an adjacent remnant. *Global Change Biology* 12:122–139.
- Kuzyakov, Y., and A. A. Larionova. 2005. Root and rhizomicrobial respiration: A review of approaches to estimate respiration by autotrophic and heterotrophic organisms in soil. *Journal of Plant Nutrition and Soil Science* 168:503–520.

- Lam, S. K., R. Norton, R. Armstrong, and D. Chen. 2014. Increased microbial activity under elevated [CO₂] does not enhance residue decomposition in a semi-arid cropping system in Australia. *Soil Biology and Biochemistry* 72:97–99.
- Leakey, A. D. B., C. J. Bernacchi, F. G. Dohleman, D. Ort, and S. P. Long. 2004. Will photosynthesis of maize (*Zea mays*) in the US Corn Belt increase in future [CO₂] rich atmospheres? An analysis of diurnal courses of CO₂ uptake under free-air concentration enrichment (FACE). *Global Change Biology* 10:951–962.
- Leakey, A. D. B., M. Uribelarrea, E. A. Ainsworth, S. L. Naidu, A. Rogers, D. R. Ort, and S. P. Long. 2006. Photosynthesis, productivity, and yield of maize are not affected by open-air elevation of CO₂ concentration in the absence of drought. *Plant Physiology* 140:779–790.
- Lenth, R. V. 2016. Least-squares means: The R package lsmeans. *Journal of Statistical Software* 69:1–33.
- Lu, M., X. Zhou, Q. Yang, H. Li, Y. Luo, C. Fang, J. Chen, X. Yang, and B. Li. 2013. Responses of ecosystem carbon cycle to experimental warming: a meta-analysis. *Ecology* 94:726–738.
- Luo, Y., S. Wan, D. Hui, and L. L. Wallace. 2001. Acclimatization of soil respiration to warming in a tall grass prairie. *Nature* 413:622–625.
- Markelz, R. J. C., R. S. Strellner, and A. D. B. Leakey. 2011. Impairment of C₄ photosynthesis by drought is exacerbated by limiting nitrogen and ameliorated by elevated [CO₂] in maize. *Journal of Experimental Botany* 62:3235–3246.
- Marriott, E. E., and M. M. Wander. 2006. Total and labile soil organic matter in organic and conventional farming systems. *Soil Science Society of America Journal* 70:950–959.

- Matamala, R. R., J. D. Jastrow, R. M. Miller, and C. T. Garten. 2008. Temporal changes in C and N stocks of restored prairie: implications for C sequestration strategies. *Ecological Applications* 18:1470–1488.
- Mayaki, J., I. Teare, and L. Stone. 1976. Top and root growth of irrigated and nonirrigated soybeans. *Crop Science* 16:92–94.
- Miglietta, F., A. Peressotti, F. P. Vaccari, A. Zaldei, P. deAngelis, and G. Scarascia-Mugnozza. 2001. Free-air CO₂ enrichment (FACE) of a poplar plantation: the POPFACE fumigation system. *New Phytologist* 150:465–476.
- Moran, K. K., and J. D. Jastrow. 2010. Elevated carbon dioxide does not offset loss of soil carbon from a corn-soybean agroecosystem. *Environmental Pollution* 158:1088–1094.
- Morgan, P. B., G. A. Bollero, R. L. Nelson, F. G. Dohleman, and S. P. Long. 2005. Smaller than predicted increase in aboveground net primary production and yield of field-grown soybean under fully open-air [CO₂] elevation. *Global Change Biology* 11:1856–1865.
- NASS. 2011. Census of Agriculture Quick Stats 2.0. National Agricultural Statistics Service, United States Department of Agriculture. http://www.nass.usda.gov/Quick_Stats/.
- NRCS. 2012. Web Soil Survey. Soil Survey Staff, Natural Resources Conservation Service, United States Department of Agriculture. <http://websoilsurvey.nrcc.usda.gov/>.
- Parton, W. J., M. D. Hartman, D. S. Ojima, and D. S. Schimel. 1998. DAYCENT and its land surface submodel: description and testing. *Global and Planetary Change* 19:35–48.
- Parton, W. J., J. A. Morgan, G. Wang, and S. J. Del Grosso. 2007. Projected ecosystem impact of the Prairie Heating and CO₂ Enrichment experiment. *New Phytologist* 174:823–834.
- Pendall, E. G., S. J. Del Grosso, J. King, D. R. LeCain, D. Milchunas, J. A. Morgan, A. Mosier, D. S. Ojima, W. J. Parton, P. Tans, and J. White. 2003. Elevated atmospheric CO₂ effects

and soil water feedbacks on soil respiration components in a Colorado grassland. *Global Biogeochemical Cycles* 17:1046.

Pendall, E. G., J. L. Heisler-White, D. G. Williams, F. A. Dijkstra, Y. Carrillo, J. A. Morgan, and D. R. LeCain. 2013. Warming reduces carbon losses from grassland exposed to elevated atmospheric carbon dioxide. *PLoS ONE* 8:e71921.

Pendall, E. G., Y. Osanai, A. L. Williams, and M. J. Hovenden. 2011. Soil carbon storage under simulated climate change is mediated by plant functional type. *Global Change Biology* 17:505–514.

Peralta, A. L., and M. M. Wander. 2008. Soil organic matter dynamics under soybean exposed to elevated [CO₂]. *Plant and Soil* 303:69–81.

Pinheiro, J., D. Bates, S. DebRoy, D. Sarkar, and R Core Team. 2016. nlme: Linear and nonlinear mixed effects models. R package version 3.1-127. <http://CRAN.R-project.org/package=nlme>.

Pregitzer, K. S., A. J. Burton, J. S. King, and D. R. Zak. 2008. Soil respiration, root biomass, and root turnover following long-term exposure of northern forests to elevated atmospheric CO₂ and tropospheric O₃. *New Phytologist* 180:153–161.

Pregitzer, K., W. Loya, M. Kubiske, and D. Zak. 2006. Soil respiration in northern forests exposed to elevated atmospheric carbon dioxide and ozone. *Oecologia* 148:503–516.

R Core Team. 2016. R: A language and environment for statistical computing. Version 3.2.4. R Foundation for Statistical Computing, Vienna, Austria. <https://www.R-project.org/>.

Rosenthal, D. M., U. M. Ruiz-Vera, M. H. Siebers, S. B. Gray, C. J. Bernacchi, and D. R. Ort. 2014. Biochemical acclimation, stomatal limitation and precipitation patterns underlie

decreases in photosynthetic stimulation of soybean (*Glycine max*) at elevated [CO₂] and temperatures under fully open air field conditions. *Plant Science* 226:136–146.

Ruiz-Vera, U. M., M. H. Siebers, D. W. Drag, D. R. Ort, and C. J. Bernacchi. 2015. Canopy warming caused photosynthetic acclimation and reduced seed yield in maize grown at ambient and elevated [CO₂]. *Global Change Biology* 21:4237–4249.

Ruiz-Vera, U. M., M. Siebers, S. B. Gray, D. W. Drag, D. M. Rosenthal, B. A. Kimball, D. R. Ort, and C. Bernacchi. 2013. Global warming can negate the expected CO₂ stimulation in photosynthesis and productivity for soybean grown in the Midwest United States. *Plant Physiology* 162:410–423.

Rustad, L., J. L. Campbell, G. M. Marion, R. J. Norby, M. J. Mitchell, A. E. Hartley, J. H. C. Cornelissen, and J. Gurevitch. 2001. A meta-analysis of the response of soil respiration, net nitrogen mineralization, and aboveground plant growth to experimental ecosystem warming. *Oecologia* 126:543–562.

Schindlbacher, A., S. Wunderlich, W. Borken, B. Kitzler, S. Zechmeister-Boltenstern, and R. Jandl. 2012. Soil respiration under climate change: prolonged summer drought offsets soil warming effects. *Global Change Biology* 18:2270–2279.

Schmidt, M. W. I., M. S. Torn, S. Abiven, T. Dittmar, G. Guggenberger, I. A. Janssens, M. Kleber, I. Kögel-Knabner, J. Lehmann, D. A. C. Manning, P. Nannipieri, D. P. Rasse, S. Weiner, and S. E. Trumbore. 2011. Persistence of soil organic matter as an ecosystem property. *Nature* 478:49–56.

Selsted, M. B., L. Linden, A. Ibrom, A. Michelsen, K. S. Larsen, J. K. Pedersen, T. N. Mikkelsen, K. Pilegaard, C. Beier, and P. Ambus. 2012. Soil respiration is stimulated by elevated CO₂ and reduced by summer drought: three years of measurements in a

- multifactor ecosystem manipulation experiment in a temperate heathland (CLIMAITE). *Global Change Biology* 18:1216–1230.
- Subke, J.-A., and M. Bahn. 2010. On the 'temperature sensitivity' of soil respiration: Can we use the immeasurable to predict the unknown? *Soil Biology and Biochemistry* 42:1653–1656.
- Suseela, V., and J. S. Dukes. 2013. The responses of soil and rhizosphere respiration to simulated climatic changes vary by season. *Ecology* 94:403–413.
- Thornton, P. E., M. M. Thornton, B. W. Mayer, N. Wilhelmi, Y. Wei, R. Devarakonda, and R. B. Cook. 2014. Daymet: Daily Surface Weather Data on a 1-km Grid for North America, Version 2. ORNL DAAC, Oak Ridge, Tennessee, USA. <http://daac.ornl.gov/>.
- Tisdall, J. M., and J. M. Oades. 1980. The effect of crop rotation on aggregation in a red-brown earth. *Australian Journal of Soil Research* 18:423–433.
- Twine, T. E., J. J. Bryant, K. Richter, C. J. Bernacchi, K. D. McConaughay, S. J. Morris, and A. D. B. Leakey. 2013. Impacts of elevated CO₂ concentration on the productivity and surface energy budget of the soybean and maize agroecosystem in the Midwest USA. *Global Change Biology* 19:2838–2852.
- Vogel, J., and D. Valentine. 2005. Small root exclusion collars provide reasonable estimates of root respiration when measured during the growing season of installation. *Canadian Journal of Forest Research* 35:2112–2117.
- Wall, G. W., J. E. T. McLain, B. A. Kimball, J. W. White, M. J. Ottman, and R. L. Garcia. 2013. Infrared warming affects intrarow soil carbon dioxide efflux during vegetative growth of spring wheat. *Agronomy Journal* 105:607–618.

- Wan, S., R. J. Norby, J. Ledford, and J. F. Weltzin. 2007. Responses of soil respiration to elevated CO₂, air warming, and changing soil water availability in a model old-field grassland. *Global Change Biology* 13:2411–2424.
- Wang, X., L. Liu, S. Piao, I. A. Janssens, J. Tang, W. Liu, Y. Chi, J. Wang, and S. Xu. 2014. Soil respiration under climate warming: differential response of heterotrophic and autotrophic respiration. *Global Change Biology* 20:3229–3237.
- Wieder, W. R., G. B. Bonan, and S. D. Allison. 2013. Global soil carbon projections are improved by modelling microbial processes. *Nature Climate Change* 3:909–912.
- Wu, Z., P. Dijkstra, G. W. Koch, J. Peñuelas, and B. A. Hungate. 2011. Responses of terrestrial ecosystems to temperature and precipitation change: a meta-analysis of experimental manipulation. *Global Change Biology* 17:927–942.

Tables and Figures

Table 2.1: Mixed effects model results for rates of soil CO₂ efflux attributed to soil heterotrophs (R_{het}), plant roots and rhizosphere organisms (R_{aut}), and whole soil (R_{tot}). The first six columns show P values for each effect. Boldface values are significant at a preselected threshold of 0.1. The main Day effect was always significant (all P < 0.02) and is not shown here to save space. The last two columns show percent change from control for each treatment, presented as the estimated differences ± 1 standard error of whole-season LS means.

Component	Heat	CO ₂	Heat × CO ₂	Heat × Day	CO ₂ × Day	Heat × CO ₂ × Day	Heat % change	CO ₂ % change
Soy 2009								
R _{aut}	0.014	0.089	0.552	0.737	0.717	0.988	-53 ± 15	-41 ± 17
R _{het}	0.035	0.068	0.271	0.790	0.495	0.724	32 ± 11	31 ± 11
R _{tot}	0.475	0.920	0.636	0.859	0.389	0.932	-6 ± 7	0 ± 8
Fallow 2009-2010¹								
R _{aut}	0.465	0.915	0.845	0.909	0.922	0.899	26 ± 50	-6 ± 43
R _{het}	0.875	0.097	0.879	0.053	0.775	0.934	5 ± 7	14 ± 7
R _{tot}	0.315	0.424	0.776	0.869	0.915	0.901	12 ± 12	8 ± 12
Maize 2010								
R _{aut}	0.716	0.806	0.917	0.561	0.317	0.277	-8 ± 19	6 ± 20
R _{het}	0.053	0.137	0.181	0.704	0.632	0.931	20 ± 8	28 ± 15
R _{tot}	0.263	0.059	0.226	0.687	0.642	0.605	8 ± 7	20 ± 7
Fallow 2010-2011								
R _{aut}	0.532	0.796	0.216	0.940	0.339	0.231	-17 ± 30	1 ± 43
R _{het}	0.740	0.800	0.687	0.636	0.310	0.752	6 ± 12	1 ± 12
R _{tot}	0.771	0.953	0.381	0.977	0.204	0.117	-2 ± 11	2 ± 17
Soy 2011								
R _{aut}	0.018	0.190	0.864	0.690	0.794	0.381	-48 ± 15	57 ± 33
R _{het}	0.047	0.224	0.700	0.801	0.739	0.091	27 ± 11	18 ± 12
R _{tot}	0.131	0.252	0.824	0.906	0.822	0.997	-11 ± 6	29 ± 21

¹Data from March 1, 2010 were excluded from the model because they contained no usable observations from heated plots.

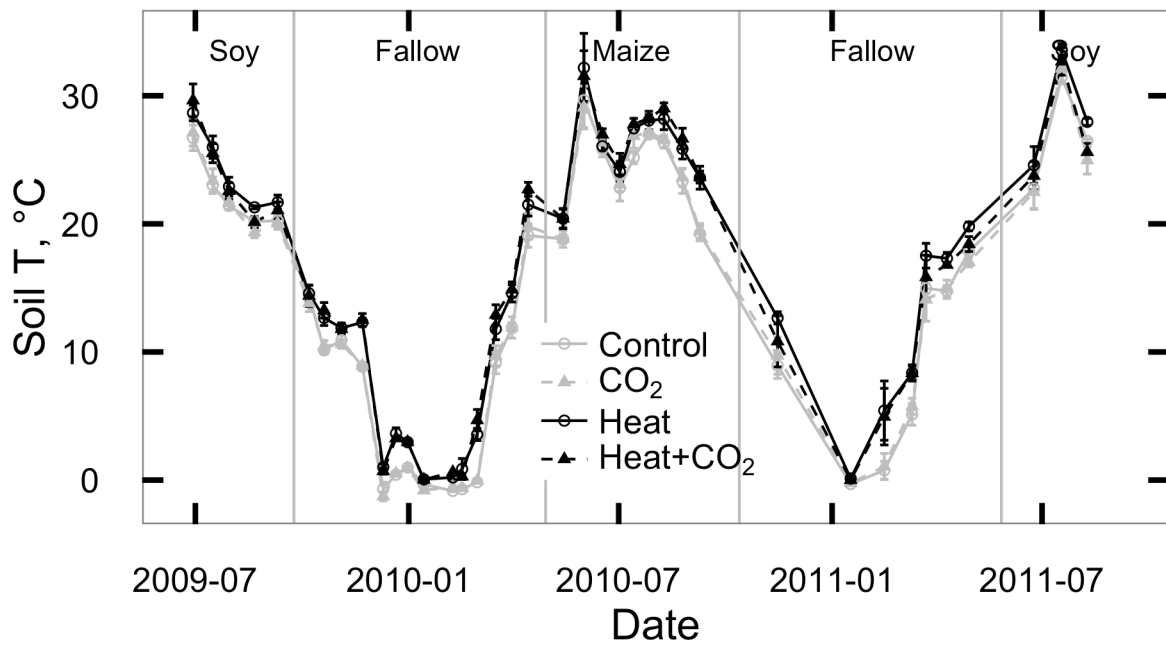


Figure 2.1: Temperature measured 5 cm below the soil surface at SoyFACE between June 2009 and October 2011. Error bars show treatment means \pm 1 standard error for each day.

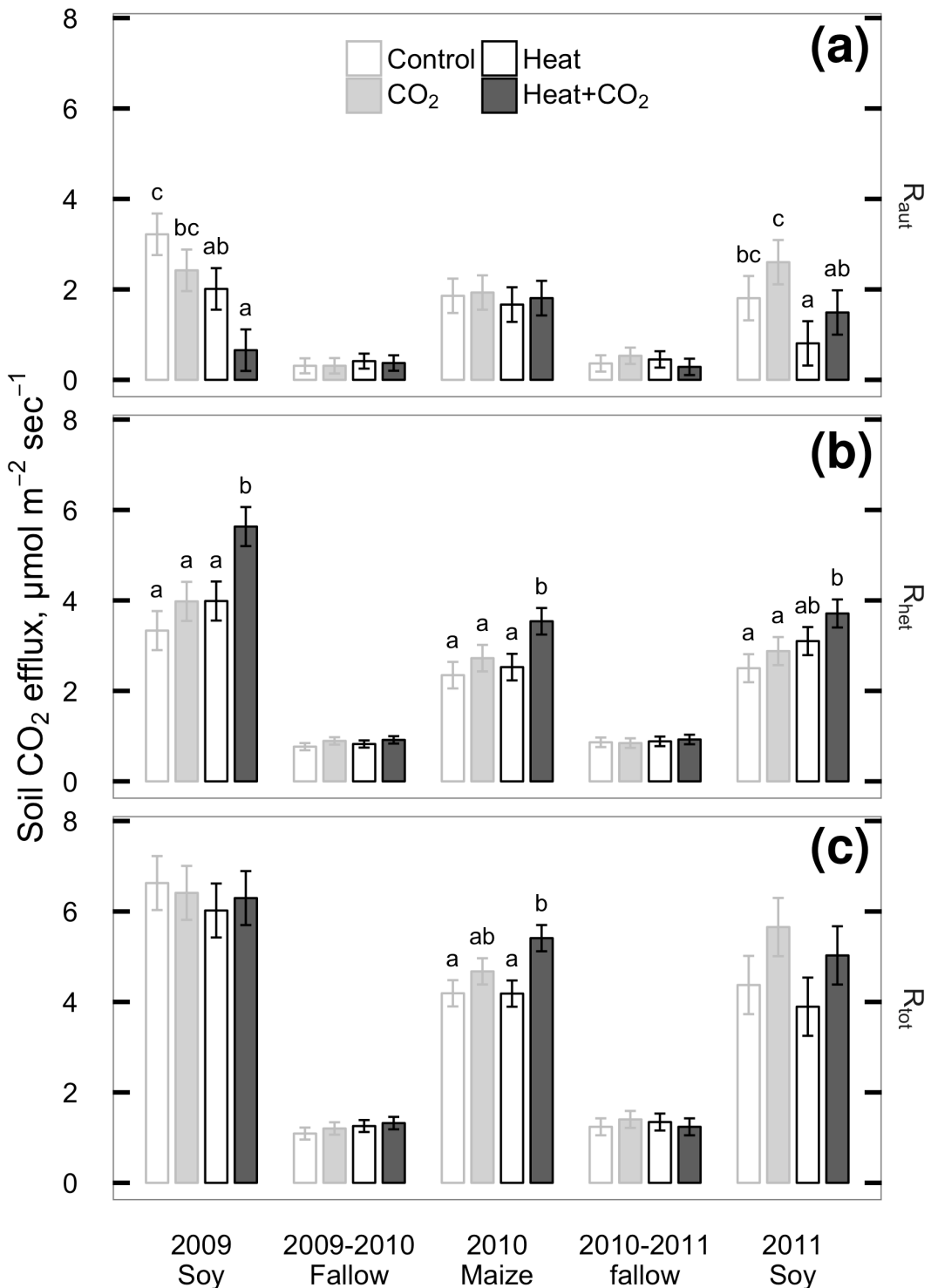


Figure 2.2: Seasonal means of CO₂ flux measured from plant roots and rhizosphere (R_{aut} ; a), soil heterotrophs (R_{het} ; b), and whole soil (R_{tot} ; c) at SoyFACE between June 2009 and October 2011. Error bars show treatment LS means \pm 1 standard error for each season. Within each season, treatments that share a letter are not statistically different ($P > 0.1$).

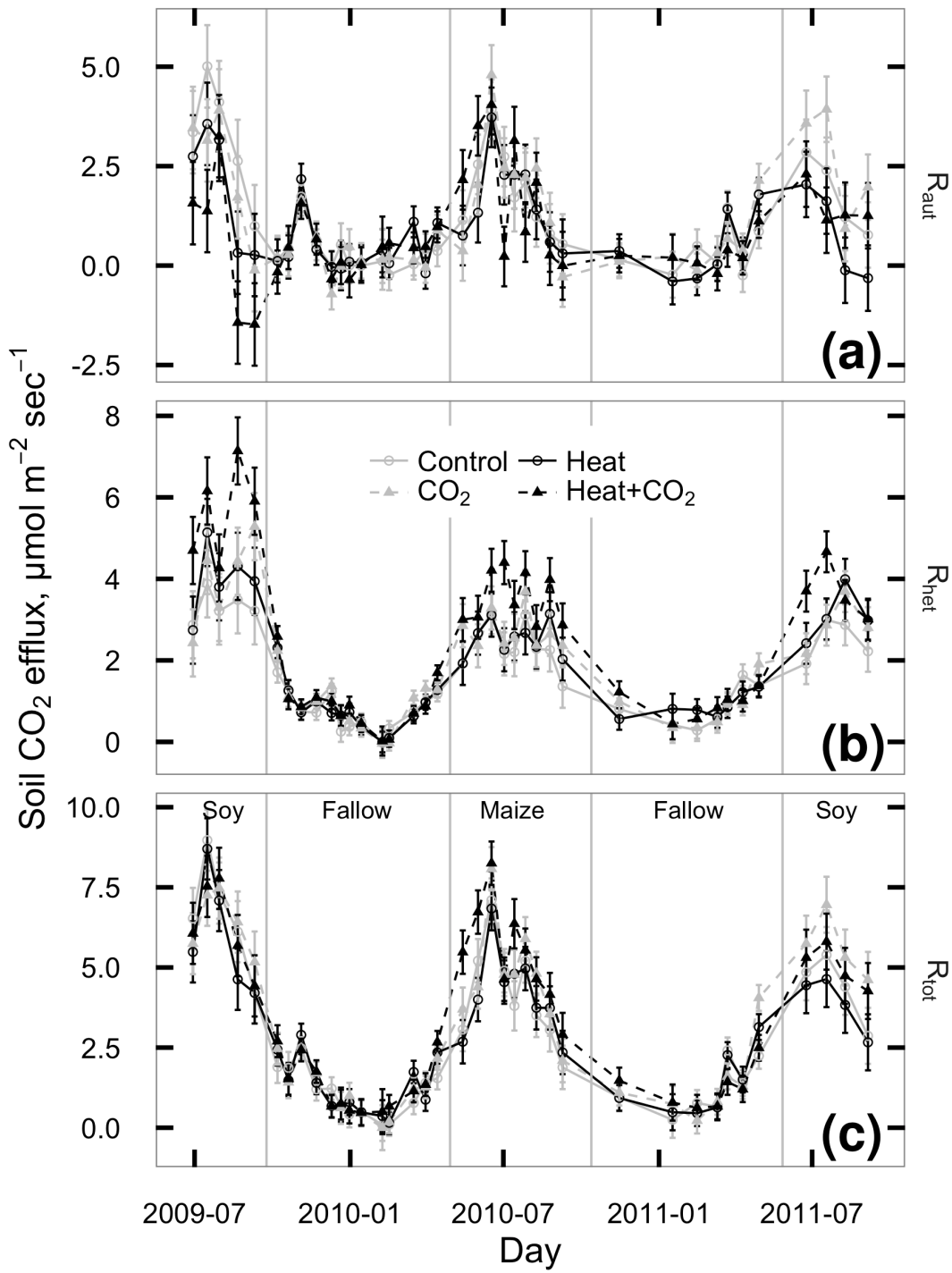


Figure 2.3: CO_2 flux measured from plant roots and rhizosphere (R_{aut} ; a), soil heterotrophs (R_{het} ; b), and whole soil (R_{tot} ; c) at SoyFACE between June 2009 and October 2011. Each season was analyzed separately; vertical grey lines indicate cutoffs between seasons. Error bars show treatment LS means ± 1 standard error for each day.

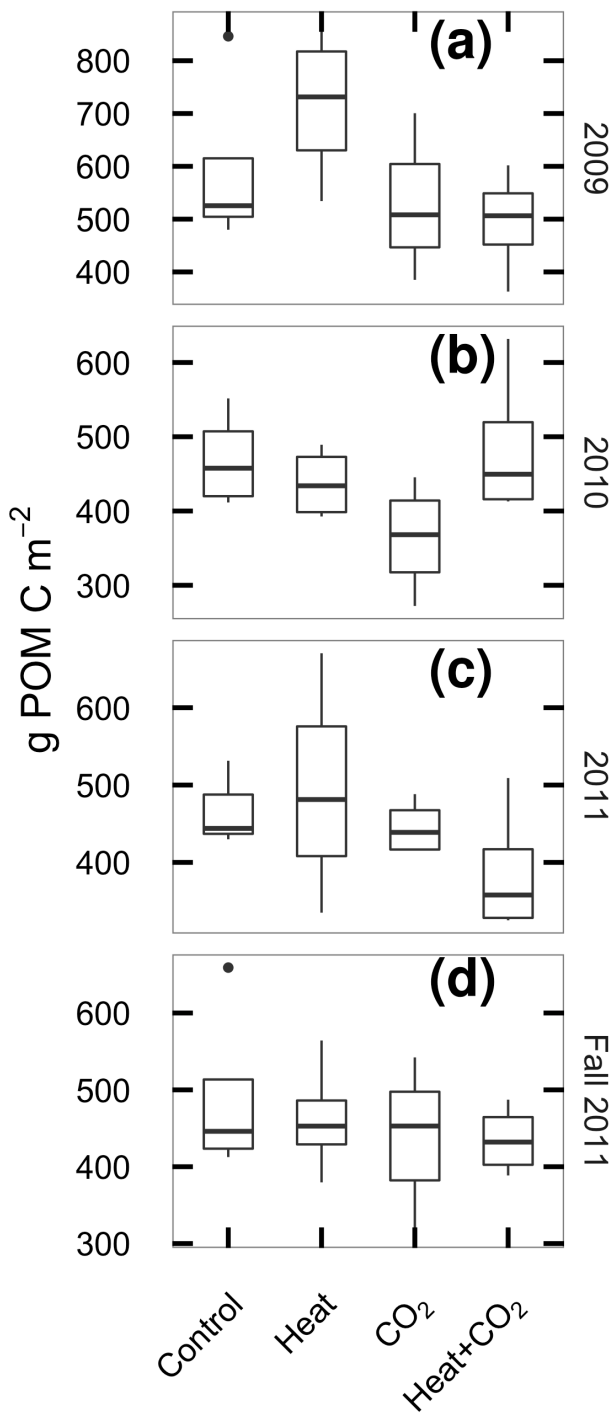


Figure 2.4: Particulate organic matter carbon (POM-C) in the top 30 cm of soil at SoyFACE, sampled in spring of 2009 (a), 2010 (b), 2011 (c) and at the end of the experiment in fall 2011 (d). Boxes cover the estimated interquartile range of each group, whiskers extend to the smaller of max/min or 1.5 IQR.

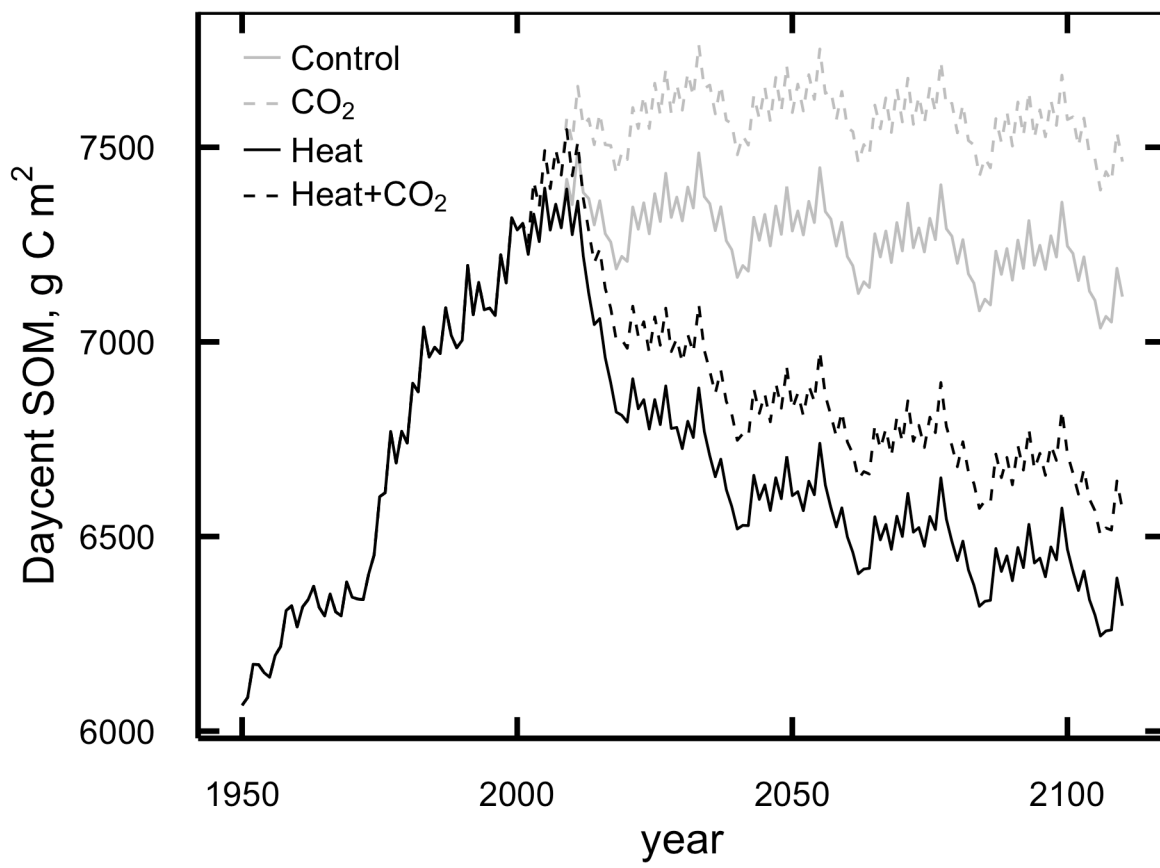


Figure 2.5: Mean annual values for total soil organic matter (g C m^{-2}) predicted by DayCent in the top 20 cm of SoyFACE soil.

Supplement 2.S1: DayCent model fit evaluation

Data availability

All the data for this paper, including raw files, data-processing scripts, and DayCent simulation files, is permanently archived in Dryad (<http://datadryad.org>) and is freely available online: <http://dx.doi.org/10.5061/dryad.bn7j3>.

Additionally, the DayCent model files, raw output, run management scripts and the majority of the model calibration data are available online at https://github.com/infotroph/soyface_daycent. Some validation was performed against unpublished datasets that were shared by collaborators in advance of publication; these are not available in this project's archive, but we intend to update the Github repository with links to those datasets at such time as their authors make them available.

Table 2.S1: Summary of model parameters changed between phases of the DayCent model run.

File	Parameter	Spin-up value	Ag value	FACE value	Remarks
sitepar.in	watertable[1-5]	1	0	0	Tile drainage lowers Jan-May water table
sitepar.in	netm_to_no3	0.05	0.8	0.8	Nitrification much lower in undisturbed grassland
fix.100	CO2PPM(1)	294	294	370	Starting [CO ₂]
fix.100	CO2PPM(2)	294	370	570	Ending [CO ₂]
fix.100	CO2RMP	1	1	0	0=step change in given year, 1=ramp
fix.100	DEC4	0.002	0.0025	0.0025	Slow-turnover OM decomposes faster in tilled, drained soil
fix.100	DEC5(1)	0.08	0.2	0.2	Intermediate-turnover OM at surface decomposes faster in tilled, drained soil
fix.100	DEC5(2)	0.1	0.25	0.25	Intermediate-turnover OM below surface decomposes faster in tilled, drained soil
fix.100	FLEACH(1)	0.7	0.4	0.4	Intercept for mineral leaching as a function of sand content
fix.100	FLEACH(2)	0.9	0.4	0.4	Slope for mineral leaching as a function of sand content
fix.100	FLEACH(3)	0.95	0.2	0.2	Leaching fraction multiplier for leached mineral N
fix.100	MINLCH	1.5	1.0	1.0	Minimum cm water flow to activate mineral leaching
fix.100	OMLECH(1)	0.03	0.05	0.05	Intercept for organic matter leaching as a function of sand content
fix.100	OMLECH(2)	0.12	0.15	0.15	Slope for organic matter leaching as a function of sand content
fix.100	OMLECH(3)	1.9	0.1	0.1	Minimum cm water flow to activate organic leaching
soyface.100	EPNFS(2)	0.017	0.005	0.005	Slope for nonsymbiotic N fixation as a function of annual precipitation

Table 2.S2: Summary of management schedule for DayCent simulations.

Years	Crop	Weather ¹	Tillage ²	N management ³
-2000–1868	Prairie	R	Fire every 5th year	Graze May–July
1869–1888	2 yr maize 1, oat, 2 yr pasture	R	Spring MD before maize & oat, fall M	Graze May–Oct after oats and during pasture
1889–1934	2 yr maize 1, oat, 2 yr pasture	H	Spring MD before maize & oat, fall M	Graze May–Oct after oats and during pasture
1935–1949	Maize 3, oat, low yield soy	H	Spring MD, fall M	Fert 40.4, graze after oats
1950–1959	Maize 5, medium yield soy	H	Spring MD, fall M	Fert 56
1960–1969	Maize 7, medium yield soy	H	Spring MD, fall M	Fert 100
1970–1979	Maize 9, medium yield soy	H	Spring CD, fall C after maize	Fert 157
1980–1998	Maize 10, high yield soy	H	Spring CD, fall C after maize	Fert 157
1999–2000	High yield soy, winter wheat	H	Spring CD, fall C after wheat	Fert 116.4
2001–2109	Maize 10, high yield soy	D	Spring CD, fall C after maize	Fert 157

¹R = randomized weather; H = historic weather from Illinois Water Survey (4.7 km from site); D = Gridded weather for site retrieved from DAYMET.

²M = Moldboard plow; D = disk; C = Chisel plow.

³Fertilization rates are in kg N ha⁻¹. Fertilizer is applied before planting of maize and wheat only; other crops are never fertilized.

Table 2.S3: Summary of DayCent parameters changed between simulated maize cultivars. All parameters not shown here are identical between cultivars; see CROP.100 in the model files for details.

Parameter	C1 ¹	C3	C5	C7	C9	C10
PRDX(1)	0.30	0.45	0.70	0.75	1.00	1.50
FRTC(5)	0.10	0.10	0.10	0.20	0.20	0.20
CFRTCN(1) ²	0.40	0.40	0.40	0.30	0.30	0.30
PRAMN(1,1)	20	20	10	10	10	10
PRAMX(1,1)	40	40	20	20	20	20
HIMAX	0.35	0.40	0.50	0.60	0.60	0.60
EFRGRN(1)	0.50	0.75	0.75	0.75	0.75	0.75
FALLRT	0.10	0.10	0.10	0.10	0.20	0.20
TMPGERM ²	10	10	10	15	15	15
DDBASE ²	1500	1500	1700	1450	1450	1450
TMPKILL ²	7	7	12	14	14	14

¹These cultivar names come from a set of 11 developed by Hudiburg et al. (2015); C2, C4, C6, C8, C11 are not shown here because they were not used in the current simulations.

²These parameters are ignored by DayCent when FRTINDEX==2, as it is for all of these cultivars, and are included here only for completeness.

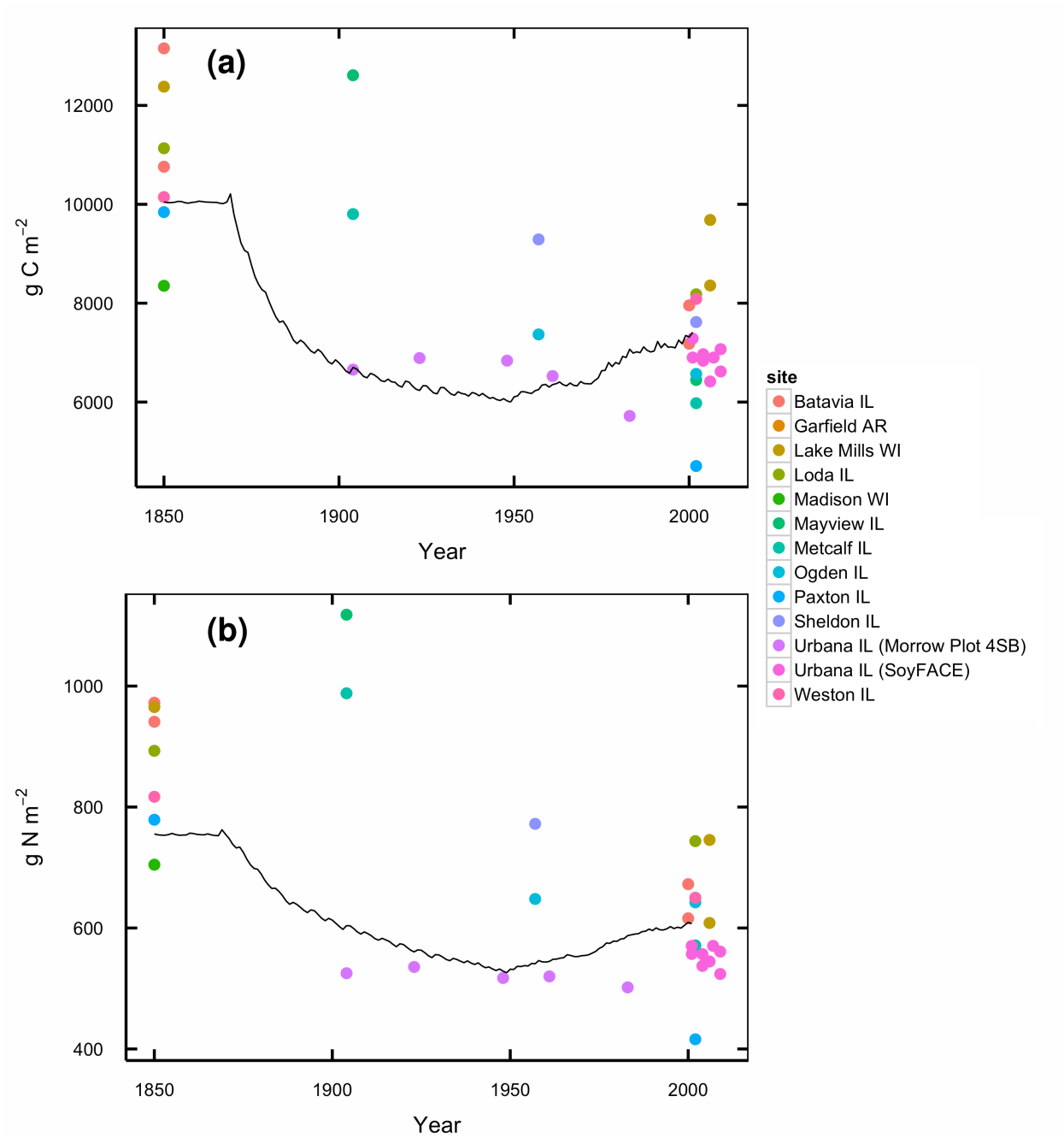


Figure 2.S1: Total organic C (a) and N (b) in soils under conversion from tallgrass prairie to agriculture. Lines show DayCent modeled soil C for the spin-up and historical agriculture phases of the model run. Points are observed SOC contents of prairie soils at comparable stages of similar management histories.

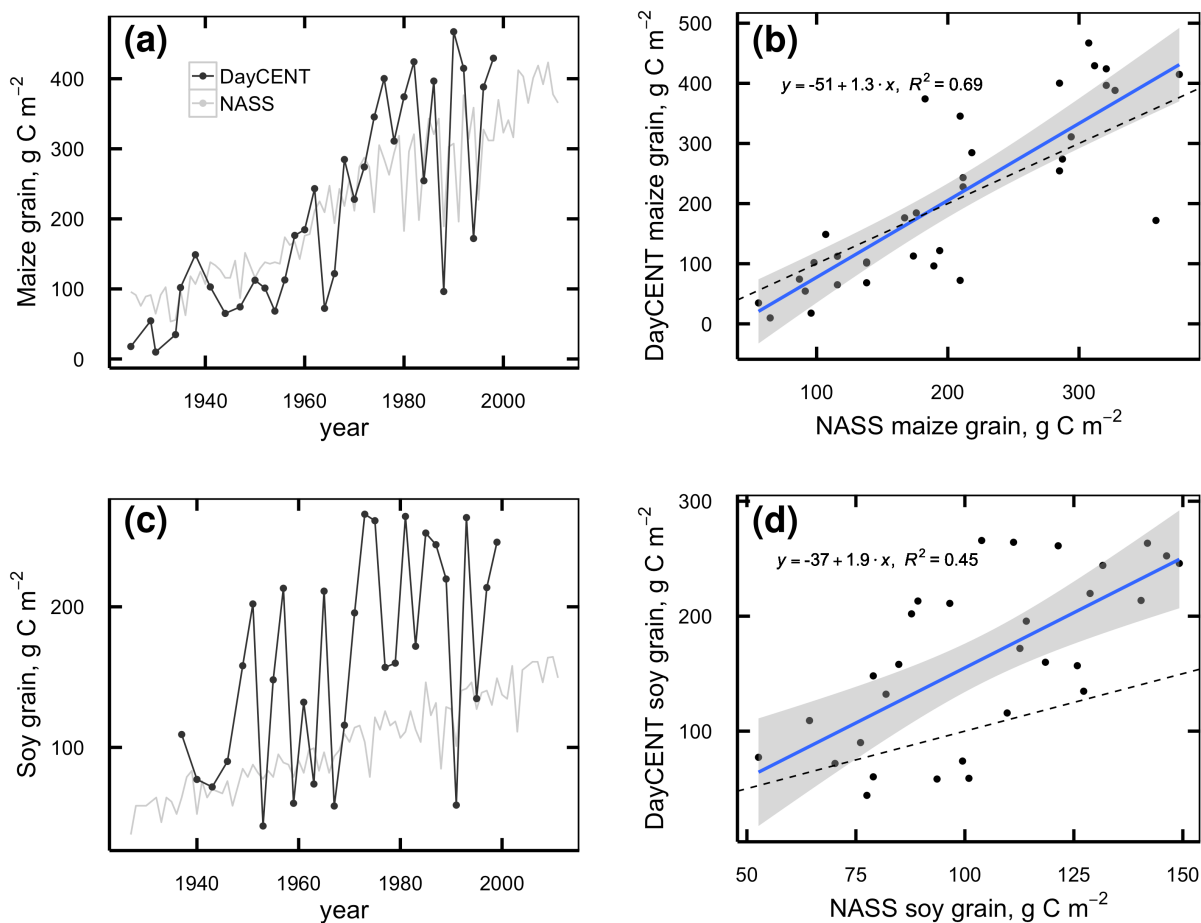


Figure 2.S2: a,c: Maize (a) and soybean (c) grain production simulated by DayCent (black lines) and Champaign County averages from NASS (grey lines). b,d, linear regression of DayCent vs. NASS maize (b) and soybean (d) yields.

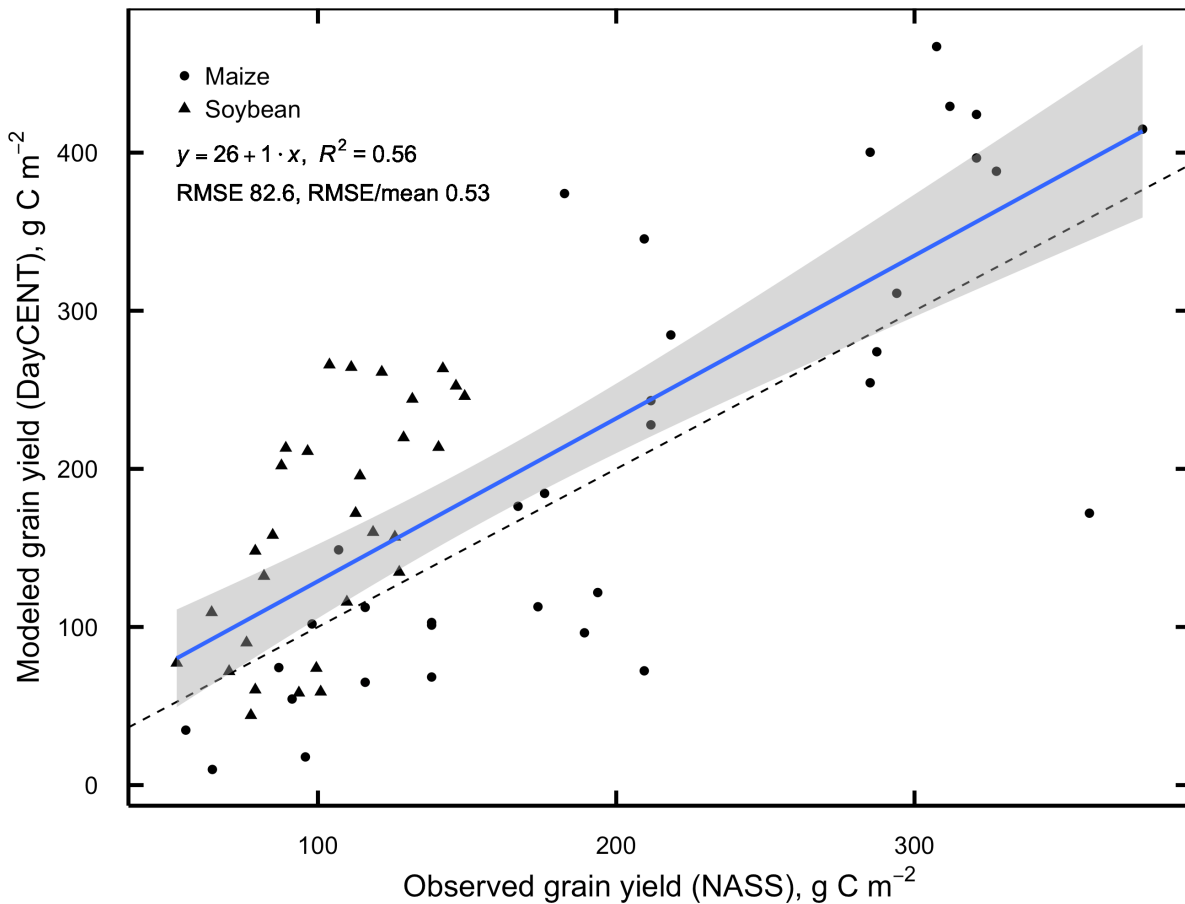


Figure 2.S3: Linear regression of DayCent vs. NASS grain yields for all years combined.

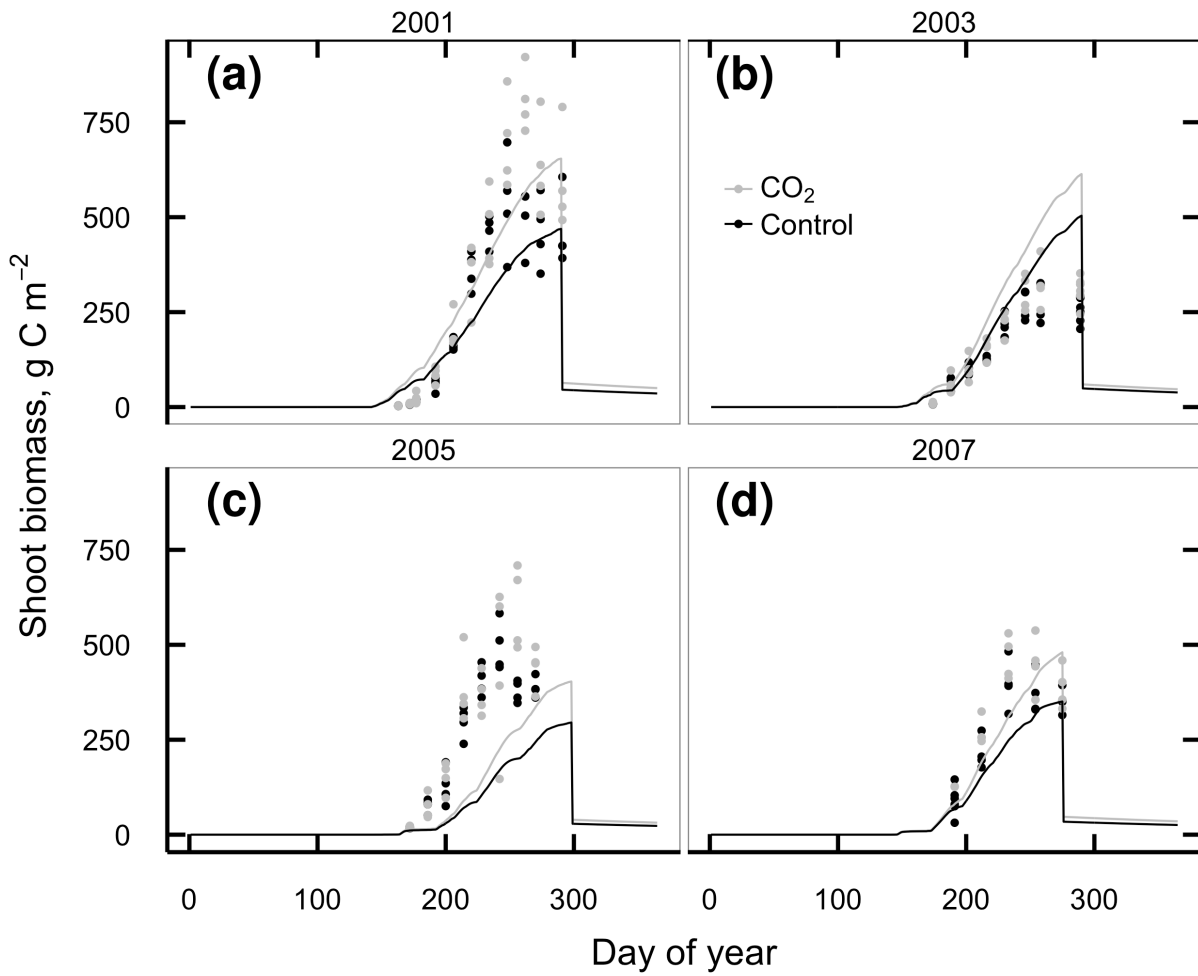


Figure 2.S4: Aboveground soybean biomass C observed at SoyFACE (dots) and simulated by DayCent in 2001 (a), 2003 (b), 2005 (c), and 2007 (d). Observations from 2003 include effects from a defoliating hailstorm on DOY 198 that is not simulated in the model.

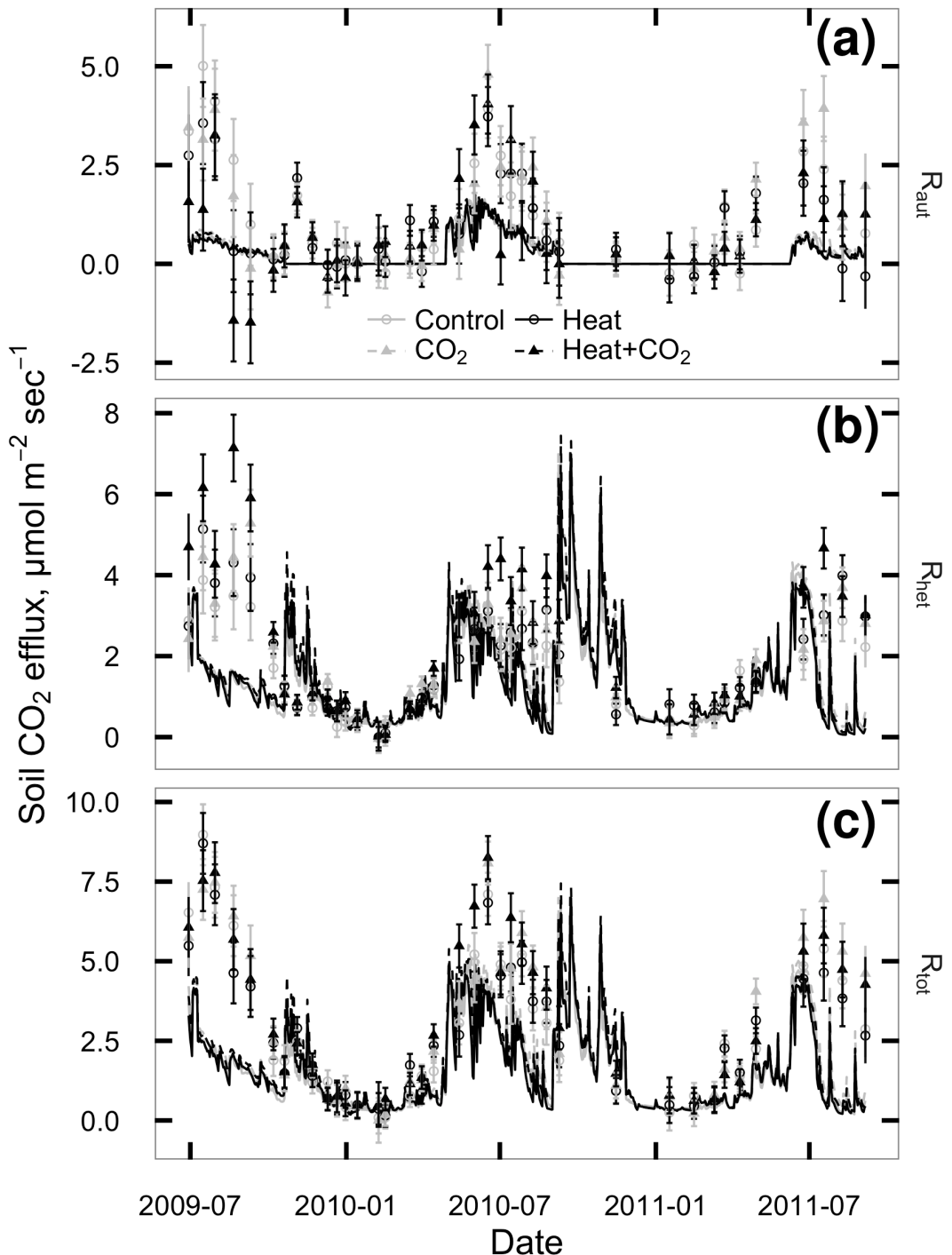


Figure 2.S5: CO_2 flux from plant roots and rhizosphere (R_{aut} ; a), soil heterotrophs (R_{het} ; b), and whole soil (R_{tot} ; c) at SoyFACE between June 2009 and October 2011. Symbols with error bars show observed treatment means ± 1 standard error for each day. Lines show values predicted by DayCent. Grey = unheated; Black = heated; Solid lines & unfilled circles = ambient CO_2 ; dashed lines & filled triangles = elevated CO_2 .

Chapter 3

Root volume distribution of maturing perennial grasses revealed by correcting for minirhizotron surface effects

Abstract

Root architecture is a key driver of plant ecology and physiology, but our current understanding of root placement in the soil profile is limited and biased by current detection methods. To better characterize the root placement and carbon-storage potential of land-use changes from conventional agriculture to perennial grass biofuels, we developed a statistical model to allow robust depth- and time-resolved measurements of standing root volume from minirhizotron images. By correcting for small sample sizes and near-surface underdetection effects, our Bayesian model explained 30% of the variation in observed root length and validated well against root mass from paired core samples. In their seventh growing season, all three perennial grasses (*Miscanthus × giganteus*, *Panicum virgatum*, and a community of 28 tallgrass prairie species) had 11-16 times more belowground biomass in total, and 2-17 times more mass at every individual depth from 0 to 128 cm, than annually tilled maize and soybean. Perennial crops showed little change in the proportion of root volume allocated to each soil layer through time, but total root volume increased through the five years of the experiment and appeared resilient to a historically hot and dry summer in 2012, suggesting that large-deep root systems helped these crops resist drought. Because the root systems produced by these grasses are large, deep, and persistent, conversion from row crops to perennial biofuel grasses is likely to sequester carbon in a large and potentially very stable soil pool.

Introduction

The placement of plant roots in the soil profile is an ecological trait that affects many ecosystem properties. Deeper roots provide structural support, give access to deep water and nutrient pools (Wasson et al. 2012, Zwicke et al. 2015), and store carbon (De Deyn et al. 2008). Meanwhile shallower roots are less costly, give access to larger but potentially less reliable water and nutrient pools (Lynch and Brown 2001, Hodge 2004, Nippert et al. 2012), and promote competitive success through root-zone exclusion (Genney et al. 2002). The existence of mycorrhizal associations lead to further tradeoffs between root architectures optimized for soil exploration by the root itself or by the mycorrhizal symbiont (Comas and Eissenstat 2009, Liu et al. 2015). Understanding root distributions is therefore fundamental to predicting ecosystem functioning (Bardgett et al. 2014) and improving management outcomes (Kochian 2016).

For the present study, we quantified root distribution in the context of evaluating the ecosystem-level effects on soil C cycling of a change in land use from annual row-crop agriculture to perennial grasses managed for biofuel production. Some researchers have suggested that biofuel grasses may build soil C because of their large root systems and minimal tillage requirements (Anderson-Teixeira et al. 2013, McCalmont et al. 2015, Agostini et al. 2015), and some have further proposed that any C gains from biofuel grasses may be especially persistent because of preferential allocation to deep soil and consequent slower turnover (Balesdent and Balabane 1996, Rasse et al. 2005, Kell 2011, Rumpel and Kögel-Knabner 2011, Agostini et al. 2015, Prieto et al. 2016, Ward et al. 2016). However, to evaluate this claim we need a better idea how much C is added, where it is distributed in the soil, and its turnover time (Agostini et al. 2015).

Understanding of root distributions is much less detailed than our understanding of aboveground traits. This lack of detail is exacerbated by notable drawbacks in the available methods of quantifying root systems (Pierret et al. 2005, Milchunas 2009, Topp et al. 2016). Pot effects mean container studies are only realistic for very small plants (Poorter et al. 2012). Destructive approaches such as coring and trenching give accurate snapshots, but require massive effort (hours to days per sample; Bohm et al. 1977) and cannot be repeated through time. Furthermore, because the effort required for coring and trenching increases rapidly with depth, many such surveys have focused only on the shallow soil layers (typically 30 cm or less), often leading to severe underestimates of deep root mass (Mokany et al. 2006). Imaging systems such as minirhizotrons give time-resolved data, but with the tradeoff that the data are noisier and indirect; the raw data are two-dimensional images that must be converted to a three-dimensional volume estimate and then converted again from a volume to a mass, with further possible noise and biases in the conversion (Metcalfe et al. 2007, Taylor et al. 2014).

Minirhizotron observations of standing root mass seem to be especially susceptible to depth biases; previous workers have often reported that minirhizotrons underdetected roots in the shallowest soil layers, probably because of movement of either the tube or the soil leading to poor contact between tube and soil in the least compacted and most frequently disturbed surface horizons (Bragg et al. 1983, Taylor et al. 1990, Parker et al. 1991, Samson and Sinclair 1994, Ephrath et al. 1999). Most previous workers who considered this bias have discarded data from the affected layers (potentially containing the majority of the root system; Samson and Sinclair 1994), used paired comparisons within layers, or equivalently developed depth-specific calibration factors. None of these approaches were satisfactory for us because we wanted to

compare both total root volume and the fraction of roots found in a given layer over time and among species.

In this study, we tracked the change in root volume associated with a change in management from annually tilled conventional row crops (maize and soybean) to untilled perennial grasses mowed annually for biofuel feedstock. We used minirhizotrons to track seasonal and interannual patterns in root distribution to a depth of >1 m, developed a statistical model to account for biases from underdetection and small samples, and verified our estimates with deep-soil core samples. We predicted that root volume under perennial grasses would be much higher than under row crops, that the root growth season would be longer, and that root systems would reach their maximum extents in the same year each crop achieved maturity as measured by aboveground yields.

Methods

Site

Measurements were made at the University of Illinois Energy Farm, ~5 km south of Urbana, Illinois (40.06N, 88.19W, elevation 220 m). Climate, soils, and site establishment have been described in detail elsewhere (Zeri et al. 2011, Smith et al. 2013, Masters et al. 2016). Briefly, the site has a highly seasonal continental climate with a mean annual temperature of 11 °C (below 0 °C December–February, over 20 °C June–August) and average annual precipitation of approximately 1 m, with approximately half falling as rain during the growing season (May–September). Soils are deep and loess-derived, mapped as Argiudolls of the Dana, Flanagan, and Blackberry series of silt loams. Four cropping treatments, each representative of a possible bioenergy cropping scheme, were established in 2008. The treatments were a three-year maize-

maize-soybean rotation that was tilled annually and managed in accordance with typical Central Illinois cropping practices, a prairie restoration mix of 28 native species (Zeri et al. 2011), and two perennial grasses: *Miscanthus × giganteus* Greef and Deuter ex Hodkinson and Renvoize (*Miscanthus*; cv “Illinois”) and *Panicum virgatum* L. (Switchgrass; cv “Cave-in-Rock”). The site was planted in a randomized complete block design replicated five times, with four blocks of 0.7 Ha plots and one block of 3.8 Ha plots (Masters et al. 2016). Each large plot was instrumented to record weather, crop growth parameters, and ecosystem C and water exchange.

Maize and soybeans were planted and harvested according to local practice. Switchgrass and prairie were planted in 2008 and not subsequently replanted; *Miscanthus* survived poorly the first winter and therefore the large *Miscanthus* plot was replanted in 2009. Standing biomass from perennials was mowed and baled after senescence each winter.

Maize was fertilized each year with 202 kg N Ha⁻¹ yr⁻¹ before planting; no fertilizer was applied to soybean. Switchgrass was fertilized with 56 kg N Ha⁻¹ yr⁻¹ applied before crop emergence. Initially, neither prairie nor *Miscanthus* were fertilized. In 2014 the small *Miscanthus* plots were split and one half of each 0.7 Ha plot remained unfertilized while the other half, and the entire 3.8 Ha plot, received 56 N Ha⁻¹. For all 2014 *Miscanthus* values, we report means averaged across fertilizer treatments.

Rhizotron tube installation and maintenance

To observe root systems over time, in May of 2009 we installed 96 clear acrylic minirhizotron tubes. We placed 24 tubes in each crop, with 4 tubes (one in each quadrant) per 0.7 Ha plot and 8 tubes (2 in each quadrant) per 3.8 Ha plot. Each tube was 1.8 m L × 51 mm ID × 57 mm OD (Bartz Technology corporation, Carpinteria CA USA) and was installed using a tractor-mounted hydraulic probe (Giddings Machine Co., Windsor, CO USA) at an angle 30°

from vertical (Bragg et al. 1983). For perennial crops, we placed tubes randomly within each quadrant. For maize and soybean, we placed half the tubes in each plot directly within rows and the other half midway between rows. Each tube's vertical angle was aligned along a row, so comparisons of root density between depths in a single tube were not confounded with row placement. Each tube was inserted until 22 cm remained aboveground or until it was stopped by soil resistance, allowing image collection from the soil surface to a depth between 115 and 140 cm. The aboveground portion of each tube was capped to minimize intrusion of light, water, or temperature swings.

Tubes in maize and soybean plots were installed immediately after planting every spring and removed after harvest to allow tillage. The tubes in perennial crops remained permanently installed, but each winter a portion of the permanent tubes developed leaks in their bottom end caps, and were replaced the following spring in a freshly bored hole at least 1 m away from the previous location. Of the original 72 tubes ‘permanently’ installed at the site, 39 survived to the end of the experiment in their initial location. Because of ongoing tube failures after repeated installation and a limited stock of replacement tubes, in 2014 we were only able to collect images from 8 tubes in maize, all in the 3.8 Ha block.

Image collection

From 2010 through 2013, we collected images approximately once a month during the growing season (May to October) using a portable minirhizotron camera (BTC-100x; Bartz Technology). In each session, we first used a long-handled swab to clean dust and condensation off the inner surface of the tube. We then mounted the camera into the tube and collected images at ~6-cm vertical increments until the camera reached the bottom of the tube (typically ~125 cm). Each tube's offset from the soil surface was remeasured periodically and used to correct

image depth estimates. The 6-cm vertical increment came from collecting images every five stops of the depth-indexing handle ($13.5 \text{ mm per stop} \rightarrow (5 \cdot 1.35)\cos(30^\circ) = 5.8 \text{ cm}$) and was chosen as the spacing that best balanced adequate sampling from each tube against the time required to process each image after collection (Johnson et al. 2001).

The resulting images were 754x510 pixels and the camera was calibrated daily by photographing a 1x1 mm grid attached to the outside of a short length of rhizotron tube (same viewing distance as the roots). The final maximum image resolution was $\sim 0.025 \text{ mm per pixel}$.

Image processing

In the laboratory, we recorded the length and diameter of every visible root segment by manual tracing using WinRhizo TRON MF v. 2009a (Regent Instruments, Québec QC, Canada) and performed all downstream analyses on the total volume of root visible in each image assuming each root segment was a perfect conic section with dimensions ($\text{Diameter}_{\text{start}} \times \text{Diameter}_{\text{end}} \times \text{length}$). Rhizotron methods have low success distinguishing living from dead root tissue (Iversen et al. 2011), so we made no attempt to classify tissue death status. Thus all our root density estimates include visible root necromass.

To minimize human variation in tracing, all technicians were trained using the same set of representative images and the agreement in traced root volume from each image was taken as an estimate of the variation among workers given the same task. The variation among workers was less than the within-worker variation (95% intervals: $\text{sd among workers} = 1.2\text{-}1.6 \text{ mm}^3 \text{ img}^{-1}$, $\text{sd within worker} = 2.4\text{-}2.7 \text{ mm}^3 \text{ img}^{-1}$; data not shown), indicating that technician identity was a minor contributor to the variation in the tracing step. Since these agreement scores were taken from novice tracers immediately after the completion of their training, it is likely that they somewhat overstate the actual variation from experienced technicians.

After tracing, each season's data were aggregated using a set of custom R scripts to adjust observed root volumes for differences in image magnification, remove data from images with poor image quality, convert locations within each tube to depths below the soil surface, and aggregate results across experimental blocks. The full data and all scripts are available online (<https://github.com/infotroph/efrhizo>).

Root mass measurements

To compare estimates of root density from minirhizotrons and destructive coring methods, we collected deep-soil cores. In August of 2011 and of 2014, when aboveground biomass of all four crops was near its yearly maximum, we collected soil cores to a depth ≥ 100 cm from 24 locations within each crop (4 from each 0.7 Ha plot, 8 from each 3.8 Ha plot) using a tractor-mounted hydraulic corer (Giddings Machine Co.). Because the heavy coring equipment necessitated trampling a large (~2-3 m) quadrat at every location, coring locations were all within 3 m of a plot edge. At each location, three 3.8 cm diameter cores were collected from within a 1-m area. We divided each core into five depth horizons (0-10, 10-30, 30-50, 50-100, and 100+ cm), pooled horizons from the same location, then separated root and rhizome material from soil by hydropneumatic elutriation (Roberts et al. 1993), separated rhizomes from roots by hand-sorting, oven-dried both to constant mass, and weighed them.

Since individual locations within a plot are pseudoreplicates, we calculated block means of root mass per cm^3 soil (for depth-resolved analyses) or per m^2 ground area (for whole-profile totals), log-transformed the result, then fitted a mixed-effects linear model where $\ln(\text{depth})$ is a continuous covariate, crop and year are categorical fixed effects (Equation 3.1), block is a categorical random effect (Equation 3.2), and residuals follow a first-order autoregressive

function within each level of the (block by crop by year) interaction to account for the autocorrelation between adjacent depths (Equation 3.3).

$$\ln(y_{ijk\ell}) = \beta_i \text{crop}_i + \beta_j \text{year}_j + \beta_k \ln(\text{depth}_k) + \gamma_\ell \text{block}_\ell + \epsilon_{ijk\ell} \quad (3.1)$$

$$\gamma_\ell \sim N(0, \psi_{ijk}^2) \quad (3.2)$$

$$\epsilon_{ijk\ell} \sim N(0, \sigma^2 \lambda_{ijk\ell}), \text{corr}(\epsilon_{ijkl}, \epsilon_{ijk\ell'}) \sim \phi^{|\ell' - \ell|} \quad (3.3)$$

All root core statistics were performed in R version 3.3.0 (R Core Team 2016) using nlme 3.1 (Pinheiro et al. 2016) for linear model fits followed by lsmeans 2.23 (Lenth 2016) for predicted marginal means and post-hoc treatment comparisons. The data from 2011 have been presented previously (Anderson-Teixeira et al. 2013); we limit our discussion here to the comparison against simultaneously collected rhizotron images from the same plots.

Bayesian modeling of root volume

To convert root areas estimated with error from minirhizotron images into an estimate of root volume distribution across depth, we used a Bayesian model to integrate image data with prior knowledge about plant architecture and growth patterns to produce a mathematically tractable and physiologically defensible estimate of root density in each crop. The basic structure of the model was formulated by Sonderegger et al. (2013) for root production estimates; we adopt it here with modifications to estimate standing root volume.

We began with a log-linear mixed model of root volume (mm^3 root observed per mm^2 of image traced) similar to the one used for root mass from cores (Equation 3.1). On a given sampling day, the expected log root density μ_{ijk} (Equation 3.4) declines with log depth according to a crop-specific intercept α_i and slope β_i , and the intercept varies for each sampling location (i.e. minirhizotron tube) as a zero-centered random effect $\gamma_j \sim N(0, \sigma^{\text{tube}})$:

$$\mu_{ijk} = \alpha_i + \gamma_j + \beta_i \ln(\text{depth}_k) + \epsilon_i. \quad (3.4)$$

We treated individual minirhizotron tubes as the unit of replication (rather than block means as in the core data) because the observed variation among individual minirhizotron tubes was much larger than the variation among blocks and therefore subsumes the block effects; it should be possible to calculate the block effect, if it is needed, as the mean of the estimated tube effect coefficients of all tubes in that block.

Next, we added an empirical correction for reduced minirhizotron root detection efficiency near the soil surface. The cause of this underdetection is still unclear, but it is commonly observed in minirhizotron studies (Bragg et al. 1983, Taylor et al. 1990, Samson and Sinclair 1994, Ephrath et al. 1999, Gray et al. 2016). We corrected for this underdetection by noting that when measured directly it appears to be sigmoid with depth, and when not measured it can be inferred by a visible deviation from the log-linear depth trend in near-surface layers, meaning the correction can be found by solving for a sigmoid underdetection function that brings near-surface observations back toward the linear depth model of Equation 3.4. Then the expected density of *detected* roots $\hat{\mu}$ (Equation 3.5) is:

$$\hat{\mu}_{ijk} = \mu_{ijk} \text{logistic}(\alpha_i^{\text{surface}} + \beta_i^{\text{surface}} \text{depth}_k), \quad (3.5)$$

where $\alpha_i^{\text{surface}}$ is the depth at which 50% of roots are detected, β_i^{surface} scales the rate of detection increase with depth, and both are estimated from observations but strongly informed by prior research (Supplement 3.S1).

Finally, we noted that individual images are small ($\sim 240 \text{ mm}^2$) compared to the scale of root system heterogeneity, and many images contain no visible roots even when root density is high. The observed root volume in an individual image (Equation 3.6) therefore follows a mixture distribution (Sonderegger et al. 2013):

$$y_{ijk} \sim \begin{cases} 0, & \text{with probability } 1 - \phi_{ijk} \\ \log\mathcal{N}(\hat{\mu}_{ijk}, \sigma^2), & \text{with probability } \phi_{ijk} \end{cases} \quad (3.6)$$

where the probability ϕ_{ijk} of observing any roots (Equation 3.7) increases with expected root density $\hat{\mu}_{ijk}$ (Equation 3.5) as

$$\text{logit}(\phi_{ijk}) = \alpha^{\text{detect}} + \beta^{\text{detect}} \hat{\mu}_{ijk}. \quad (3.7)$$

We fitted this model separately to each day of data using the Rstan (Stan Development Team 2016a) interface to the Stan probabilistic programming language (Stan Development Team 2016b), which computes the joint likelihood of all model parameters given the observed data and uses Hamiltonian Monte Carlo sampling to draw from their posterior distributions. For each model, we ran five independent chains for 5000 iterations each, then discarded the first 1000 iterations as warmup, giving a total of 20000 Monte Carlo samples for each parameter and an effective posterior sample size (after accounting for autocorrelation) of at least 1000. We checked for convergence both visually by plotting the chains and by checking that the potential scale reduction factor was close to 1.0 (Gelman and Rubin 1992). All scripts needed to reproduce the analysis are available online (<https://github.com/infotroph/efrhizo>).

Results

Soil core samples

Perennials produced far more root biomass than maize, and the difference became larger as the perennials matured (Figure 3.1). The belowground biomass of the perennial grasses in core samples increased dramatically from 2011 to 2014 ($F_{1,28} > 66$; $p < 0.01$), from 5-8 times greater than maize in 2011 whether measured as roots or as total biomass (Anderson-Teixeira et al. 2013) to 8-11 (root alone) or 11-16 (root+rhizome) times greater than maize in 2014 (Figure 3.1;

all Tukey $t_{28} > 7$; all $p << 0.01$). When we considered roots alone there was an interaction between year and crop, with increases for *Miscanthus* and prairie (both more than tripled from 2011 to 2014; $t_{28} > 5.5$, $p << 0.01$) but not for maize or switchgrass (root mass was greater by 62% and 76% respectively, but the difference was not significant after correcting for multiple comparisons; $t_{28} < 2.8$; $p > 0.15$). When we considered total root+rhizome biomass, the year-over-year changes were similar in magnitude to those for roots alone, but the variability was greater and the year by crop interaction was not significant ($F_{3,28}=2.2$; $p > 0.1$).

There were no statistically resolvable differences in belowground biomass among perennials in either year (all Tukey $t_{28} < 1.6$; $p > 0.4$), but the rank order of total mass depended on the year and the pool measured because of increases in rhizome mass. In 2011 switchgrass had the greatest mass (860 ± 126 g root m^{-2} , no rhizomes detected) and *Miscanthus* was second for total biomass (819 ± 130 g root+rhizome m^{-2}) but third for roots alone (535 ± 79 g root m^{-2}), while in 2014 prairie had the greatest root mass (1924 ± 282 g root m^{-2}) but *Miscanthus* had the greatest total mass (2793 ± 444 g root m^{-2}). For comparison, maize root mass was 109 ± 17 (2011) and 177 ± 26 (2014) g root m^{-2} (Figure 3.1).

Biomass in core samples declined approximately log-linearly with depth (Figure 3.2), but the distribution of biomass through the soil profile varied by species ($F_{3,180} = 8.69$, $p << 0.01$). Prairie roots were more concentrated near the surface and declined more quickly with depth than *Miscanthus* or maize ($t_{180} > 3.5$; $p < 0.01$). The decline in switchgrass was intermediate between prairie and maize and not significantly different from either one (all $t_{180} < 2.6$; $p > 0.05$), although the comparison with prairie was marginal in 2014 ($t_{180} = 2.59$; $p = 0.0501$), and switchgrass declined more quickly than *Miscanthus* in 2011 ($t_{180} = 3.50$; $p < 0.01$) but not in 2014 ($t_{180} = 1.02$, $p = 0.69$). When we modeled total root+rhizome biomass instead of roots

alone, the slope by year interaction became significant ($F_{1,180} = 4.99$, $p < 0.05$), with the mass of all crops declining more with depth in 2014 than in 2011. With rhizome mass included there were no statistically resolvable differences in slope among perennials in either year, but *Miscanthus* and switchgrass changed from similar to maize in 2011 ($t_{180} < 1.9$; $p > 0.2$) to greater declines in 2014 ($t_{180} > 2.9$, $p < 0.02$) because of dramatic increases in rhizome biomass near the surface.

Despite the observation that root biomass for maize was more evenly distributed through the soil profile (less negative slope terms) than the perennial crops, the root mass of perennials at any given depth was greater than that of maize even at the bottom of the soil profile (Figure 3.1). Perennials had 2-17 times more root biomass than maize (post-hoc contrasts on fitted LS means; $t_{180} > 3$; $p << 0.01$) all the way to 128 cm, the mean maximum depth of our core samples, with the exception that in 2011 the difference between prairie and maize was marginal at depths greater than 1 m ($t_{180} < 2.6$; $0.05 < p < 0.1$).

Minirhizotron images: model evaluation

The Bayesian model of root distribution compensated well for poor surface root detection by the minirhizotron, explained ~30% of the total variance in log root volume, and showed little bias: 90% prediction intervals for individual images included the observed value 90% of the time, and 50% intervals about 50% of the time, indicating that both the mean and variance components were consistent with the data (Figure 3.S1).

Much of the remaining ~70% of variation is attributable to the inherent variability among source images and could be reduced by aggregating multiple images before testing model fit, but this is prevented by the model structure. After incorporating detection and surface effects, model predictions are in units of expected *corrected* root volume and their means can no longer be

compared directly against the observed means of raw images, meaning the direct comparison of observed vs. predicted values is only valid at the level of individual images. Although the model structure prevents a quantitative comparison, qualitatively the shape of the depth function and the ranking of species differences agreed well with the patterns seen in soil cores (Figure 3.3), and did not show the reduction in near-surface root volume observed in the raw images. The model treated the variance from individual minirhizotron tubes σ^{tube} and the detection probability parameters a^{detect} and b^{detect} as identical across crops, while the intercept, slope, surface underdetection parameters α^{surface} and β^{surface} , and residual variance σ , were fit separately for each crop. Half-detection depths (α^{surface} ; the estimated depth where the surface underdetection effect reduces to observations 50% of true root volume) ranged from 1 to 36 cm in maize, 14-35 in *Miscanthus*, 9-24 in switchgrass, and 11-26 in prairie, and tended to be greatest in midseason. We also attempted to fit an alternate model with α^{surface} and β^{surface} identical across all crops, but encountered numerical difficulties and lack of sampler convergence that suggested a very poor model fit (data not shown).

Although the model predicts root *volume* per area of image rather than root mass directly, predicted root volume for midsummer 2011 and 2014 scaled positively and log-linearly against simultaneously collected root masses from coring (Figure 3.S3) and overlapped with the values expected from a simple conversion based on previous research. If root volume per image area = (root mass)(depth of view)/(root tissue density), the dashed lines in Figure 3.S3 show the root volume expected from core mass assuming 0.78 mm depth of view (Taylor et al. 2014) and root tissue densities of 0.08 g cm⁻³ for maize (Pahlavanian and Silk 1988), 0.20 for *Miscanthus* (Wahl and Ryser 2000, Roumet et al. 2006, Picon-Cochard et al. 2012), 0.19 for switchgrass (Craine et al. 2001) and 0.15 for prairie (Craine et al. 2001). With the exceptions of maize (0%) and

Miscanthus (45%) in 2011, model predictions accounted for at least 75% of the variation in block means of root mass from cores (Figure 3.S3).

Minirhizotron images: changes in root distribution through time

Across the five years of the experiment, all three perennials increased their root volume (95% intervals for 2010 and 2014 model intercepts did not overlap; Figure 3.S2), while maize and soybean did not (95% intervals overlapped; Figure 3.S2), even though both annuals and perennials had the numerically lowest midsummer root volume in 2010 and the highest in 2014 (Figure 3.3).

The distribution of root volume with depth showed little change over time. Prairie roots were more concentrated near the surface in 2014 than in either 2011 or 2012 (slope term was more negative; 95% intervals do not overlap; Figure 3.S2) but no other crop showing detectable changes from year to year. Intriguingly, though, maize, *Miscanthus*, and prairie all showed their most even distribution and widest uncertainty intervals in 2012, a very hot drought year. This change can be seen in the predicted depth profiles as a reduction in near-surface root volume in maize, *Miscanthus*, and prairie, but no apparent change was seen in switchgrass (Figure 3.3).

When we followed root volume from month to month within individual growing seasons, the perennials showed strong seasonal changes in 2010 but did not change from month to month in 2012. In 2010 root volume under all four crops was higher in August than either May or October (95% intervals for intercept term do not overlap; Figure 3.S2). In soybean the distribution of roots in the soil also changed, with root volume strongly decreasing with depth in June and July but essentially vertical from midsummer through senescence (Figure 3.4; slope interval overlapped zero in August and October; Figure 3.S2). In contrast, root volume in the perennial crops rose from June through August and dropped again in October, but the depth

distribution did not change substantially except in *Miscanthus*, where roots were more concentrated near the surface in July than in August (Figure 3.4; Figure 3.S2). In 2012, maize root volume increased from May through August (Figure 3.S2), but shifted its distribution dramatically from roots concentrated very near the surface in the first three observations to evenly distributed across depths in August (Figure 3.5). The 2012 maize crop senesced in August because of drought and was harvested in September, so no images were collected from maize in October. All three perennials, by contrast, were consistent in both total root volume and in depth distribution throughout the season. All three appeared to slightly reduce near-surface root volume late in the season (Figure 3.5), but these changes were not statistically resolvable except in prairie, where roots were concentrated nearer the surface in May than in either early August or October (Figure 3.S2).

Discussion

In repeated observations of four crop systems, we observed much more root both by mass and by volume in perennial grasses than in annual maize-soybean. The root systems of the perennials continued expanding across five years of observations, appeared resilient to a major drought, and allocated large quantities of carbon to the deep subsoil. By explicitly correcting for depth-dependent detection biases, we found good agreement between minirhizotron and core-based measurements of root mass, which may allow nondestructive monitoring of root structure and C stocks in familiar units. The combination of greatly increased root mass and allocation deep in the soil suggest that conversion from row cropping to perennial grass biofuels could result in large-scale soil C increases.

Our measured root masses agree well with previous work that shows much larger root systems in perennial grasses than in annual crops, and that root mass stays high even during the spring and fall when annual fields are fallow. We observed switchgrass root masses comparable to those from other stands of similar age that were sampled to a depth of ≥ 90 m (Frank et al. 2004, Monti and Zatta 2009, Collins et al. 2010, Garten et al. 2010, Dohleman et al. 2012) and higher than those sampled to shallower depths (Bransby et al. 1998). *Miscanthus* root masses were comparable but generally at the high end of totals seen in other studies (Neukirchen et al. 1999, Beuch et al. 2000, Christian et al. 2006, Monti and Zatta 2009, Amougou et al. 2011, Dohleman et al. 2012) and the values reported by other studies are highly correlated with sampling depth. *Miscanthus* rhizome mass, by contrast, was comparable but generally at the low end of totals seen in other studies, comparable to previous work on crops of similar ages (Beuch et al. 2000, Christian et al. 2006, Amougou et al. 2011, Dohleman et al. 2012). Taken together, this suggests that *Miscanthus* invested especially heavily in roots over rhizomes at our highly fertile, deep-soil site. The minirhizotron method never detected rhizomes, so all image-based results should be considered to show root volume only.

We expected that root development would approximately parallel aboveground stand development, with belowground biomass nearing steady state in year 3-4. Instead, perennials explored the whole soil profile very early in development (we detected roots beyond 126 cm even in the first imaging sessions) but their root volume continued to increase through the whole period of the study even after each crop reached maximum aboveground biomass (2010-2012; Joo et al. 2016). This increase was especially evident in the prairie treatment, which consistently had the lowest aboveground productivity among our four crop systems (Anderson-Teixeira et al. 2013) but reached 608 ± 89 g root m^{-2} by 2011 and 1924 ± 306 g root m^{-2} by 2014 (Figure 3.1),

making the root mass of this prairie comparable to 20-year-old restorations in its fourth year and, remarkably, comparable in its seventh year to undisturbed native prairie remnants (Kucharik et al. 2006, Matamala et al. 2008, Jelinski et al. 2011).

During the unusually hot and dry summer of 2012, both *Miscanthus* and switchgrass maintained essentially the same root volume and depth distribution as other years, while maize and prairie shifted from shallower to deeper roots as the season progressed. This may reflect a difference in ecological drought resilience strategies, with both *Miscanthus* and switchgrass apparently able to access deep soil water and maintain growth through the drought. Although measurements of net ecosystem exchange suggest that our *Miscanthus* may have suffered some delayed consequences of 2012 drought stress in the form of reduced 2013 productivity (Joo et al. 2016), we saw no negative effects on root volume. By contrast, Mann et al (2013) reported very shallow root systems and severe biomass reductions from young *Miscanthus* grown in water-limited mesocosms while young switchgrass explored deep soil whether irrigated or water-limited. The difference between these results and ours may indicate that mature, established deep roots are crucial to *Miscanthus* drought resistance. It is probable that the shift in prairie root distribution came from changes in relative dominance of species with different rooting habits rather than from individual species reallocating mass within the soil profile, but this is speculative because the minirhizotron images do not allow us to distinguish among roots of different species. Furthermore, the presence of deep roots from a particular species is not necessarily sufficient for effective access to deep soil water (Nippert et al. 2012).

By modeling the root distribution as a log-linear function of depth and explicitly estimating two forms of detection noise (zeroes from small samples and bias from the surface underdetection effect), we gained sensitivity to detect changes in root volume that would have

been invisible in a conventional minirhizotron analysis of root length density. However, this method has some limitations. It requires a large sample size (probably at least 15-20 tubes per treatment) to achieve reasonable precision, especially for the underdetection parameter estimates. In particular, estimates of the surface underdetection factor are positively correlated with model slope, so the model requires enough data from deep soil (where the underdetection factor is zero) to accurately separate these effects. In our data this was especially visible early in 2012, when few maize roots were present below the surface layers and therefore the model predicted unrealistically high maize root density in the surface layers (Figure 3.5).

Previous work on the underdetection of near-surface roots by minirhizotron images has usually concluded that the underdetection is similar across species (Ephrath et al. 1999). Our model differs by estimating the correction separately for each crop; we tested an alternate model with a common correction factor, but found that it fit poorly and frequently overestimated near-surface root volume in maize and soybean. It is possible that this difference can be explained as a difference in time since tube installation: We re-installed the minirhizotron tubes in maize-soybean each year but left the perennial tubes in place. Consistent with this hypothesis, we note that the estimated correction factor differed more between maize-soybean and perennials than it did among perennials, but we cannot test for time effects in more detail because installation time and crop are confounded in our experimental design.

We also emphasize that our conversion from root volume to mass (Figure 3.S3) is based solely on mean root tissue densities from the literature; it assumes constant tissue density across depth, root age and size class, and plant development stage. This assumption was necessary because few depth- and time-resolved reports of tissue density are available. Indeed, what evidence we do have suggests variation in tissue density across all of these factors (Craine et al.

2003, Bernier et al. 2005, Monti and Zatta 2009, de Vries et al. 2016). The precision of rhizotron-based root mass estimates could likely be improved by incorporating more specific tissue density conversions when they are available.

Overall we found that perennial biofuel grasses consistently had many more roots than maize and soybean at every depth, and the deep soil layers (> 50 cm) contained more perennial roots than were present in the entire soil profile under maize or soybean. This deep rooting appears to be important for resilience to summer drought, and is also a large flux of carbon into stable, rarely disturbed soil. Consistent with strongly negative net ecosystem carbon balance for perennial crops compared to positive values for maize-soybean rotation (Zeri et al. 2011), we therefore speculate that the conversion from row crops to perennial biofuel grasses may result in large and persistent increases in soil C storage.

Acknowledgements

We are grateful to R. J. Cody Markelz, John Brehm, and Laurel Brehm for statistical advice, and to Abishek Pal, Christopher Sligar, Edwin Albrarran, Jacob Rosenthal, Michael Donovan, and Taylor Wright for their endless patience performing the root tracing. This research was funded by the Energy Biosciences Institute.

References

Agostini, F., A. S. Gregory, and G. M. Richter. 2015. Carbon sequestration by perennial energy crops: is the jury still out? BioEnergy Research 8:1057–1080.

- Amougou, N., I. Bertrand, J.-M. Machet, and S. Recous. 2011. Quality and decomposition in soil of rhizome, root and senescent leaf from *Miscanthus x giganteus*, as affected by harvest date and N fertilization. *Plant and Soil* 338:83–97.
- Anderson-Teixeira, K. J., M. D. Masters, C. K. Black, M. Zeri, M. Z. Hussain, C. J. Bernacchi, and E. H. DeLucia. 2013. Altered belowground carbon cycling following land-use change to perennial bioenergy crops. *Ecosystems* 16:508–520.
- Balesdent, J., and M. Balabane. 1996. Major contribution of roots to soil carbon storage inferred from maize cultivated soils. *Soil Biology and Biochemistry* 28:1261–1263.
- Bardgett, R. D., L. Mommer, and F. T. De Vries. 2014. Going underground: root traits as drivers of ecosystem processes. *TRENDS in Ecology and Evolution* 29:692–699.
- Bernier, P. Y., G. Robitaille, and D. Rioux. 2005. Estimating the mass density of fine roots of trees for minirhizotron-based estimates of productivity. *Canadian Journal of Forest Research* 35:1708–1713.
- Beuch, S., B. Boelcke, and L. Belau. 2000. Effect of the organic residues of *Miscanthus × giganteus* on the soil organic matter level of arable soils. *Journal of Agronomy and Crop Science* 183:111–119.
- Bohm, W., H. Maduakor, and H. M. Taylor. 1977. Comparison of five methods for characterizing soybean rooting density and development. *Agronomy Journal* 69:415–419.
- Bragg, P. L., G. Govi, and R. Q. Cannell. 1983. A comparison of methods, including angled and vertical minirhizotrons, for studying root growth and distribution in a spring oat crop. *Plant and Soil* 73:435–440.
- Bransby, D. I., S. B. McLaughlin, and D. J. Parrish. 1998. A review of carbon and nitrogen balances in switchgrass grown for energy. *Biomass & Bioenergy* 14:379–384.

- Christian, D. G., P. R. Poulton, A. B. Riche, N. E. Yates, and A. D. Todd. 2006. The recovery over several seasons of ^{15}N -labelled fertilizer applied to *Miscanthus* \times *giganteus* ranging from 1 to 3 years old. *Biomass & Bioenergy* 30:125–133.
- Collins, H. P., J. L. Smith, S. Fransen, A. K. Alva, C. E. Kruger, and D. M. Granatstein. 2010. Carbon sequestration under irrigated switchgrass (*Panicum virgatum* L.) production. *Soil Science Society of America Journal* 74:2049–2058.
- Comas, L. H., and D. M. Eissenstat. 2009. Patterns in root trait variation among 25 co-existing North American forest species. *New Phytologist* 182:919–928.
- Craine, J. M., J. Froehle, D. G. Tilman, D. A. Wedin, and F. S. Chapin III. 2001. The relationships among root and leaf traits of 76 grassland species and relative abundance along fertility and disturbance gradients. *Oikos* 93:274–285.
- Craine, J. M., D. A. Wedin, F. S. Chapin III, and P. B. Reich. 2003. The dependence of root system properties on root system biomass of 10 North American grassland species. *Plant and Soil* 250:39–47.
- De Deyn, G. B., J. H. C. Cornelissen, and R. D. Bardgett. 2008. Plant functional traits and soil carbon sequestration in contrasting biomes. *Ecology Letters* 11:516–531.
- de Vries, F. T., C. Brown, and C. J. Stevens. 2016. Grassland species root response to drought: consequences for soil carbon and nitrogen availability. *Plant and Soil* 10.1007/s11104-016-2964-4.
- Dohleman, F. G., E. A. Heaton, R. A. Arundale, and S. P. Long. 2012. Seasonal dynamics of above- and below-ground biomass and nitrogen partitioning in *Miscanthus* \times *giganteus* and *Panicum virgatum* across three growing seasons. *Global Change Biology Bioenergy* 4:534–544.

- Ephrath, J. E., M. Silberbush, and P. Berliner. 1999. Calibration of minirhizotron readings against root length density data obtained from soil cores. *Plant and Soil* 209:201–208.
- Frank, A. B., J. D. Berdahl, J. D. Hanson, M. A. Liebig, and H. A. Johnson. 2004. Biomass and carbon partitioning in switchgrass. *Crop Science* 44:1391–1396.
- Garten, C. T., Jr, J. L. Smith, D. D. Tyler, J. E. Amonette, V. L. Bailey, D. J. Brice, H. F. Castro, R. L. Graham, C. A. Gunderson, R. C. Izaurralde, P. M. Jardine, J. D. Jastrow, M. K. Kerley, R. R. Matamala, M. A. Mayes, F. B. Metting, R. M. Miller, K. K. Moran, W. M. Post III, R. D. Sands, C. W. Schadt, J. R. Phillips, A. M. Thomson, T. Vugteveen, T. O. West, and S. D. Wullschleger. 2010. Intra-annual changes in biomass, carbon, and nitrogen dynamics at 4-year old switchgrass field trials in west Tennessee, USA. *Agriculture, Ecosystems & Environment* 136:177–184.
- Gelman, A. 2006. Prior distributions for variance parameters in hierarchical models (comment on article by Browne and Draper). *Bayesian Analysis* 1:515–534.
- Gelman, A., and D. B. Rubin. 1992. Inference from iterative simulation using multiple sequences. *Statistical Science* 7:457–472.
- Genney, D. R., I. J. Alexander, and S. E. Hartley. 2002. Soil organic matter distribution and below-ground competition between *Calluna vulgaris* and *Nardus stricta*. *Functional Ecology* 16:664–670.
- Gray, S. B., O. Dermody, S. P. Klein, A. M. Locke, J. M. McGrath, R. E. Paul, D. M. Rosenthal, U. M. Ruiz-Vera, M. H. Siebers, R. Strellner, E. A. Ainsworth, C. J. Bernacchi, S. P. Long, D. R. Ort, and A. D. B. Leakey. 2016. Intensifying drought eliminates the expected benefits of elevated carbon dioxide for soybean. *Nature Plants* 2:16132.

- Hodge, A. 2004. The plastic plant: root responses to heterogeneous supplies of nutrients. *New Phytologist* 162:9–24.
- Iversen, C. M., M. T. Murphy, M. F. Allen, J. Childs, D. M. Eissenstat, E. A. Lilleskov, T. M. Sarjala, V. L. Sloan, and P. F. Sullivan. 2011. Advancing the use of minirhizotrons in wetlands. *Plant and Soil* 352:23–39.
- Jelinski, N. A., C. J. Kucharik, and J. B. Zedler. 2011. A test of diversity-productivity models in natural, degraded, and restored wet prairies. *Restoration Ecology* 19:186–193.
- Johnson, M. G., D. T. Tingey, D. L. Phillips, and M. J. Storm. 2001. Advancing fine root research with minirhizotrons. *Environmental and Experimental Botany* 45:263–289.
- Joo, E., M. Z. Hussain, M. Zeri, M. D. Masters, J. N. Miller, N. Gomez-Casanovas, E. H. DeLucia, and C. J. Bernacchi. 2016. The influence of drought and heat stress on long-term carbon fluxes of bioenergy crops grown in the Midwestern USA. *Plant Cell and Environment* 39:1928–1940.
- Kell, D. B. 2011. Breeding crop plants with deep roots: their role in sustainable carbon, nutrient and water sequestration. *Annals of Botany* 108:407–418.
- Kochian, L. V. 2016. Root architecture. *Journal of Integrative Plant Biology* 58:190–192.
- Kucharik, C. J., N. J. Fayram, and K. N. Cahill. 2006. A paired study of prairie carbon stocks, fluxes, and phenology: comparing the world's oldest prairie restoration with an adjacent remnant. *Global Change Biology* 12:122–139.
- Lenth, R. V. 2016. Least-squares means: The R package lsmeans. *Journal of Statistical Software* 69:1–33.

- Liu, B., H. Li, B. Zhu, R. T. Koide, D. M. Eissenstat, and D. Guo. 2015. Complementarity in nutrient foraging strategies of absorptive fine roots and arbuscular mycorrhizal fungi across 14 coexisting subtropical tree species. *New Phytologist* 208:125–136.
- Lynch, J. P., and K. M. Brown. 2001. Topsoil foraging – an architectural adaptation of plants to low phosphorus availability. *Plant and Soil* 237:225–237.
- Mann, J. J., J. N. Barney, G. B. Kyser, and J. M. DiTomaso. 2013. Root system dynamics of *Miscanthus × giganteus* and *Panicum virgatum* in response to rainfed and irrigated conditions in California. *BioEnergy Research* 6:678–687.
- Masters, M. D., C. K. Black, I. B. Kantola, K. P. Woli, T. Voigt, M. B. David, and E. H. DeLucia. 2016. Soil nutrient removal by four potential bioenergy crops: *Zea mays*, *Panicum virgatum*, *Miscanthus × giganteus*, and prairie. *Agriculture, Ecosystems & Environment* 216:51–60.
- Matamala, R. R., J. D. Jastrow, R. M. Miller, and C. T. Garten. 2008. Temporal changes in C and N stocks of restored prairie: implications for C sequestration strategies. *Ecological Applications* 18:1470–1488.
- McCalmont, J. P., A. Hastings, N. P. McNamara, G. M. Richter, P. Robson, I. S. Donnison, and J. Clifton-Brown. 2015. Environmental costs and benefits of growing *Miscanthus* for bioenergy in the UK. *Global Change Biology Bioenergy* 10.1111/gcbb.12294.
- Metcalfe, D. B., P. Meir, and M. Williams. 2007. A comparison of methods for converting rhizotron root length measurements into estimates of root mass production per unit ground area. *Plant and Soil* 301:279–288.
- Milchunas, D. G. 2009. Estimating root production: comparison of 11 methods in shortgrass steppe and review of biases. *Ecosystems* 12:1381–1402.

- Mokany, K., R. J. Raison, and A. S. Prokushkin. 2006. Critical analysis of root : shoot ratios in terrestrial biomes. *Global Change Biology* 12:84–96.
- Monti, A., and A. Zatta. 2009. Root distribution and soil moisture retrieval in perennial and annual energy crops in Northern Italy. *Agriculture, Ecosystems & Environment* 132:252–259.
- Neukirchen, D., M. Himken, J. Lammel, U. Czypionka-Krause, and H. W. Olfs. 1999. Spatial and temporal distribution of the root system and root nutrient content of an established *Miscanthus* crop. *European Journal of Agronomy* 11:301–309.
- Nippert, J., R. Wieme, T. Ocheltree, and J. M. Craine. 2012. Root characteristics of C₄ grasses limit reliance on deep soil water in tallgrass prairie. *Plant and Soil* 355:385–394.
- Pahlavanian, A. M., and W. K. Silk. 1988. Effect of temperature on spatial and temporal aspects of growth in the primary maize root. *Plant Physiology* 87:529–532.
- Parker, C. J., M. K. V. Carr, N. J. Jarvis, B. O. Puplampu, and V. H. Lee. 1991. An evaluation of the minirhizotron technique for estimating root distribution in potatoes. *Journal of Agricultural Science* 116:341–350.
- Picon-Cochard, C., R. Pilon, E. Tarroux, L. Pagès, J. Robertson, and L. A. Dawson. 2012. Effect of species, root branching order and season on the root traits of 13 perennial grass species. *Plant and Soil* 353:47–57.
- Pierret, A., C. J. Moran, and C. Doussan. 2005. Conventional detection methodology is limiting our ability to understand the roles and functions of fine roots. *New Phytologist* 166:967–980.

- Pinheiro, J., D. Bates, S. DebRoy, D. Sarkar, and R Core Team. 2016. nlme: Linear and nonlinear mixed effects models. R package version 3.1-128. <http://CRAN.R-project.org/package=nlme>.
- Poorter, H., J. Bühler, D. van Dusschoten, J. Climent, and J. A. Postma. 2012. Pot size matters: a meta-analysis of the effects of rooting volume on plant growth. *Functional Plant Biology* 39:839–850.
- Prieto, I., A. Stokes, and C. Roumet. 2016. Root functional parameters predict fine root decomposability at the community level. *Journal of Ecology* 104:725–733.
- R Core Team. 2016. R: A language and environment for statistical computing. Version 3.3.0. R Foundation for Statistical Computing, Vienna, Austria. <https://www.R-project.org/>.
- Rasse, D. P., C. Rumpel, and M.-F. Dignac. 2005. Is soil carbon mostly root carbon? Mechanisms for a specific stabilisation. *Plant and Soil* 269:341–356.
- Roberts, M. J., S. P. Long, L. L. Tieszen, and C. L. Beadle. 1993. Measurement of plant biomass and net primary production of herbaceous vegetation. Pages 1–21 in D. O. Hall, J. M. O. Scurlock, H. R. Bolhar-Nordenkampf, R. C. Leegood, and S. P. Long, editors. *Photosynthesis and production in a changing environment: A field and laboratory manual*. Chapman; Hall.
- Roumet, C., C. Urcelay, and S. Díaz. 2006. Suites of root traits differ between annual and perennial species growing in the field. *New Phytologist* 170:357–368.
- Rumpel, C., and I. Kögel-Knabner. 2011. Deep soil organic matter—a key but poorly understood component of terrestrial C cycle. *Plant and Soil* 338:143–158.
- Samson, B. K., and T. R. Sinclair. 1994. Soil core and minirhizotron comparison for the determination of root length density. *Plant and Soil* 161:225–232.

- Smith, C. M., M. B. David, C. A. Mitchell, M. D. Masters, K. J. Anderson-Teixeira, C. J. Bernacchi, and E. H. DeLucia. 2013. Reduced nitrogen losses after conversion of row crop agriculture to perennial biofuel crops. *Journal of Environmental Quality* 42:219–228.
- Sonderegger, D. L., K. Ogle, R. D. Evans, S. Ferguson, and R. S. Nowak. 2013. Temporal dynamics of fine roots under long-term exposure to elevated CO₂ in the Mojave Desert. *New Phytologist* 198:127–138.
- Stan Development Team. 2016a. RStan: the R interface to Stan. R package version 2.12.1. <https://cran.r-project.org/web/packages/rstan/>.
- Stan Development Team. 2016b. Stan Modeling Language Users Guide and Reference Manual, version 2.12.0. <http://mc-stan.org>.
- Taylor, B. N., K. V. Beidler, A. E. Strand, and S. G. Pritchard. 2014. Improved scaling of minirhizotron data using an empirically-derived depth of field and correcting for the underestimation of root diameters. *Plant and Soil* 374:941–948.
- Taylor, H. M., D. Upchurch, and B. McMichael. 1990. Application and limitation of rhizotrons and minirhizotrons for root studies. *Plant and Soil* 129:29–35.
- Topp, C. N., A. L. Bray, N. A. Ellis, and Z. Liu. 2016. How can we harness quantitative genetic variation in crop root systems for agricultural improvement? *Journal of Integrative Plant Biology* 58:213–225.
- Wahl, S., and P. Ryser. 2000. Root tissue structure is linked to ecological strategies of grasses. *New Phytologist* 148:459–471.

- Ward, S. E., S. M. Smart, H. Quirk, J. R. B. Tallowin, S. R. Mortimer, R. S. Shiel, A. Wilby, and R. D. Bardgett. 2016. Legacy effects of grassland management on soil carbon to depth. *Global Change Biology* 22:2829–2938.
- Wasson, A. P., R. A. Richards, R. Chatrath, S. C. Misra, S. V. Sai Prasad, G. J. Rebetzke, J. A. Kirkegaard, J. Christopher, and M. Watt. 2012. Traits and selection strategies to improve root systems and water uptake in water-limited wheat crops. *Journal of Experimental Botany* 63:3485–3498.
- Zeri, M., K. J. Anderson-Teixeira, G. C. Hickman, M. D. Masters, E. H. DeLucia, and C. J. Bernacchi. 2011. Carbon exchange by establishing biofuel crops in Central Illinois. *Agriculture Ecosystems & Environment* 144:319–329.
- Zwicke, M., C. Picon-Cochard, A. Morvan-Bertrand, M.-P. Prud'homme, and F. Volaire. 2015. What functional strategies drive drought survival and recovery of perennial species from upland grassland? *Annals of Botany* 116:1001–1015.

Figures

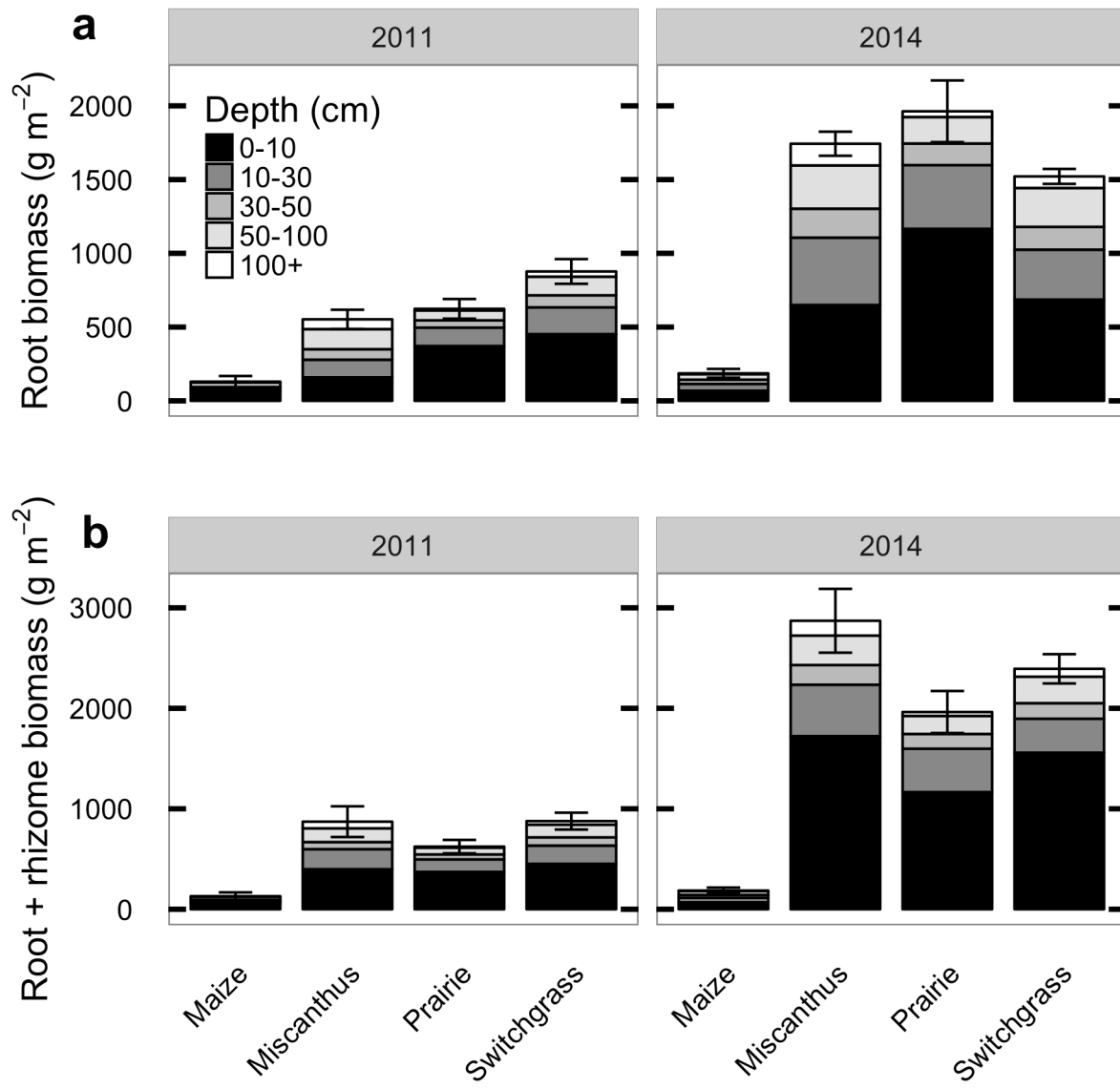


Figure 3.1: Biomass in roots and rhizomes of biofuel crops, as measured by coring in 2011 and again in 2014, divided by depth horizon. Error bars show mean ± 1 standard error of total profile biomass in each block. The 2011 data are re-plotted from (Anderson-Teixeira et al. 2013).

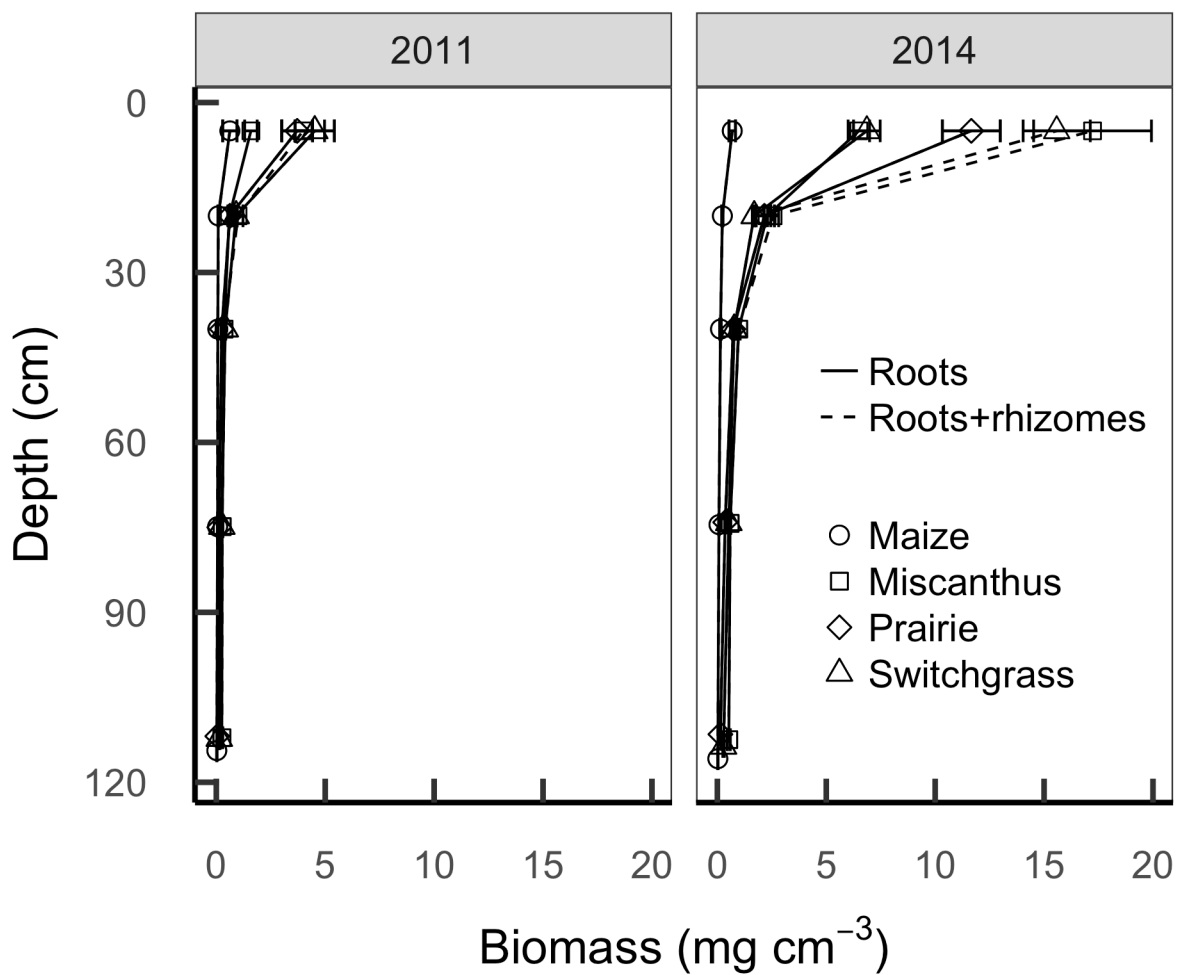


Figure 3.2: Depth profiles of root and root+rhizome mass measured by deep coring in 2011 (left) and again in 2014 (right). The 2011 data are replotted from (Anderson-Teixeira et al. 2013).

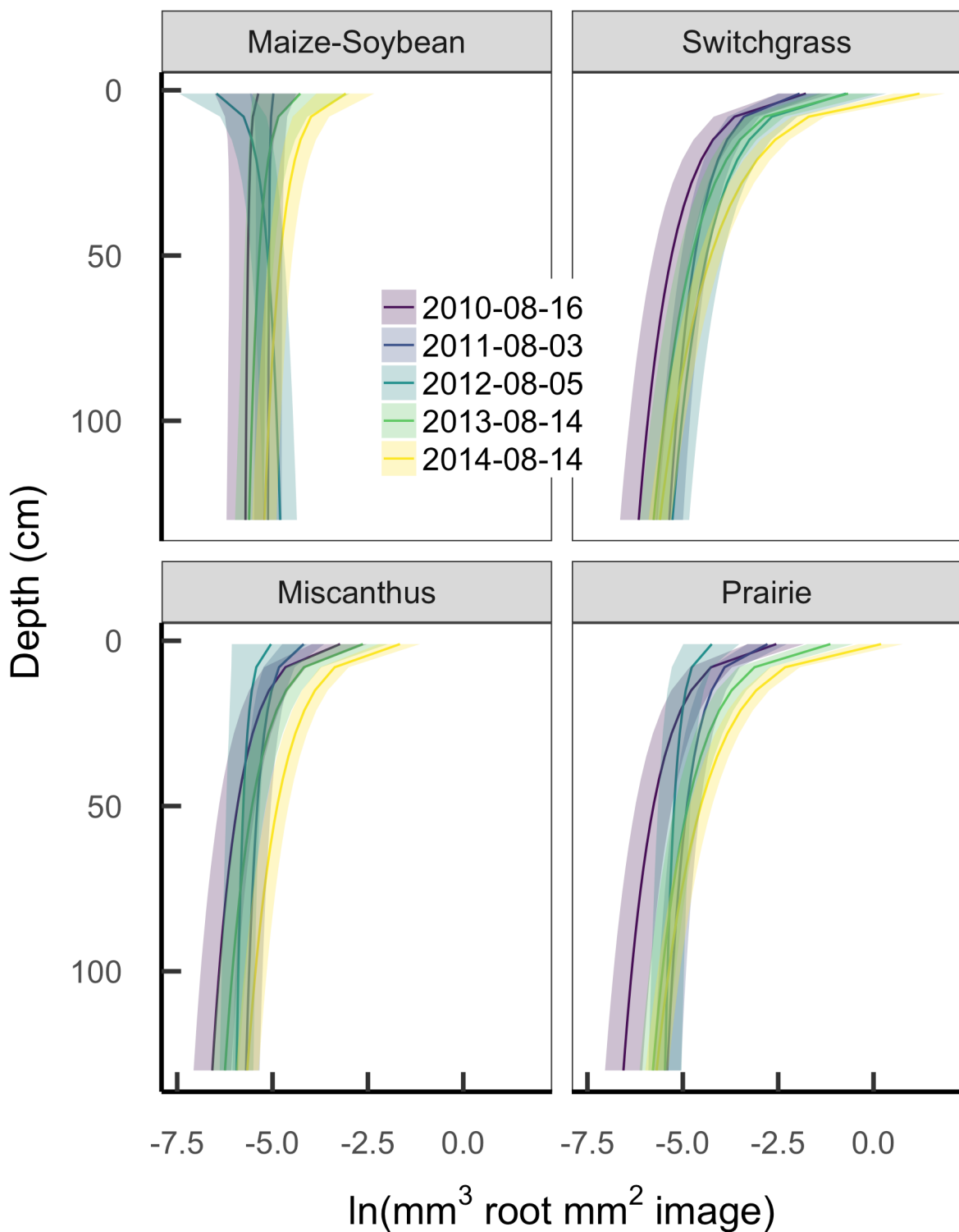


Figure 3.3: Mean \pm 50% intervals of estimated root volume density from minirhizotron images collected at peak aboveground biomass each year from 2010-2014.

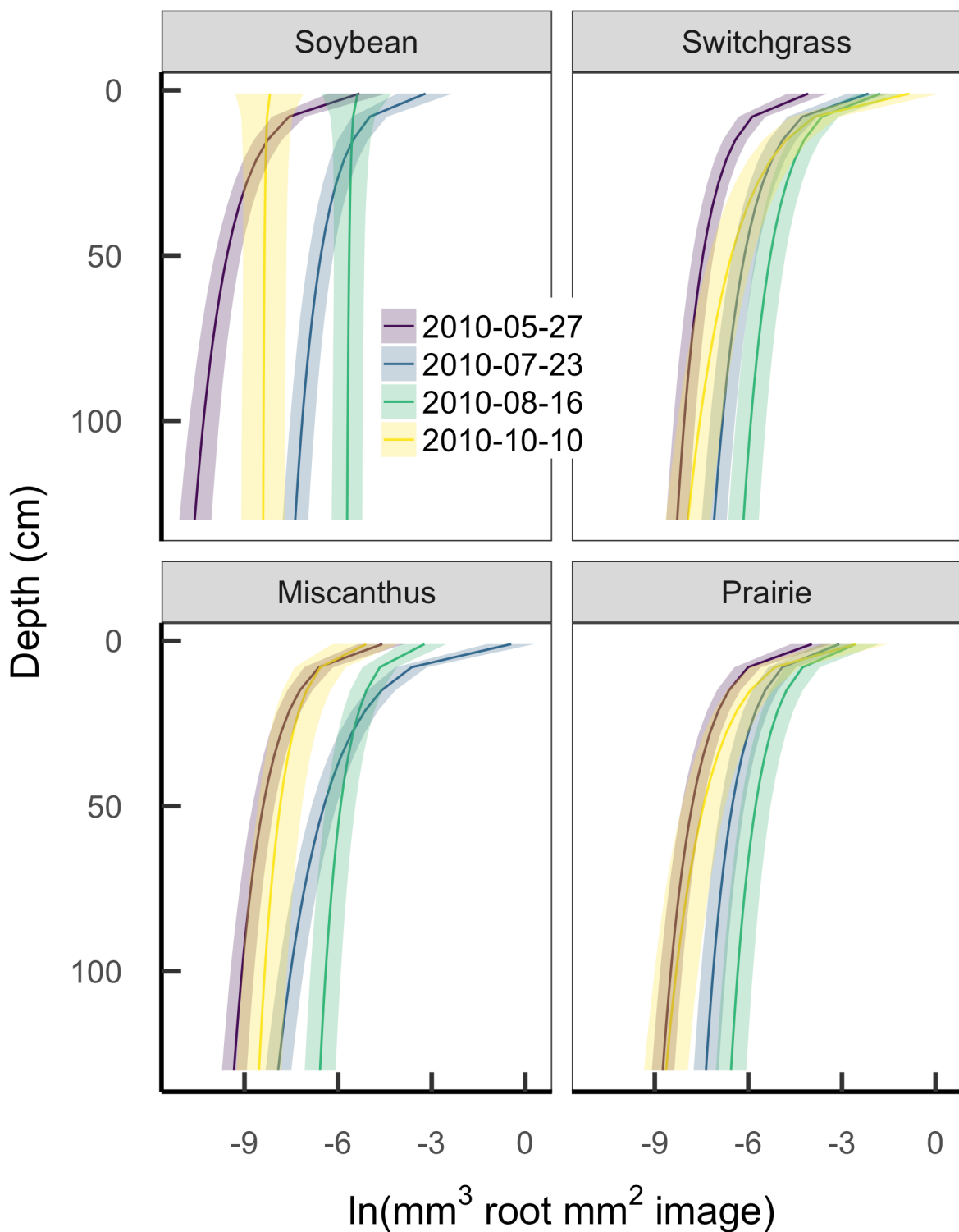


Figure 3.4: Mean \pm 50% intervals of estimated root volume density from minirhizotron images collected in summer 2010. Each color shows a different sampling session.

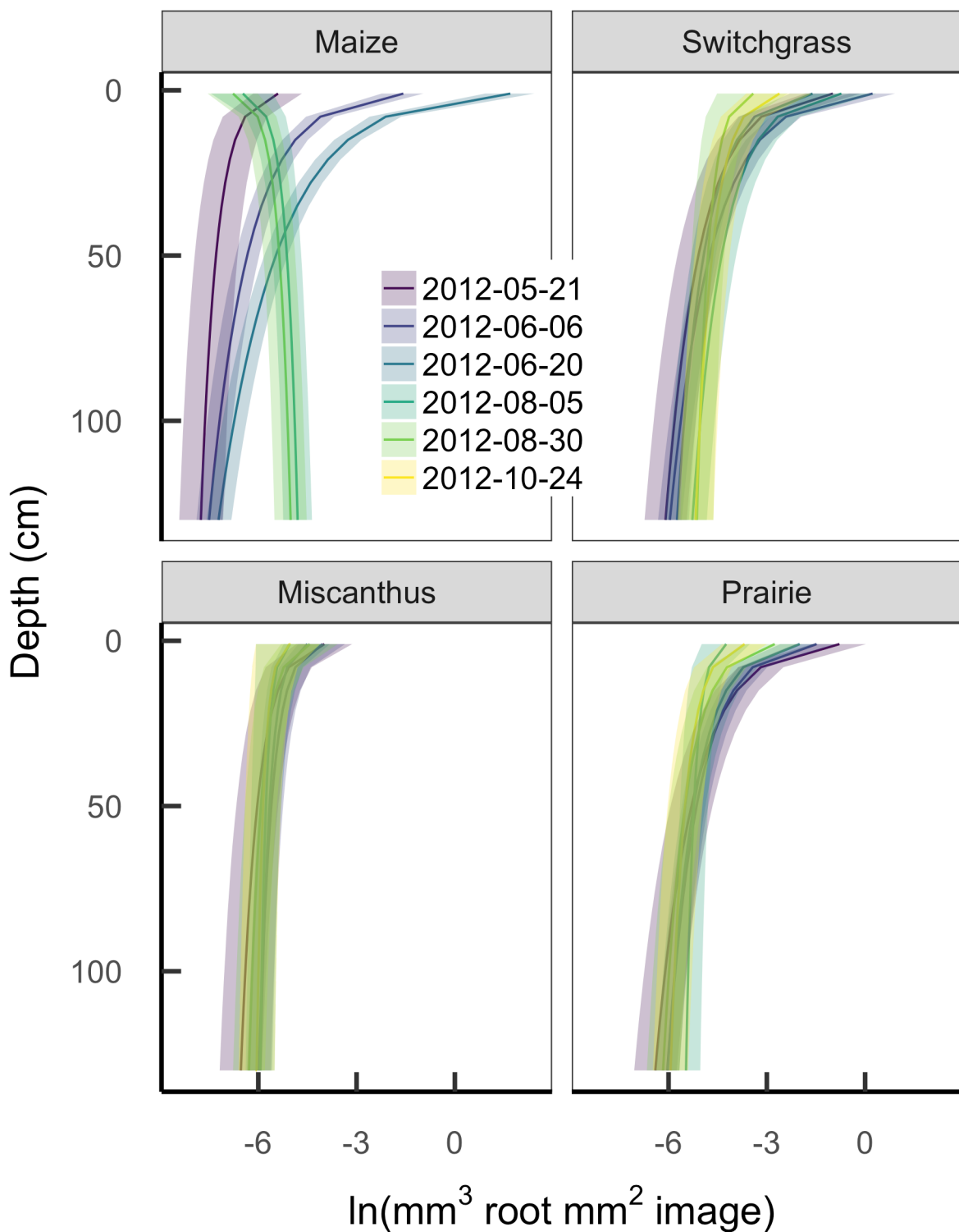


Figure 3.5: Mean \pm 50% intervals of estimated root volume density from minirhizotron images collected in summer 2012. Each color shows a different sampling session.

Supplement 3.1: Selection of priors for model parameters

Our goal for most model parameters was to provide priors that were weakly informative in the sense of Gelman (2006). That is, we aimed to have our posterior estimates mostly informed by the data but with the priors adding sufficient information to avoid unreasonable parameter combinations, thus aiding identifiability and reducing computation difficulty. In particular, our priors for the surface underdetection parameters α^{surface} and β^{surface} use information from other published minirhizotron work but for all other parameters we set our priors with reference to the numeric constraints on visible root volume per image rather than directly from previous biological research.

As a starting point for parameters that need to be specified on the same scale as the data, we derived the expected range of observations by reasoning that root volume cannot exceed 1 mm³ root mm⁻³ soil and is probably undetectable when roots occupy less than 1 pixel per image, or $(0.02/2)^2 \cdot \pi \cdot 0.02 \approx 6 \times 10^{-6}$ mm³ at our typical magnification levels of 0.02-0.025 mm² px⁻¹. Therefore, when modeling on the log scale we expect observed root volumes to fall within a range narrower than $[\ln(6 \times 10^{-6}), \ln(1)]$, or roughly -12 to 0. This leads to the following priors:

- The model intercept term α_i is the expected log volume at mean depth for a given species, and should be able to take any value in the range of observable root volumes. We set it separately to $N(-6, 6)$ for each crop.
- The slope term β_i is the change in expected log volume per log cm of depth. Prior minirhizotron work has usually found that root volume decreases with depth but is still detectable (i.e. $\ln(\text{root volume}) > -12$) at depths greater than 1 m. Since $\ln(\text{root volume at surface}) \leq 0$, this implies a change of less than $-12/\ln(100) \approx -2.6$, but we allow the

possibility of steeper slopes (e.g. annuals that have not yet achieved full rooting depth) and set the prior separately to $N(-1,5)$ for each crop.

- Residual variance ϵ_i cannot be less than zero or greater than the variance of the whole dataset. Taking (-12, 0) again as the maximum possible observed range of the full dataset and approximating the range of a Normal distribution as four sigmas, $0 \leq \epsilon_i \leq 12/4 = 3$, so we set the prior to a folded Normal(0, 3).
- Variation among individual minirhizotron tubes σ^{tube} has the same possible range as ϵ , so we use the same prior: folded $N(0,3)$.
- The location α^{detect} and scale β^{detect} of the root detection probability $\phi = p(\text{detect} | \hat{\mu}, \alpha^{\text{detect}}, \beta^{\text{detect}})$ can vary between two conceptual extremes: If zeroes arise mostly from low root volume, then ϕ will have a sharp threshold at some low $\hat{\mu}$ corresponding to the boundary of effective image resolution. Conversely, if zeroes arise mostly from heterogeneity around a relatively high volume, then ϕ will rise slowly and α^{detect} will be large. Interpolating between these extremes, we reason that the effective image resolution must be coarser than 1 pixel and that even with pure heterogeneity and infinitely small samples we would still expect to detect roots more than 50% of the time if roots fill more than 50% of the soil volume, so $-12 \leq \alpha^{\text{detect}} \leq \ln(0.5) = -0.69$. Since this reasoning is extremely vague, we add that our detection is probably better than chance (our samples are not infinitely small) and set our prior to be quite weak but with its peak below the center of the possible range: $N(-8,10)$.
- Reasoning similarly for β^{detect} as for α^{detect} , if ϕ is “low” (say, less than 0.05, or approximately -3 on the standard logistic scale) at $\hat{\mu} \leq -12$ and at least 0.5 (=0 on the standard logistic scale) at $\hat{\mu} \geq -0.69$, this corresponds to a change of at least 3 units on

the standard logistic scale in the space of 11 log units, or $\beta^{\text{detect}} \leq 11/3 \approx 3.66$, or possibly much less if ϕ is a steep threshold. This too is vaguely reasoned, so we set the prior weak enough to allow values somewhat outside this range if they are consistent with the data: folded $N(0,6)$.

For the surface underdetection function, the expected scale of the root volume data offers little guidance. Instead, we relied on previously published data, especially on a comparison of minirhizotron and core break root counts in a spring oat crop (Bragg et al. 1983, especially their Table 1). Assuming that these observations apply to other grasses and that the underdetection for root counts is comparable to that for root volume, the key finding from this and other papers (Samson and Sinclair 1994, Ephrath et al. 1999) is that only about 10-20% of roots were detected in the surface soil, rising to “full detection” ($>95\%$) at depths greater than about 30 cm. Converting these percentages to the log-odds scale, this is a change of $(| - \ln(1/0.1 - 1)| = 2.19) + (-\ln(1/0.95 - 1) = 2.94) \approx 5$ units on the standard logistic scale, implying that the half-detection depth α^{surface} is around 13 cm and the scale β^{surface} is about 6. This is qualitatively comparable with other papers that report underdetection near the surface by minirhizotron methods, but few others have reported the comparison in enough detail to plot the curve. We set our prior for α^{surface} as $N(13,10)$ and β^{surface} as $N(6,5)$.

Supplement 3.2: Supplemental figures

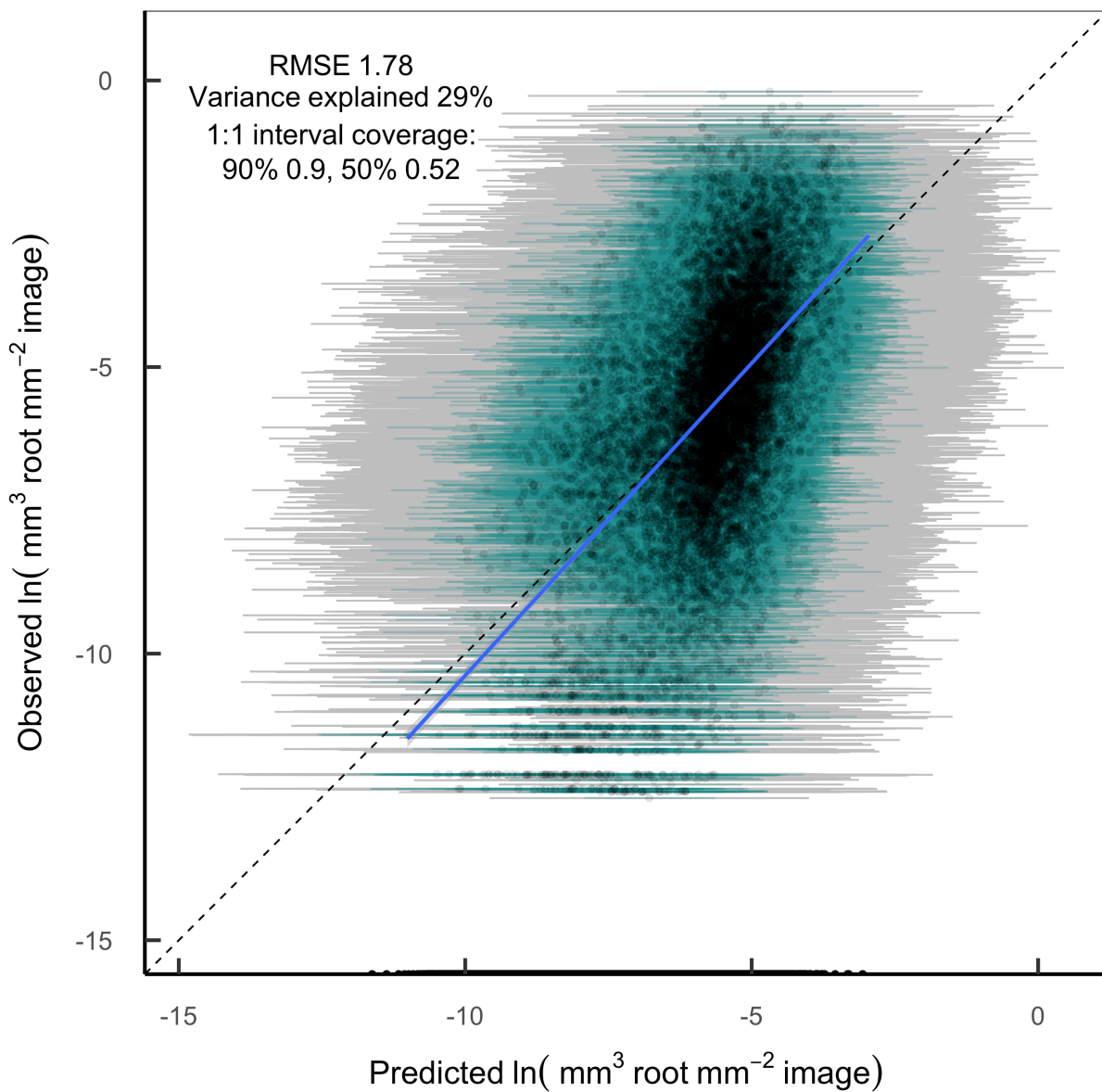


Figure 3.S1: Observations versus predictions of visible root volume in individual minirhizotron images. Bars show prediction intervals (grey: 90%; blue: 50%), for newly observed images at the same location. The points along the bottom of the image indicate model predictions for images with zero observed roots and are not included in the regression.

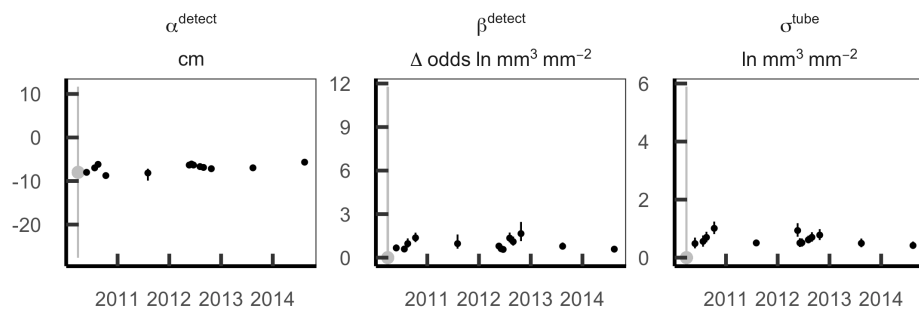
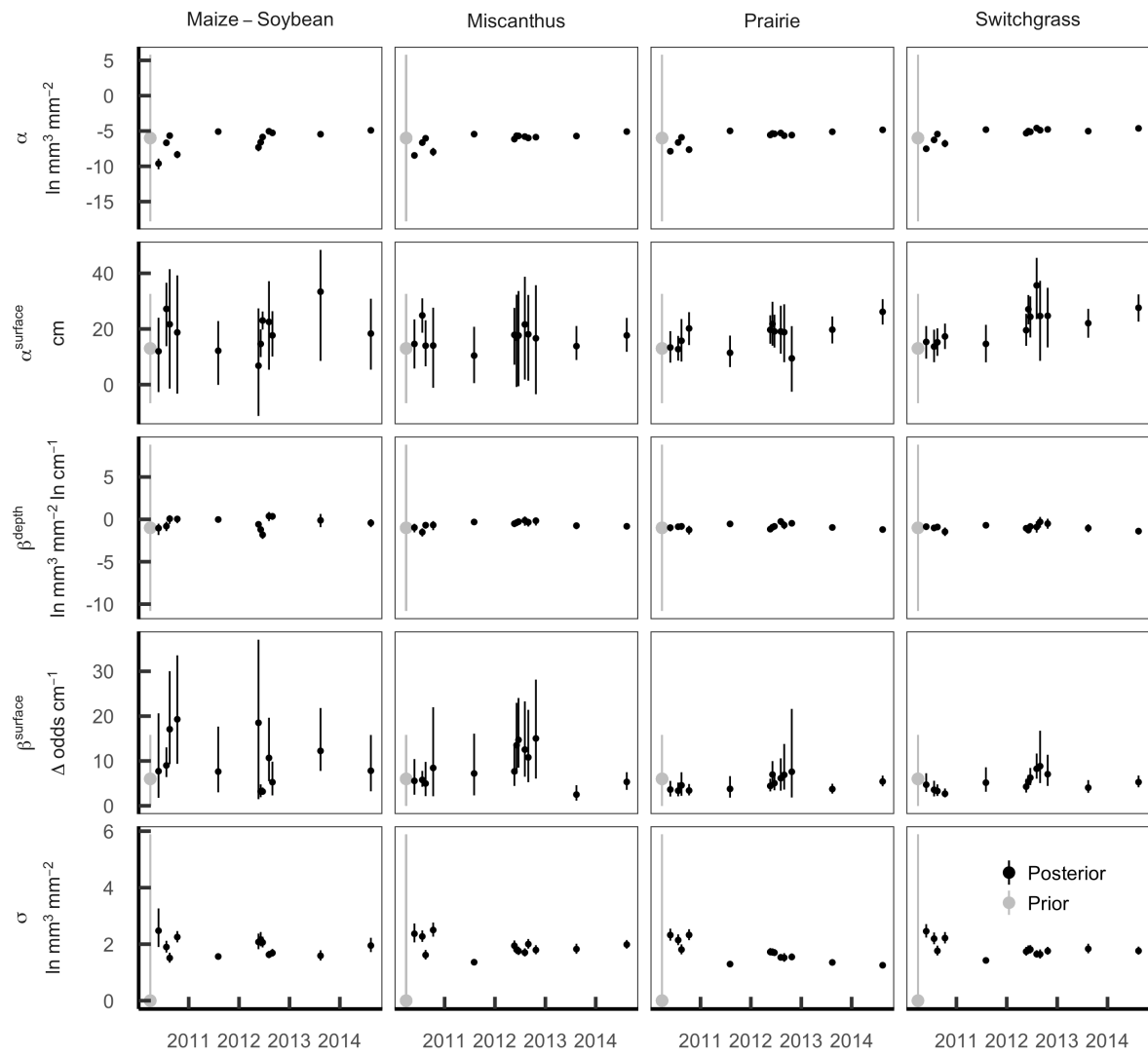


Figure 3.S2: Model parameter estimates. The grey bar at the left edge of each panel shows the mean \pm 95% credible interval of the prior distribution; black bars show posterior mean \pm 95% credible interval for each sample day.

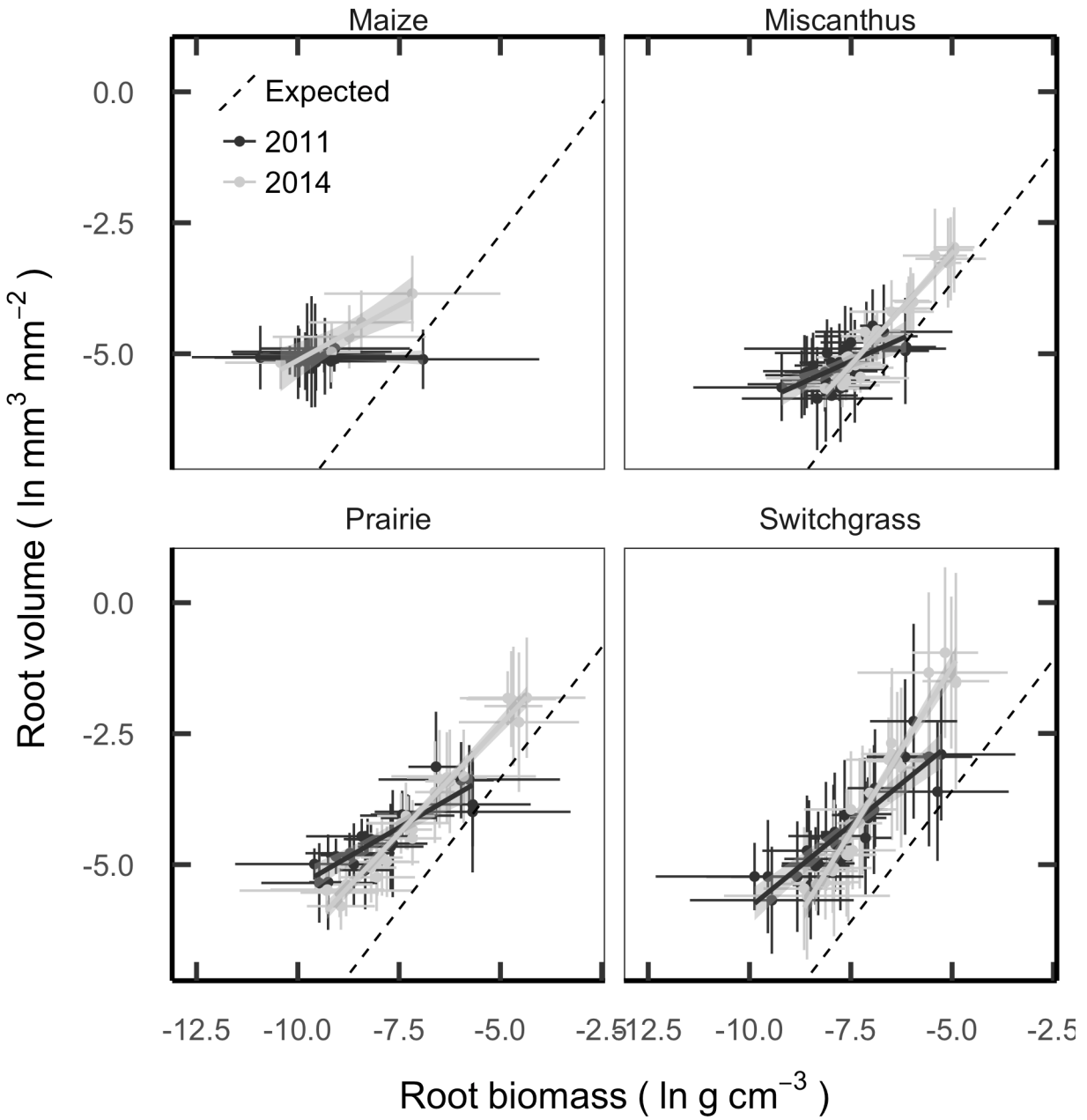


Figure 3.S3: Comparison between root mass measured from soil cores and estimated from minirhizotron images taken in midsummer 2011 and 2014. Each point shows the mean \pm 95% interval for one depth layer (0-10, 10-30, 30-50, 50-100 cm) in one experimental plot. Dashed lines show the expected relationship between root mass and volume assuming a 0.78 mm depth of view and constant root tissue densities of 0.08 (maize), 0.20 (*Miscanthus*), 0.19 (switchgrass), or 0.15 (prairie) g cm^{-3} .

Chapter 4

Molecular analysis shows taxonomic partitioning of root placement by depth in a prairie plant community

Abstract

The question of how diversity affects ecosystem resilience is urgent in the face of climate change, yet poorly addressed for belowground contexts. In particular, it is not clear to what extent different species change their behavior when grown in mixed root communities to achieve better partitioning of the available functional and spatial niches. In mixed root samples taken from varying depths in a tallgrass prairie restoration managed for biomass production, we identified taxa by using microfluidic PCR and high-throughput sequencing to obtain DNA barcodes for the *ITS2* region, and asked whether taxa from different functional groups had recognizable spatial roles or co-occurrence patterns. We found that grasses increased in prevalence with depth and forbs from the Asteraceae decreased with depth, and consequently that grasses and forbs showed negative co-occurrence (spatial segregation) overall. Most other taxa were found equally at all depths and showed random or positive co-occurrence, suggesting that there is little overall spatial partitioning at this site. Aboveground cover and belowground read abundance were positively correlated, but with a lower slope for grasses than for dicots. We suggest that in this managed, high-evenness system on uniform, fertile soils, the relatively small fraction of belowground biomass found in the form of grass roots in deep soil layers may be disproportionately important for functions such as water uptake, N leaching prevention, and C storage that affect the resilience of the whole ecosystem.

Introduction

In a rapidly changing world, one of the most pressing questions in ecology is which ecosystem properties promote stability and which lead to rapid state changes. It is now well recognized that diversity generally promotes resilience in ecosystem productivity (Tilman et al. 2001), partly through facilitation but primarily through functional complementarity that allows more effective partitioning and therefore more complete exploitation of niche space, producing a more stable overall allocation of resources across the community (Fornara and Tilman 2008, 2009, De Deyn et al. 2008). This implies that the resilience benefits of niche partitioning will only be realized if different species in the community possess functions that are actually complementary to each other. For example, N and water availability are often strongly anticorrelated in grassland soils, leading *Festuca ovina* and *Achillea millefolium* to extract N from different depths when competing in mixed-species stands than when they are grown alone, while *Phleum pratense* and *Trifolium pratense* showed no such vertical partitioning (Jumpponen et al. 2002).

In addition to functional complementarity, the resilience of grassland systems may rely on diversity in *spatial* partitioning as well. Prairie plant communities are noted for maintaining a large proportion of their biomass below ground (Jackson et al. 1996), and the importance of belowground interactions between species with differing root traits for determining community productivity has long been recognized (Weaver 1919, Bardgett et al. 2014). Grassland plant communities may be more strongly structured belowground than aboveground (Kesanakurti et al. 2011, Hiiesalu et al. 2012, Wilson 2014) and the physiological capacity to exploit soil resources may be a strong predictor of competitive success (Tucker et al. 2011, de Kroon et al. 2012, Hendriks et al. 2015). Therefore, to understand the potential responses of

multiplespecies communities to destabilized conditions such as a changing climate, it is necessary to understand the physical placement of the different species in the community as well as the between-species differences in resource allocation and niche partitioning strategies.

Progress in understanding these belowground dynamics is slowed by the challenges of studying belowground environments, especially for mixed-species samples. Because harvesting root systems requires digging and root systems show extreme spatial variability that increases the sample size needed to characterize a system, all methods are laborious and most require destructive harvests, often in the form of massive excavations to identify roots by physically tracing them to the plant crown (Weaver and Voigt 1950). Visual identification of roots based on anatomical or morphological characteristics is sometimes possible (Wardle and Peltzer 2003) but is an inherently low-throughput method that requires a trained specialist and becomes much more challenging for very fine roots or highly diverse communities. Minirhizotron methods can provide some information on root placement, but have limited success at distinguishing between species (Rewald et al. 2012).

With the increasing availability of high-throughput DNA sequencing, molecular methods now provide a partial solution to this dilemma. DNA-based methods can use smaller samples and therefore less-destructive sampling techniques, allow distinctions between visually identical roots, and permit quantitative comparisons. Additionally, because DNA persists to some extent in dead tissue, sequencing potentially can integrate longer timescales by detecting species that are present in the community but were dormant or senesced at the time of sampling. The internal transcribed spacer between the 5.8S and 26S regions of the nuclear ribosomal DNA (ITS2) is a popular choice for barcoding of mixed root species recovered from soil: It is easily extracted from all plant groups, widely used in root sequencing (Jackson et al. 1999) and therefore well

represented in databases, and short enough (~200 bases) to sequence on an Illumina platform. Although higher taxonomic resolution can be obtained from multiple barcodes (e.g. *rcbL* and *matK*; Staats et al. 2016), assigning identities to multiple barcodes in mixed samples is challenging (Rewald et al. 2012) and ITS2 alone provides comparable resolution to other single barcodes (Chen et al. 2010, Fahner et al. 2016).

The objective of this study was to identify the root species present at varying soil depths (0-100 cm) in a restored prairie in central Illinois, and to use these identities to infer differences in species roles for water usage, N uptake, and carbon storage. We used a DNA metabarcoding approach: we collected fine root samples by coring and extracted whole-community DNA for ITS2 amplicon library construction (Fluidigm Access Array) followed by sequencing (Illumina MiSeq 2x300), then identified the detected sequences to genus level by database search and compared the resulting abundance estimates against those from aboveground surveys.

Methods

Experimental site

Our experimental site is the University of Illinois Energy Farm (Urbana, Illinois, USA: 40.06N, 88.19W, elevation 220 m), where five plots of restored prairie were planted in 2008 (four 0.7 Ha plots plus one 3.8 Ha plot). The site has a continental climate with a mean annual temperature of 11°C and approximately 1 m of precipitation annually. It is established on deep, highly fertile Mollisol soils (Argiudolls, mapped as Dana, Flanagan and Blackberry silt loam) with organic C contents more than 1% throughout the top 50 cm (Figure 4.1). The site was used for agriculture for at least 100 years before establishment of the current experiment. For further

details on the establishment and management of the site, see previous work by (Zeri et al. 2011, Smith et al. 2013, Masters et al. 2016).

The prairie plots were established by seeding with a mix of 28 species native to Illinois (Table 4.1). Species were chosen to balance four stated goals: Maximum biomass production, ecosystem resilience, trophic diversity, and locally adapted species. Seeds were obtained from Pizzo and Associates (Leland IL), treated at planting time with a mycorrhizal inoculum (“AM 120”; Reforestation Technologies International; Gilroy CA) that is primarily *Glomus intraradices* (Neal Anderson, RTI Inc.; personal communication), and overseeded with a spring oat (*Avena sativa*) cover crop. The plots were mowed after senescence each year and the above-ground biomass was baled and removed. 25 of these 28 species remained detectable in 2011 (Feng and Dietze 2013) and in 2012 a total of 32 species were censused in the plots, with the five most common species *Andropogon gerardii*, *Sorghastrum nutans*, *Ratibida pinnata*, *Helianthus grosseserratus*, and *Coreopsis tripteris* collectively providing about 75% of total cover (Table 4.1).

Sample collection

To characterize the spatial distribution of species with depth, we collected mixed root samples on July 15-18 of 2013, after most late-season grasses were well emerged but before most early-season plants began to senesce. At 24 locations (one in each quadrant of each 0.7 Ha plot, two in each quadrant of the 3.8 Ha plot), we used an 8 cm bucket auger to collect roots and soil from five depth increments (0-10, 10-30, 30-50, 50-75, and 75-100 cm) of 3 cores within a 2 m radius. We pooled all three cores from each location, collected a ~0.5-1 kg subsample of mixed roots and soil from each depth, and returned the remaining material to the holes. The

resulting 120 samples were stored on ice in 1-gallon Ziplok bags for transport to the laboratory, then frozen at -80 °C the same day and stored until further analysis.

To characterize the genetic diversity of our target species and generate a mock community for use as a sequencing control, we collected voucher specimens on August 31 and September 1, 2013. For each of the 33 plant species present in aboveground surveys (X. Feng, unpublished data), we located 3-5 individuals, identified them to species by leaf and flower morphology, and used a trowel to extract roots still attached to their well-identified crown. We pooled all roots from each species, placed them in Ziplok bags, placed them on ice for transport to the laboratory, and froze them at -80 °C the same day for storage until further analysis.

Root recovery

To separate roots from soil, we thawed mixed samples overnight at 4 °C, then screened them through a 2 mm sieve followed by manually picking all visible roots using forceps. The picking process took about 30-90 minutes per sample and all sieves, forceps, and gloves were wiped with ethanol immediately before use to minimize contamination by non-sample DNA. After root picking, a subsample of the root-free bulk soil was collected and lyophilized, then ground and combusted to determine total carbon and nitrogen content (4010 CHNSO Elemental Analyzer; Costech, Valencia CA).

We then rinsed all roots in three changes of sterile water, with the final rinse including 10 minutes of sonication to dislodge any residual soil from the the root surface, then lyophilized all samples and stored them at room temperature. Single-species root voucher samples were treated identically to the mixed root samples, with the exception that bulk soil had been removed at collection time and therefore no sieving or hand-picking steps were necessary.

DNA extraction and amplification

To maximize extraction of DNA from tough root tissue, we ground all samples once in a dry mortar and pestle at room temperature, then again in liquid nitrogen to a very fine powder. We then weighed ~100 mg of tissue from each sample and extracted whole DNA using a Powersoil-htp isolation kit (Mo Bio Laboratories, Carlsbad CA) according to the manufacturer's directions, including an optional initial bead-beating step (GenoGrinder; 4 x 30 sec at 1750 RPM, 2 min between rounds) followed by a 60 min incubation at 65 °C with 1% proteinase K. We then performed a post-extraction cleanup using materials from the same kit (E. Adams, Mo Bio; personal communication): We diluted the DNA to a volume of 100 µL with DNase-free water, added 50 µL of bead beating solution and inverted to mix, then added 25 µL each of solutions C2 and C3, inverted to mix, and centrifuged at 10000 xg for 2 minutes. We then collected the supernatant, added 2 volumes of solution C4, vortexed, and loaded the sample onto a spin filter. Finally, we washed with 500 µL of solution C5 and eluted with 50 µL of C6.

After extraction, we submitted whole DNA to the W.M. Keck Center (Urbana, IL, USA) for amplification and sequencing. In addition to DNA extracted from mixed samples, we included nominally pure extracts of root DNA from four species with high aboveground abundance (*Andropogon gerardii*, *Sorghastrum nutans*, *Silphium perfoliatum*, and *Elymus nutans*; Feng 2014), water extractions as a negative control on the DNA extraction + PCR + sequencing process taken as a whole, and a mock community of DNA from 29 species combined in equimolar quantity plus one species (*Heliospopsis helianthoides*) at twice the concentration of the others. The second internal transcribed spacer of the nuclear ribosome gene (ITS2) was amplified from each sample by microfluidic PCR using the Fluidigm Access Array chip and sequenced by synthesis for 2x301 paired-end cycles (MiSeq, V3 chemistry, Illumina Inc, San Diego CA). The

5' linker construct for each sequence consisted of Illumina flowcell-binding primer i5, Fluidigm linker pad CS1, and plant-specific ITS2 primer S2F (Chen et al. 2010) for a final forward linker sequence of 5' -AATGATAACGGCGACCACCGAGATCT-ACACTGACGACATGGTTCTACA- ATGCGATACTTGGTGTGAAT. The 3' linker construct for each sequence consisted of the Illumina flowcell-binding primer i7, a 10-base oligonucleotide barcode that was unique for each sample, Fluidigm linker pad CS2, and plant-specific ITS2 primer S3R (Chen et al. 2010) for a final reverse linker sequence of 5' -CAAGCAGAAGACGGCATACGAGAT-XXXXXX- TACGGTAGCAGAGACTTGGTCT-GACGCTTCTCCAGACTACAAT, where XXXXXXXX indicates the variable barcode sequence.

Data processing

The raw Illumina read files were preprocessed by sequencing center staff before delivery by using CASAVA 1.8 to remove sequencing primers, PhiX reference reads, and reads from unrelated samples sequenced in the same flowcell lane. We then used cutadapt 1.8.1 (Martin 2011) to trim primers, discard all reads that did not begin with the expected primer, and trim 3' bases with a Phred quality score below 20. We then joined the overlapping ends of each read using the RDP maximum likelihood algorithm (Cole et al. 2013) as implemented in Pandaseq 2.10 (Masella et al. 2012) using a minimum alignment quality of 0.8, a minimum assembled length of 25 bases, and a minimum overlap of at least 20 “bits saved” (corresponds to ~10 bases; see Cole et al. 2013). We then used the `split_libraries_fastq.py` script in QIIME 1.9.1 (Caporaso et al. 2010) to assign sequences to samples by barcode matching.

To assign sequences to taxonomic units, we used a de novo clustering approach. We dereplicated sequences and removed singletons and suspected PCR chimeras using VSEARCH 2.0.4 (Rognes et al. 2016), extracted full-length ITS2 variable regions using ITSx 1.0.11

(Bengtsson-Palme et al. 2013), clustered the results using VSEARCH with a similarity threshold of 99%, and assigned taxonomy to each cluster using BLAST+ (Camacho et al. 2009) against the GenBank nt database. We then mapped taxonomy for the full dataset by using VSEARCH to search the full sequence file (including singletons and chimeras) against these cluster centroids, also with a similarity threshold of 99%. After taxonomy assignment, we collapsed all clusters assigned as the same phylotype (species, genus, or family depending on the analysis of interest) into single taxon groups using the phyloseq 1.16.2 package (McMurdie and Holmes 2013) in R 3.3.1 (R Core Team 2016), then corrected for between-sample differences in sequencing depth by transforming raw read counts for each taxon group into sample proportions. Taxa with a mean abundance less than 1% per sample were removed from plots, but included in multivariate analyses.

To visualize the effects of depth and C/N content on root community composition, we performed nonmetric multidimensional scaling followed by permutational MANOVA using the adonis function of vegan 2.4-1 (Oksanen et al. 2016) in R 3.31 (R Core Team 2016), using Jaccard distance as the response variable; depth, C, and N as environmental variables; ‘plot:location’ as a blocking effect. To assess species co-occurrence patterns, we used the package cooccur 1.3 (Griffith et al. 2016) in R 3.31.

Full analysis scripts and raw sequence data are available online (https://github.com/infotroph/Prairie_seq).

Results

The MiSeq run and sequence cleanup produced ample, high-quality sequences for the planned analysis: The raw file contained 1286163 plant ITS2 reads, of which 730235 were

successfully end-paired, quality filtered, and assigned back from barcodes to samples. These clean reads contained 494505 unique sequences, of which 459986 were observed only once in the dataset (singletons). Of the 34519 sequences observed at least twice, 2219 were identified as probable or borderline PCR chimeras by `vsearch`. These chimeric sequences accounted for a total of 8526 reads, or ~1.2% of the raw dataset. A further 75 sequences were identified as incomplete or undetectable ITS2 regions by `ITSx`, leaving a total of 32225 ITS2 sequences to be clustered at 99% similarity into 1347 OTUs, which we then used as reference sequences at 99% similarity to map the 730235 reads (singletons included) of the cleaned sequence file, for a final sequence-by-sample table of 576650 reads. Sample coverage was excellent, with 110 of the 120 mixed root samples having more than 1000 reads (1355-8998), sufficient for confident analysis. There was no apparent change in total read count between samples from differing depths.

After obtaining best-match barcode identities for each of the 1347 OTUs clustered at 99%, we collapsed OTUs to phylotypes by combining groups of OTUs that all yielded the same taxon as their top BLAST hit. When we collapsed at the species level, we obtained 158 phylotypes that were identified as coming from 70 genera across 16 families, which is notably higher than the 32 species, 22 genera, and 6 families known from site vegetation surveys (Table 4.1). Many samples contained high read counts from several different “species” of genera that have only one known species at the site (Figure 4.S2). From this we infer that, at least with current databases, ITS2 barcode identities may be more reliable at the genus level than the species level.

Of the genera detected both belowground and aboveground, per-plot mean belowground read proportion was positively correlated with percent aboveground cover, but the slope of the relationship was much lower for grasses than for any dicot group (Figure 4.2), possibly

indicating a lower sensitivity to detect grasses by this ITS method. Similarly, the number of reads obtained from grasses in our mock community was consistently lower than calculated from input DNA concentrations, and neither of two species from the Lamiaceae was ever detected either in the mock community or the mixed samples (Figure 4.S2).

To test for spatial partitioning between species, we examined how often pairs of species were found together in a given sample. Most species co-occurred with each other at rates broadly compatible with random occurrence. Of the pairs that appeared nonrandom, more were positively correlated (overdispersion) than were negatively correlated (spatial partitioning), and there were no evident differences in co-occurrence rate between samples from different depths (Figure 4.S5). However, these effects differed between functional types: Species from the Asteraceae showed neutral to positive co-occurrence with species from all families, while Poaceae species had positive co-occurrence with other Poaceae but negative co-occurrence with most species from other families (Figure 4.3).

The overall taxonomic makeup of roots shifted with depth: The proportion of reads identified as grasses increased from roughly 10% of near-surface reads to approximately one-third of reads in the 75-100 cm layer. Forbs from the Asteraceae declined somewhat with depth, while legumes were relatively consistent across depths (Figure 4.4). These partitionings were consistent across groups within each functional type: When grouped by genus, all grasses were more abundant in deep layers than near the surface. Within the Asteraceae, only *Silphium* was more abundant in middle layers rather than shallow, possibly attributable to being the only genus at the site with a mix of tap-rooted (*S. laciniatum*, *S. terebinthinaceum*) and fibrous-rooted (*S. integrifolium*, *S. perfoliatum*) species.

Our observation of increasing grass dominance in deeper layers was supported by multivariate analyses: Nonmetric multidimensional scaling produced a first axis highly correlated with depth (Figure 4.5), with grasses associated with deeper layers, Asteraceae with shallow layers, and legumes orthogonal to the depth axis. The largest single explanatory variable was sampling location, which we treated as a conditioning variable and which explained ~40% of total inertia; after accounting for location, depth added a small (~8%) but significant (PERMANOVA pseudo- $F=8.7$; $p=0.001$) further increase in inertia explained. Organic C, N, and C:N were all strongly anticorrelated with depth and neither they nor their interactions with depth added any further explanatory power (PERMANOVA; all $R^2 < 0.01$; all $p > 0.4$).

Discussion

Root placement in our prairie plots appears to be weakly partitioned by taxonomy, with grasses increasing in abundance relative to forbs at greater depths (Figure 4.4) but little evidence of spatial patterning among other functional groups (Figure 4.3). The aboveground and belowground abundances of most species appeared to scale together (Figure 4.2), but with very different slopes for grasses than for dicots. Given the high overall proportion of reads identified as Asteraceae and especially given their dominance in the shallow soil layers that contain over 80% of the total root mass in this system (Figure 4.1), it is likely that much of the root mass in these plots originates from forbs rather than grasses. However, even if grass root mass in the deep soil layers is small relative to the surface and relative to other taxa, it may still be ecologically important for access to water, nutrient economy, and carbon storage.

One goal of this study was to infer the species composition of root mixtures, to allow richer insights from other studies where bulk biomass samples are collected without identifying

their component mixtures. We found that most genera were at least occasionally present at all depths, that the majority of the sequences obtained were from forbs in the Asteraceae, that these were especially dominant in the shallow soil layers, and that despite grasses dominating aboveground measurements of cover and biomass we detected few reads from grass roots near the surface and only some in the deeper layers. Considering biomass and taxon identity together, it is thus likely that relatively shallow forb roots account for a substantial fraction of the root C input to this prairie. However, this does not necessarily mean that grasses are a minor component of total root mass: To attempt a quantitative conversion from reads to tissue mass requires knowing the potentially species-specific relationships between root biomass and DNA yield (Rewald et al. 2012, Zeng et al. 2015), which we did not attempt to characterize here. The lower slope of grasses in the aboveground-belowground relationship (Figure 4.2) and the apparent lower detection of grasses in our mock community (Figure 4.S2) are suggestive of a possible extraction or sequencing bias against grasses, but even if present we expect this to be constant across samples and thus should not affect comparisons of relative functional group dominance between depths.

An additional caution for our method is that the precision and accuracy of our barcode identifications are limited by the taxonomic resolution of the ITS2 region, the potential for intraspecific variation (Álvarez and Wendel 2003), and the completeness of available sequence databases. Following previous workers (e.g. Fahner et al. 2016), we regard all species identities from this dataset to be tentative, and in a few cases even genus assignment was uncertain. This was particularly evident in the C4 grasses, for many of which we obtained BLAST ties with multiple best results widely spread across the PACMAD clade. However, because our site has only a few congeneric species (Table 4.1) and our hypotheses were focused at the level of

phylogenetically-distinct functional groups, further refinements of sequence identity are unlikely to change the conclusions. Using multiple primer sets may help to increase taxonomic resolution and would be straightforward to add to future work using the Fluidigm PCR platform (Brown et al. 2016), but in our mixed-sample setting the bioinformatic challenge of resolving multiple markers would likely be prohibitive (Fahner et al. 2016).

Previous work on the spatial structure of grassland root communities has found mixed results. An old-field site in Ontario (Kesanakurti et al. 2011) was similar to ours in finding positive correlations between aboveground and belowground abundance and in finding less roots from grasses than expected from aboveground data, but differed in finding very strong spatial partitioning. This difference may be attributable to differences in spatial scale (they extracted individual roots from 5x5x5-cm soil blocks, we pooled roots from multiple cores in each ~2 m sampling area) or to differing environmental controls in a heterogeneous old-field environment than in a planted site under active crop management. By contrast, two grasslands with differing soil water regimes in Wyoming showed co-occurrence patterns much like those we observed, with most species present in all samples and only weak changes in detection with depth (Frank et al. 2015). In addition, mapping of individual roots at the mm scale in these same Wyoming grasslands were consistent with our finding of more positive than negative species co-occurrences (Frank et al. 2015). Taken together, these findings support the conclusion of Price and co-workers (2012) that belowground community structure is largely determined by *abiotic* filtering; perhaps we should not be surprised to find little spatial structure in our highly fertile, previously tilled, evenly planted, annually mowed site.

Although root mass in the deep soil was low relative to the surface layers, these roots are likely to be ecologically important. By allocating proportionally more roots to the deep soil than

other groups, the grasses in this prairie may gain access to more reliable water supplies and reduced competition for nutrients that help maintain their aboveground dominance. Even small increases in the amount of deep root can contribute to drought survival of grasses (Nippert et al. 2012), reduce N leaching losses (Smith et al. 2013), and increase soil C storage (De Deyn et al. 2008, Anderson-Teixeira et al. 2013), implying that the taxonomic partitioning we observed is likely to increase the management value of prairie restorations as well as their ecological resilience.

Acknowledgments

We thank Xiaohui Feng for plant species identifications and for providing the aboveground survey data, Mark Band and Alvaro Hernandez (W. M. Keck Center) for technical advice, library preparation, and sequencing, James Doroghazi, Shawn P. Brown, Elizabeth Bach, and Aleel Grennan for valuable discussions, Michael D. Masters for soil CN analysis and lab logistics, and Robert A. Cachro, Jacob N. Rosenthal, Taylor A. Wright, and Derick A. Carnazzola for assistance with sample processing. This project was partially funded by the Energy Biosciences Institute and by an award to SAW through the Institute for Genomic Biology Fellows program.

References

Anderson-Teixeira, K. J., M. D. Masters, C. K. Black, M. Zeri, M. Z. Hussain, C. J. Bernacchi, and E. H. DeLucia. 2013. Altered belowground carbon cycling following land-use change to perennial bioenergy crops. *Ecosystems* 16:508–520.

- Álvarez, I., and J. F. Wendel. 2003. Ribosomal ITS sequences and plant phylogenetic inference. *Molecular Phylogenetics and Evolution* 29:417–434.
- Bardgett, R. D., L. Mommer, and F. T. de Vries. 2014. Going underground: root traits as drivers of ecosystem processes. *TRENDS in Ecology and Evolution* 29:692–699.
- Bengtsson-Palme, J., M. Ryberg, M. Hartmann, S. Branco, Z. Wang, A. Godhe, P. De Wit, M. Sánchez-García, I. Ebersberger, F. de Sousa, A. S. Amend, A. Jumpponen, M. Unterseher, E. Kristiansson, K. Abarenkov, Y. J. K. Bertrand, K. Sanli, K. M. Eriksson, U. Vik, V. Veldre, and R. H. Nilsson. 2013. Improved software detection and extraction of ITS1 and ITS2 from ribosomal ITS sequences of fungi and other eukaryotes for analysis of environmental sequencing data. *Methods in Ecology and Evolution* 4:914–919.
- Brown, S. P., A. Ferrer, J. W. Dalling, and K. D. Heath. 2016. Don't put all your eggs in one basket: a cost-effective and powerful method to optimize primer choice for rRNA environmental community analyses using the Fluidigm Access Array. *Molecular Ecology Resources* 16:946–956.
- Camacho, C., G. Coulouris, V. Avagyan, N. Ma, J. Papadopoulos, K. Bealer, and T. L. Madden. 2009. BLAST+: architecture and applications. *BMC Bioinformatics* 10:421.
- Caporaso, J. G., J. Kuczynski, J. Stombaugh, K. Bittinger, F. D. Bushman, E. K. Costello, N. Fierer, A. González Peña, J. K. Goodrich, J. I. Gordon, G. A. Huttley, S. T. Kelley, D. Knights, J. E. Koenig, R. E. Ley, C. A. Lozupone, D. McDonald, B. D. Muegge, M. Pirrung, J. Reeder, J. R. Sevinsky, P. J. Turnbaugh, W. A. Walters, J. Widmann, T. Yatsunenko, J. Zaneveld, and R. Knight. 2010. QIIME allows analysis of high-throughput community sequencing data. *Nature Methods* 7:335–336.

- Chen, S., H. Yao, J. Han, C. Liu, J. Song, L. Shi, Y. Zhu, X. Ma, T. Gao, X. Pang, K. Luo, Y. Li, X. Li, X. Jia, Y. Lin, and C. Leon. 2010. Validation of the ITS2 region as a novel DNA barcode for identifying medicinal plant species. PLoS ONE 5:e8613.
- Cole, J. R., Q. Wang, J. A. Fish, B. Chai, D. M. McGarrell, Y. Sun, C. T. Brown, A. Porras-Alfaro, C. R. Kuske, and J. M. Tiedje. 2013. Ribosomal Database Project: data and tools for high throughput rRNA analysis. Nucleic Acids Research 42:D633–D642.
- De Deyn, G. B., J. H. C. Cornelissen, and R. D. Bardgett. 2008. Plant functional traits and soil carbon sequestration in contrasting biomes. Ecology Letters 11:516–531.
- de Kroon, H., M. Hendriks, J. van Ruijven, J. Ravenek, F. M. Padilla, E. Jongejans, E. J. W. Visser, and L. Mommer. 2012. Root responses to nutrients and soil biota: drivers of species coexistence and ecosystem productivity. Journal of Ecology 100:6–15.
- Fahner, N. A., S. Shokralla, D. J. Baird, and M. Hajibabaei. 2016. Large-scale monitoring of plants through environmental DNA metabarcoding of soil: Recovery, resolution, and annotation of four DNA markers. PLoS ONE 11:e0157505.
- Feng, X. 2014. Productivity, physiology, community dynamics, and ecological impacts of a grassland agro-ecosystem: integrating field studies and ecosystem modeling. PhD thesis, University of Illinois at Urbana-Champaign; University of Illinois at Urbana-Champaign.
- Feng, X., and M. Dietze. 2013. Scale dependence in the effects of leaf ecophysiological traits on photosynthesis: Bayesian parameterization of photosynthesis models. New Phytologist 200:1132–1144.
- Fornara, D. A., and D. Tilman. 2008. Plant functional composition influences rates of soil carbon and nitrogen accumulation. Journal of Ecology 96:314–322.

- Fornara, D. A., and D. Tilman. 2009. Ecological mechanisms associated with the positive diversity-productivity relationship in an N-limited grassland. *Ecology* 90:408–418.
- Frank, D. A., A. W. Pontes, E. M. Maine, and J. D. Fridley. 2015. Fine-scale belowground species associations in temperate grassland. *Molecular Ecology* 24:3206–3216.
- Griffith, D. M., J. A. Veech, and C. J. Marsh. 2016. cooccur: Probabilistic species co-occurrence analysis in R. *Journal of Statistical Software, Code Snippets* 69:1–17.
- Hendriks, M., J. M. Ravenek, A. E. Smit-Tiekstra, J. W. van der Paauw, H. de Caluwe, W. H. van der Putten, H. de Kroon, and L. Mommer. 2015. Spatial heterogeneity of plant-soil feedback affects root interactions and interspecific competition. *New Phytologist* 207:830–840.
- Hiiesalu, I., M. Öpik, M. Metsis, L. Lilje, J. Davison, M. Vasar, M. Moora, M. Zobel, S. D. Wilson, and M. Pärtel. 2012. Plant species richness belowground: higher richness and new patterns revealed by next-generation sequencing. *Molecular Ecology* 21:2004–2016.
- Jackson, R. B., J. G. Canadell, J. R. Ehleringer, H. A. Mooney, O. E. Sala, and E. D. Schulze. 1996. A global analysis of root distributions for terrestrial biomes. *Oecologia* 108:389–411.
- Jackson, R. B., L. A. Moore, W. A. Hoffmann, W. T. Pockman, and C. R. Linder. 1999. Ecosystem rooting depth determined with caves and DNA. *Proceedings of the National Academy of Sciences of the United States of America* 96:11387–11392.
- Jumpponen, A., P. Höglberg, K. Huss-Danell, and C. P. H. Mulder. 2002. Interspecific and spatial differences in nitrogen uptake in monocultures and two-species mixtures in north European grasslands. *Functional Ecology* 16:454–461.

- Kesanakurti, P. R., A. J. Fazekas, K. S. Burgess, D. M. Percy, S. G. Newmaster, S. W. Graham, S. C. H. Barrett, M. Hajibabaei, and B. C. Husband. 2011. Spatial patterns of plant diversity below-ground as revealed by DNA barcoding. *Molecular Ecology* 20:1289–1302.
- Martin, M. 2011. Cutadapt removes adapter sequences from high-throughput sequencing reads. *EMBnet.journal* 17:10–12.
- Masella, A. P., A. K. Bartram, J. M. Truszkowski, D. G. Brown, and J. D. Neufeld. 2012. PANDAseq: PAired-eND Assembler for Illumina sequences. *BMC Bioinformatics* 13:31.
- Masters, M. D., C. K. Black, I. B. Kantola, K. P. Woli, T. Voigt, M. B. David, and E. H. DeLucia. 2016. Soil nutrient removal by four potential bioenergy crops: *Zea mays*, *Panicum virgatum*, *Miscanthus × giganteus*, and prairie. *Agriculture, Ecosystems & Environment* 216:51–60.
- McMurdie, P. J., and S. Holmes. 2013. phyloseq: An R package for reproducible interactive analysis and graphics of microbiome census data. *PLoS ONE* 8:e61217.
- Nippert, J., R. Wieme, T. Ocheltree, and J. M. Craine. 2012. Root characteristics of C₄ grasses limit reliance on deep soil water in tallgrass prairie. *Plant and Soil* 355:385–394.
- Oksanen, J., F. G. Blanchet, M. Friendly, R. Kindt, P. Legendre, D. McGlinn, P. R. Minchin, R. B. O'Hara, G. L. Simpson, P. Solymos, M. H. H. Stevens, E. Szoecs, and H. Wagner. 2016. vegan: Community ecology package. <https://CRAN.R-project.org/package=vegan>.
- Price, J. N., I. Hiiesalu, P. Gerhold, and M. Pärtel. 2012. Small-scale grassland assembly patterns differ above and below the soil surface. *Ecology* 93:1290–1296.
- R Core Team. 2016. R: A language and environment for statistical computing. Version 3.3.1. R Foundation for Statistical Computing, Vienna, Austria. <https://www.R-project.org/>.

- Rewald, B., C. Meinen, M. Trockenbrodt, J. E. Ephrath, and S. Rachmilevitch. 2012. Root taxa identification in plant mixtures – current techniques and future challenges. *Plant and Soil* 359:165–182.
- Rognes, T., T. Flouri, B. Nichols, C. Quince, and F. Mahé. 2016. VSEARCH: a versatile open source tool for metagenomics. *PeerJ* 4:e2584.
- Smith, C. M., M. B. David, C. A. Mitchell, M. D. Masters, K. J. Anderson-Teixeira, C. J. Bernacchi, and E. H. DeLucia. 2013. Reduced nitrogen losses after conversion of row crop agriculture to perennial biofuel crops. *Journal of Environmental Quality* 42:219–228.
- Staats, M., A. J. Arulandhu, B. Gravendeel, A. Holst-Jensen, I. Scholtens, T. Peelen, T. W. Prins, and E. Kok. 2016. Advances in DNA metabarcoding for food and wildlife forensic species identification. *Analytical and Bioanalytical Chemistry* 408:4615–4630.
- Tilman, D., P. B. Reich, J. Knops, D. Wedin, T. Mielke, and C. Lehman. 2001. Diversity and productivity in a long-term grassland experiment. *Science* 294:843–845.
- Tucker, S. S., J. M. Craine, and J. B. Nippert. 2011. Physiological drought tolerance and the structuring of tallgrass prairie assemblages. *Ecosphere* 2:48.
- Wardle, D. A., and D. A. Peltzer. 2003. Interspecific interactions and biomass allocation among grassland plant species. *Oikos* 100:497–506.
- Weaver, J. E. 1919. *The Ecological Relations of Roots*. Carnegie Institution of Washington, Washington, D.C.
- Weaver, J. E., and J. W. Voigt. 1950. Monolith method of root-sampling in studies on succession and degeneration. *Botanical Gazette* 111:286–299.

- Wilson, S. D. 2014. Below-ground opportunities in vegetation science. *Journal of Vegetation Science* 25:1117–1125.
- Zeng, W., B. Zhou, P. Lei, Y. Zeng, Y. Liu, C. Liu, and W. Xiang. 2015. A molecular method to identify species of fine roots and to predict the proportion of a species in mixed samples in subtropical forests. *Frontiers in Plant Science* 6:313.
- Zeri, M., K. J. Anderson-Teixeira, G. C. Hickman, M. D. Masters, E. H. DeLucia, and C. J. Bernacchi. 2011. Carbon exchange by establishing biofuel crops in Central Illinois. *Agriculture, Ecosystems & Environment* 144:319–329.

Tables and Figures

Table 4.1: Plant species planted or found present (*) during aboveground vegetation surveys of permanent quadrats in prairie restoration plots at the University of Illinois Energy Farm. Mean and standard deviation of stem abundance and percent cover across growing season 2012 were recalculated from X. Feng (unpublished data).

Functional type	Family	Species	% cover	sd
C3 grass	Cyperaceae	<i>Carex bicknellii</i>	1.4	2.3
C3 grass	Poaceae	<i>Elymus canadensis</i>	2.2	3.4
C4 grass	Poaceae	<i>Andropogon gerardii</i>	34.3	13.7
C4 grass	Poaceae	<i>Schizachyrium scoparium</i>	3.0	3.4
C4 grass	Poaceae	<i>Sorghastrum nutans</i>	21.2	10.5
Forb	Asteraceae	<i>Coreopsis palmata</i>	0.1	0.5
Forb	Asteraceae	<i>Coreopsis tripteris</i>	4.9	6.1
Forb	Asteraceae	<i>Echinacea pallida</i>	0.1	0.4
Forb	Asteraceae	<i>Felicia hirta</i> *	0.3	0.8
Forb	Asteraceae	<i>Helianthus grosseserratus</i>	7.2	8.2
Forb	Asteraceae	<i>Heliopsis helianthoides</i>	0.1	0.3
Forb	Asteraceae	<i>Parthenium integrifolium</i>	0.4	1.2
Forb	Asteraceae	<i>Ratibida pinnata</i>	8.3	5.4
Forb	Asteraceae	<i>Rudbeckia hirta</i> *	0.0	0.2
Forb	Asteraceae	<i>Rudbeckia subtomentosa</i>	2.9	4.2
Forb	Asteraceae	<i>Silphium integrifolium</i>	1.6	2.8
Forb	Asteraceae	<i>Silphium laciniatum</i>	0.2	0.8
Forb	Asteraceae	<i>Silphium perfoliatum</i>	0.5	2.0
Forb	Asteraceae	<i>Silphium terebinthinaceum</i>	0.1	0.7
Forb	Asteraceae	<i>Solidago canadensis</i> *	3.2	6.4
Forb	Asteraceae	<i>Solidago rigida</i>	1.3	2.7
Forb	Asteraceae	<i>Symphyotrichum novae-angliae</i>	4.0	3.8
Forb	Asteraceae	<i>Taraxacum officinale</i> *	0.1	0.5
Forb	Lamiaceae	<i>Monarda fistulosa</i>	1.0	2.0
Forb	Lamiaceae	<i>Pycnanthemum virginianum</i>	0.6	0.8
Forb	Plantaginaceae	<i>Penstemon digitalis</i>	0.5	2.2
Forb	Plantaginaceae	<i>Veronicastrum virginicum</i>	0.2	0.8
N fixer	Fabaceae	<i>Astragalus canadensis</i>	0.0	0.2
N fixer	Fabaceae	unidentified <i>Baptisia</i> sp.*	0.1	0.4
N fixer	Fabaceae	<i>Baptisia alba</i>	0.7	1.5
N fixer	Fabaceae	<i>Dalea purpurea</i>	0.2	0.6
N fixer	Fabaceae	<i>Desmodium canadense</i>	4.8	5.7
N fixer	Fabaceae	<i>Lespedeza capitata</i>	0.2	0.5

*Indicates a species not present in the seed mix planted during plot establishment in 2008.

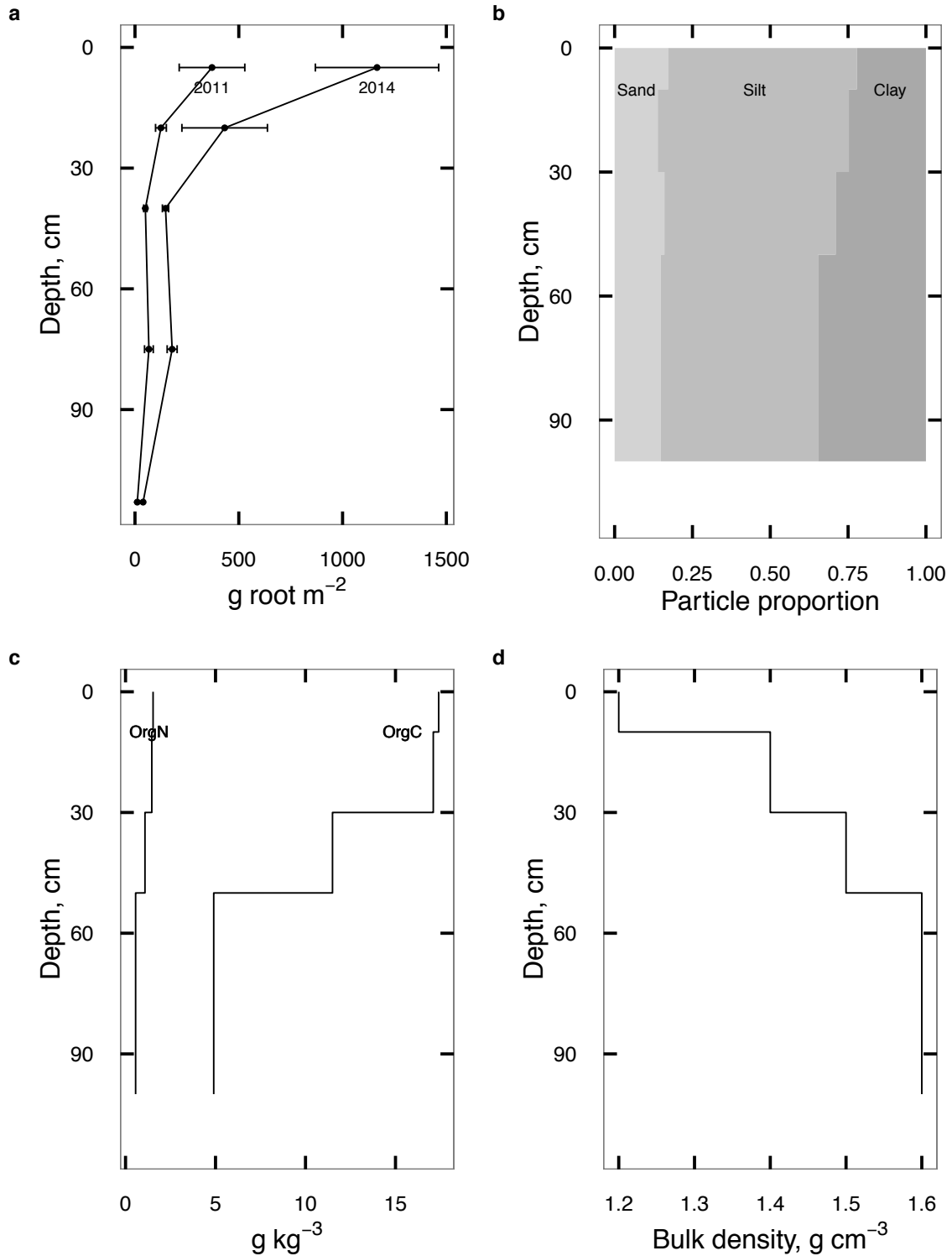


Figure 4.1: (a) total root mass of prairie plots measured in mid-August of 2011 (Replotted from Anderson-Teixeira et al. 2013) and 2014 (Replotted from Black et al., in prep). Error bars show mean \pm 1 standard deviation of 24 cores. Remaining panels show means of soil properties measured when the plots were established in 2008 (replotted from Smith et al. 2013): (b) soil texture; (c) soil organic C and N content; (d) soil bulk density.

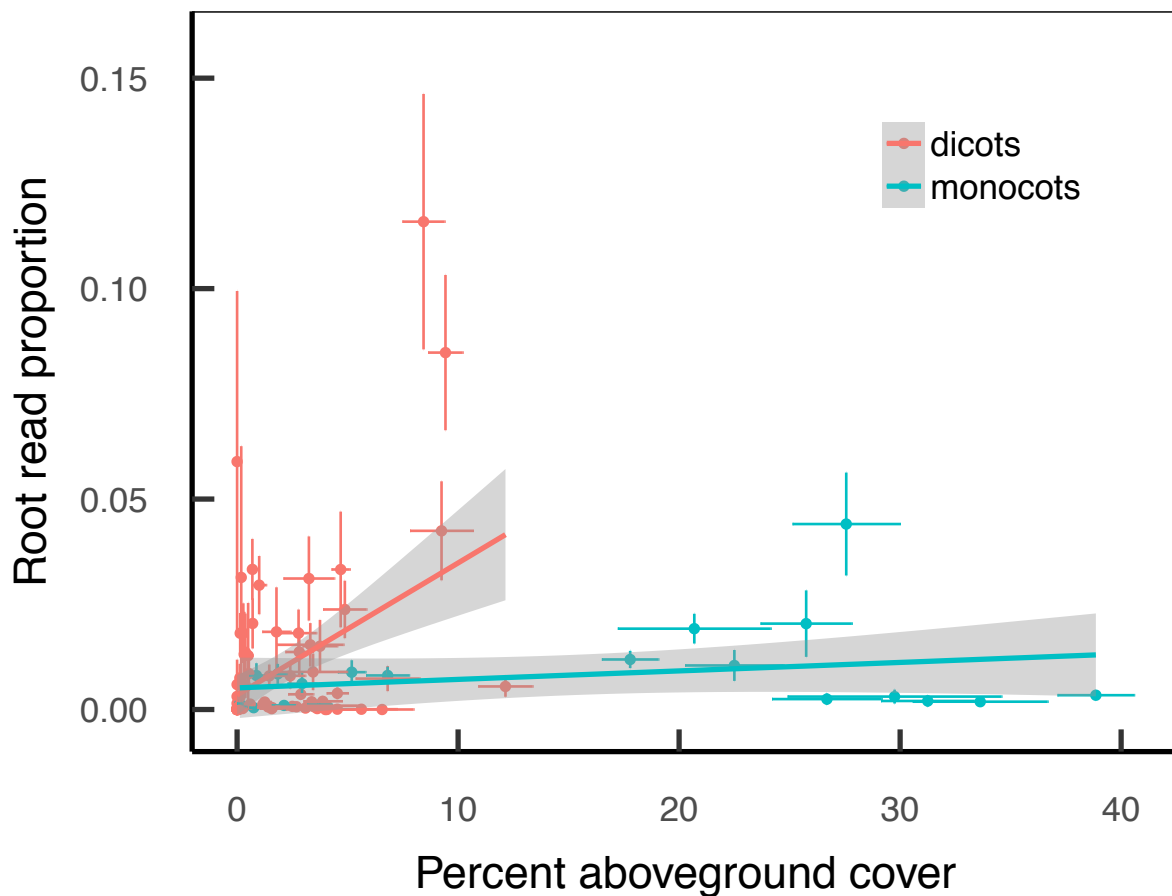


Figure 4.2: Correlation between percent aboveground cover (horizontal axis) and read proportion per root sample (vertical axis). Points are genus means for one experimental plot ($N=5$ plots); bars are 1 standard errors in each direction. Root proportions are averaged across all depths.

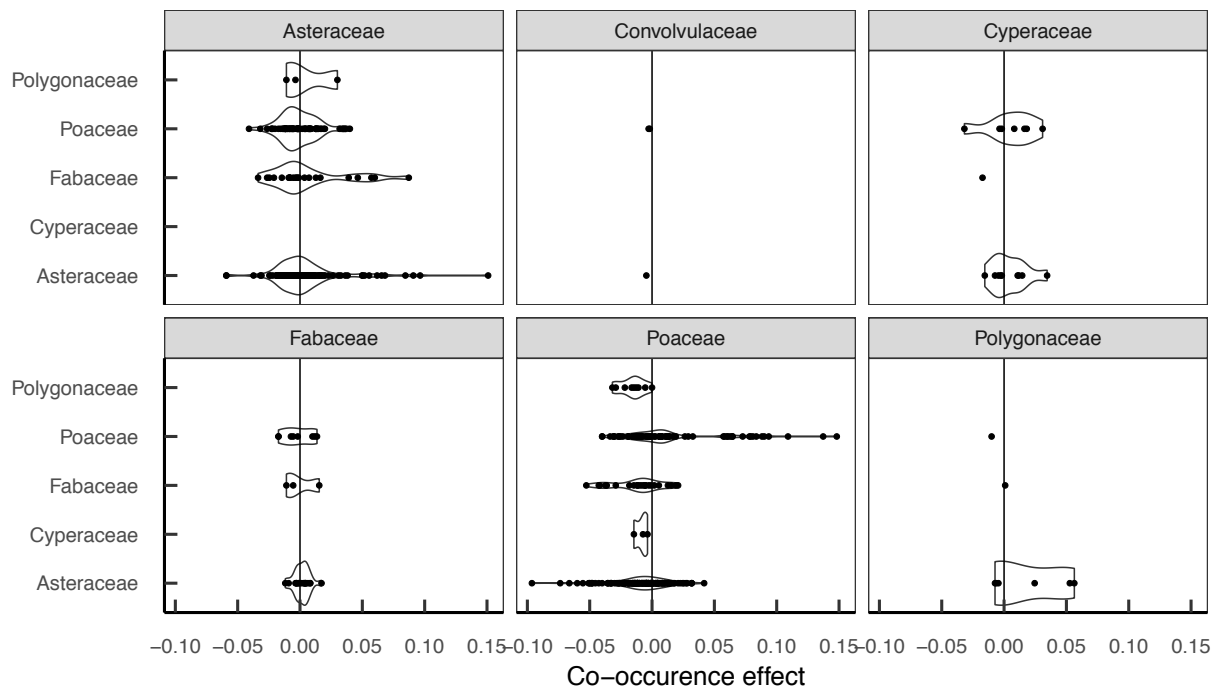


Figure 4.3: Standardized effect sizes for observed co-occurrence rates. Each point is one pair of species; violin shapes show density distribution for each group. Vertical axes show family identity of the first species in the pair, panel labels show the family identity of the second species. Co-occurrence was defined as mixed root samples with more than 1% of ITS2 reads from both species. Larger positive effect sizes indicate species pairs that are found together in more samples than expected for independently-occurring species; negative values indicate pairs that are found together less than expected.

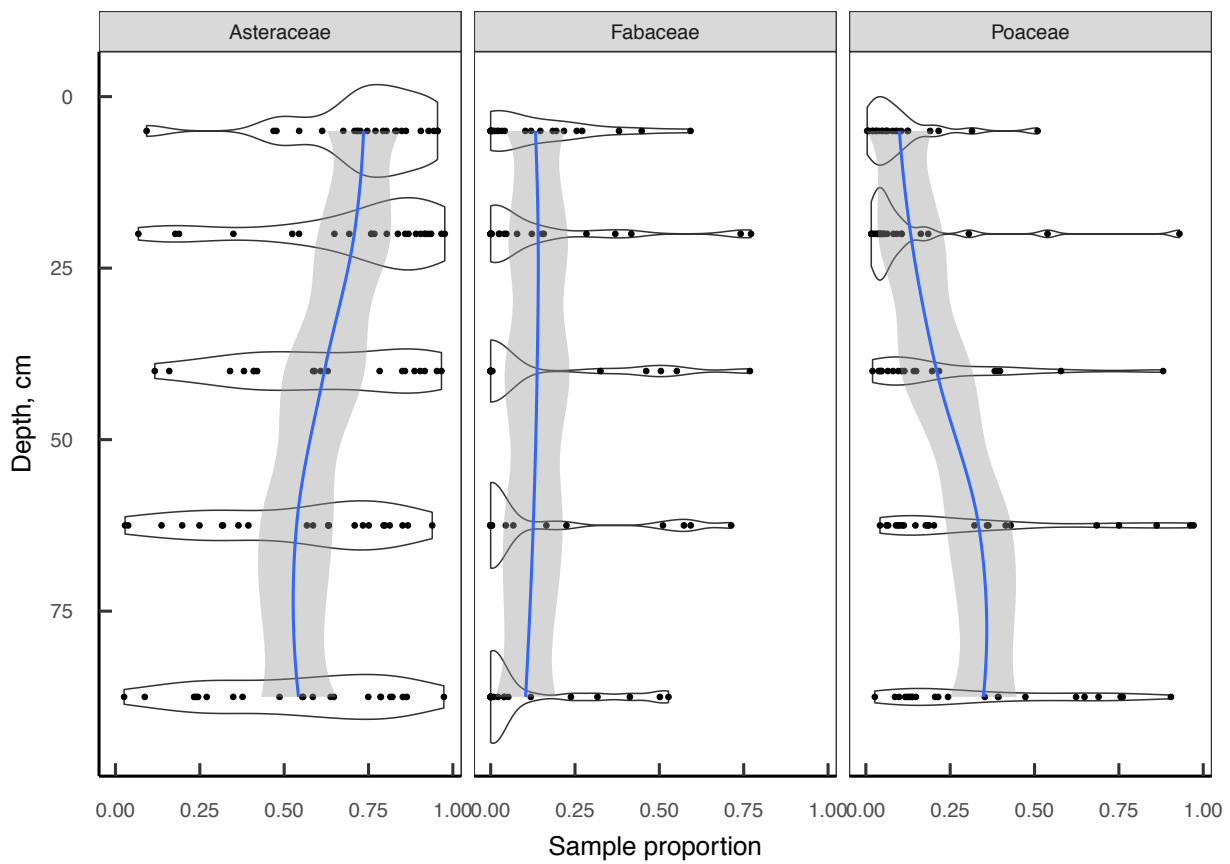


Figure 4.4: Relative abundance (fraction of reads from each sample) as a function of sample depth for each observed plant family. Sequences were clustered at 99% similarity and identified to species according to the closest BLAST match against the Genbank nt database. Taxa were then collapsed by family and groups with a mean abundance less than 1% per sample were removed for plotting.

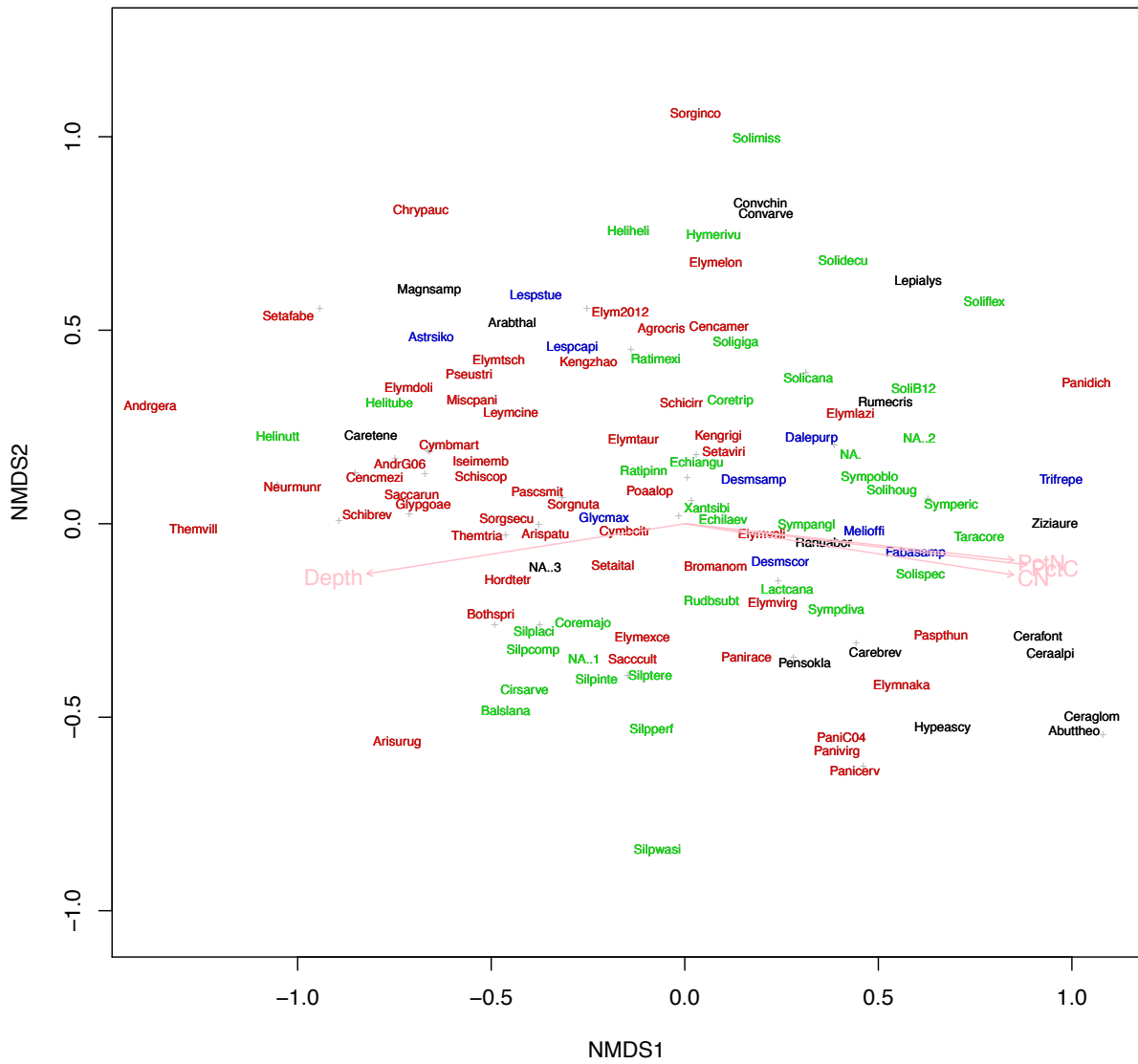


Figure 4.5: Nonmetric multidimensional scaling plot showing centroids for all detected species. Red: Poaceae. Green: Asteraceae. Blue: Fabaceae. Black: Other families. Grey crosses: Low-abundance species, unlabeled for figure clarity. Pink arrows show best fits for environmental vectors of depth in soil, organic C and N content, and C:N ratio.

Supplement 4.S1: Supplemental figures

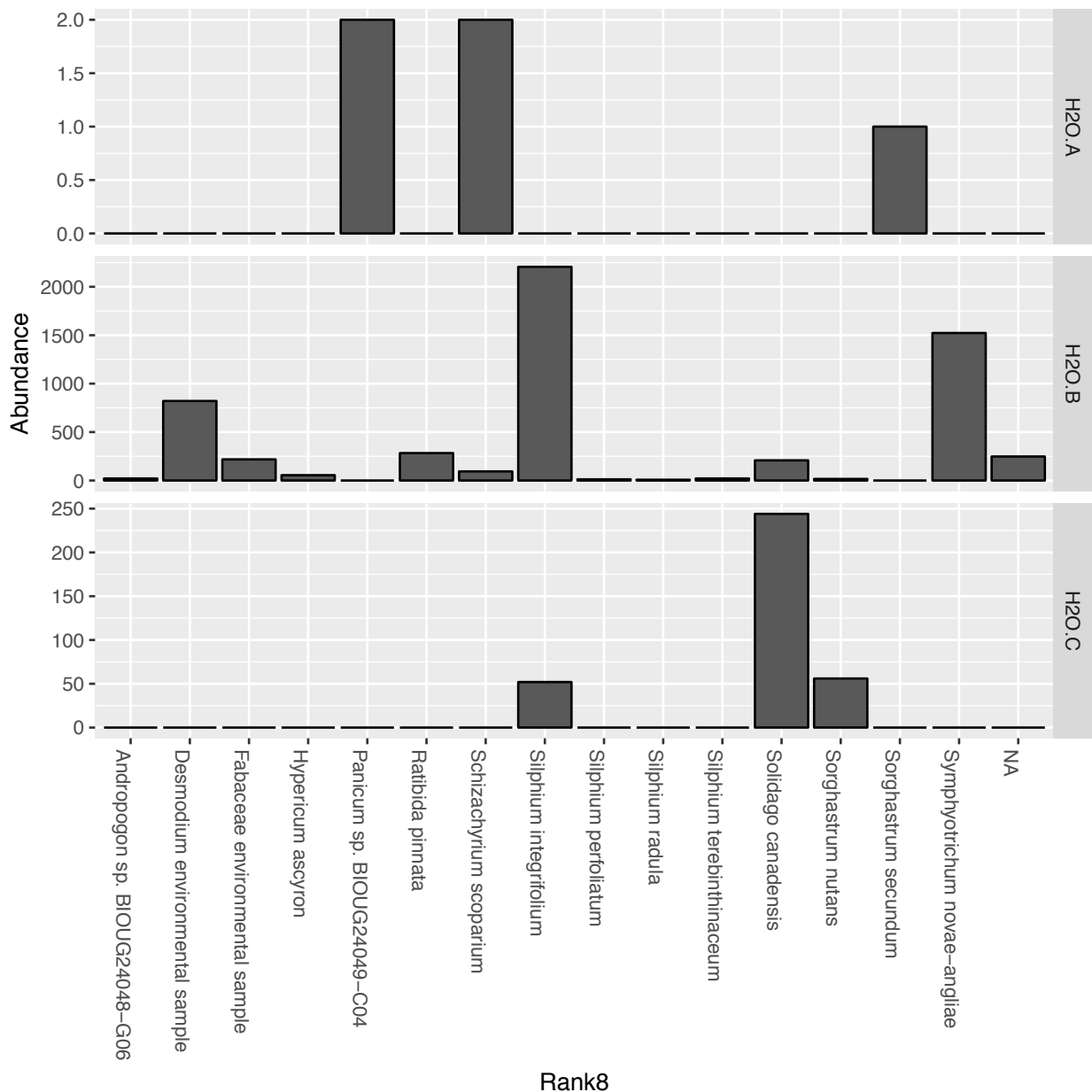


Figure 4.S1: Read counts obtained from water controls, binned by assigned genus. Each panel shows reads from a separate aliquot of DNA-free water processed simultaneously through the same DNA extraction, PCR, and sequencing pipeline as the root samples. Notice that the y-axis shows raw read counts (not sample proportions as in other figures) and that the scale differs between panels.

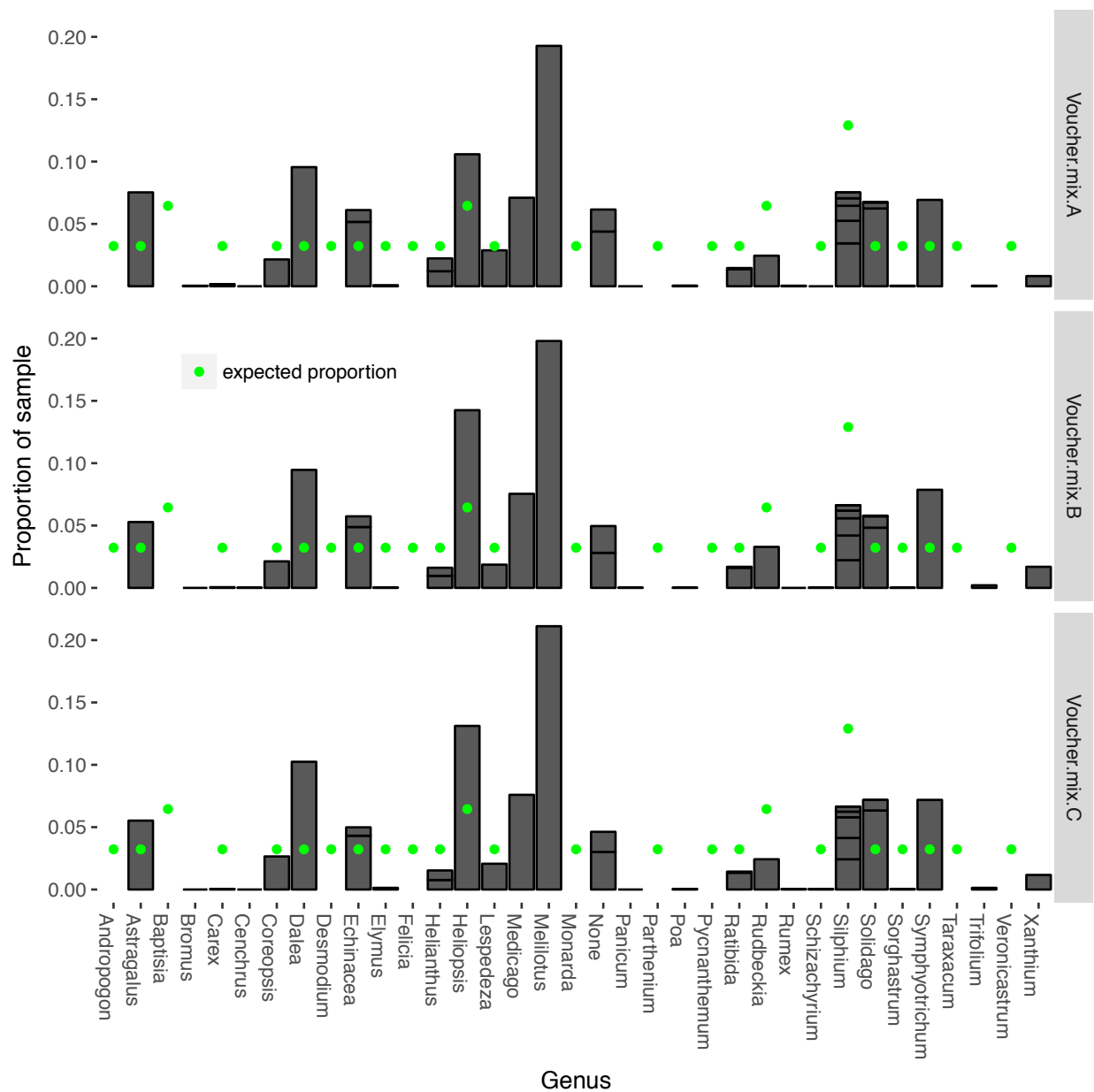


Figure 4.S2: Genus identities of reads obtained from a mock community of DNA obtained from known-species root samples. Green dots show proportion of template DNA added to the mixture. Black bars show the proportion of reads obtained. Panels are technical replicates, each separately amplified and sequenced from the same aliquot of mixed DNA.

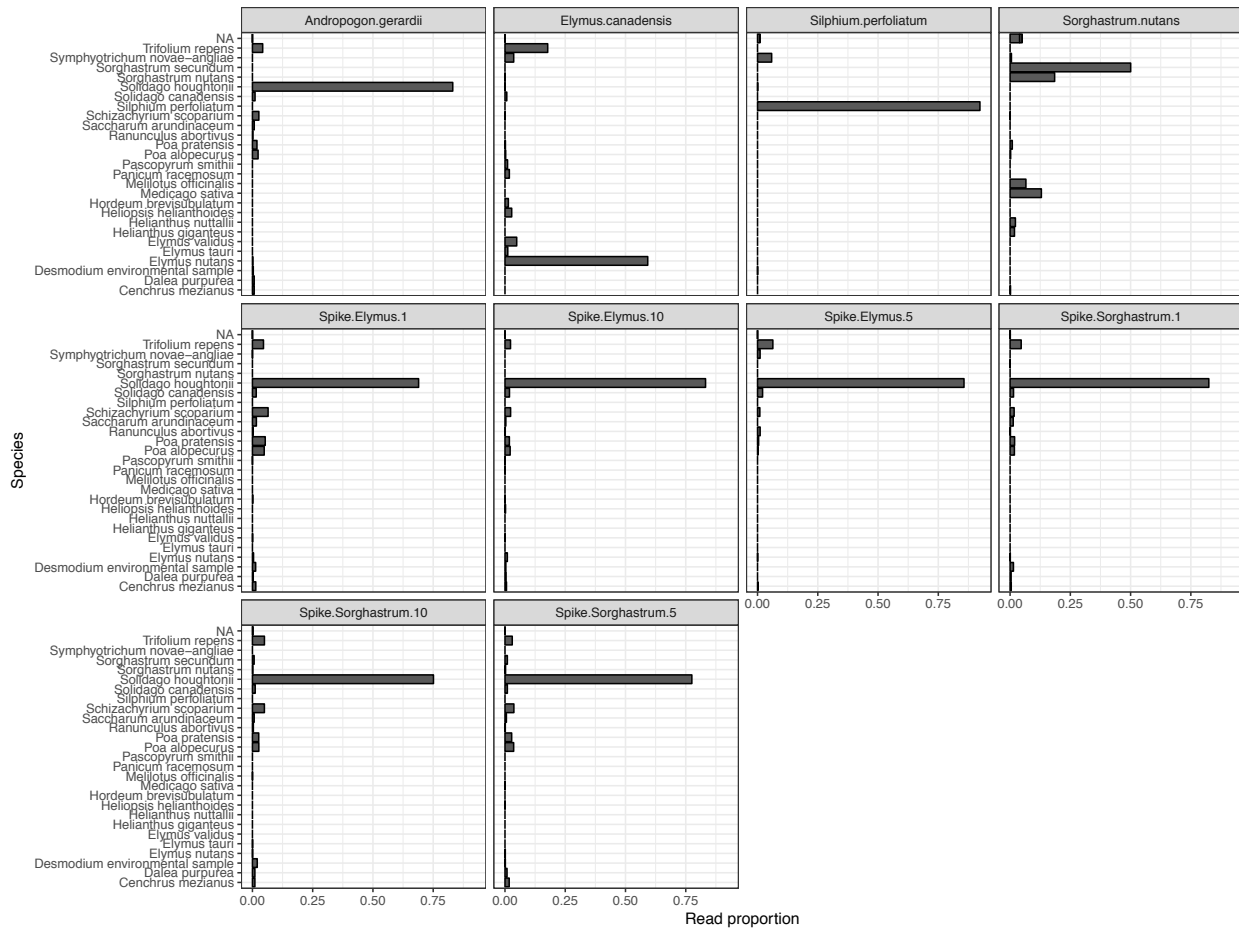


Figure 4.S3: Species identities of reads obtained from (top row) DNA extracted from single-species root samples, and (second two rows) DNA from the “*Andropogon gerardii*” sample spiked with 1%, 5%, or 10% *Elymus canadensis* or *Sorghastrum nutans* DNA. Notice that the barcoding assignment identifies the dominant sequence from the “*Andropogon gerardii*” sample as *Solidago*, not a grass!

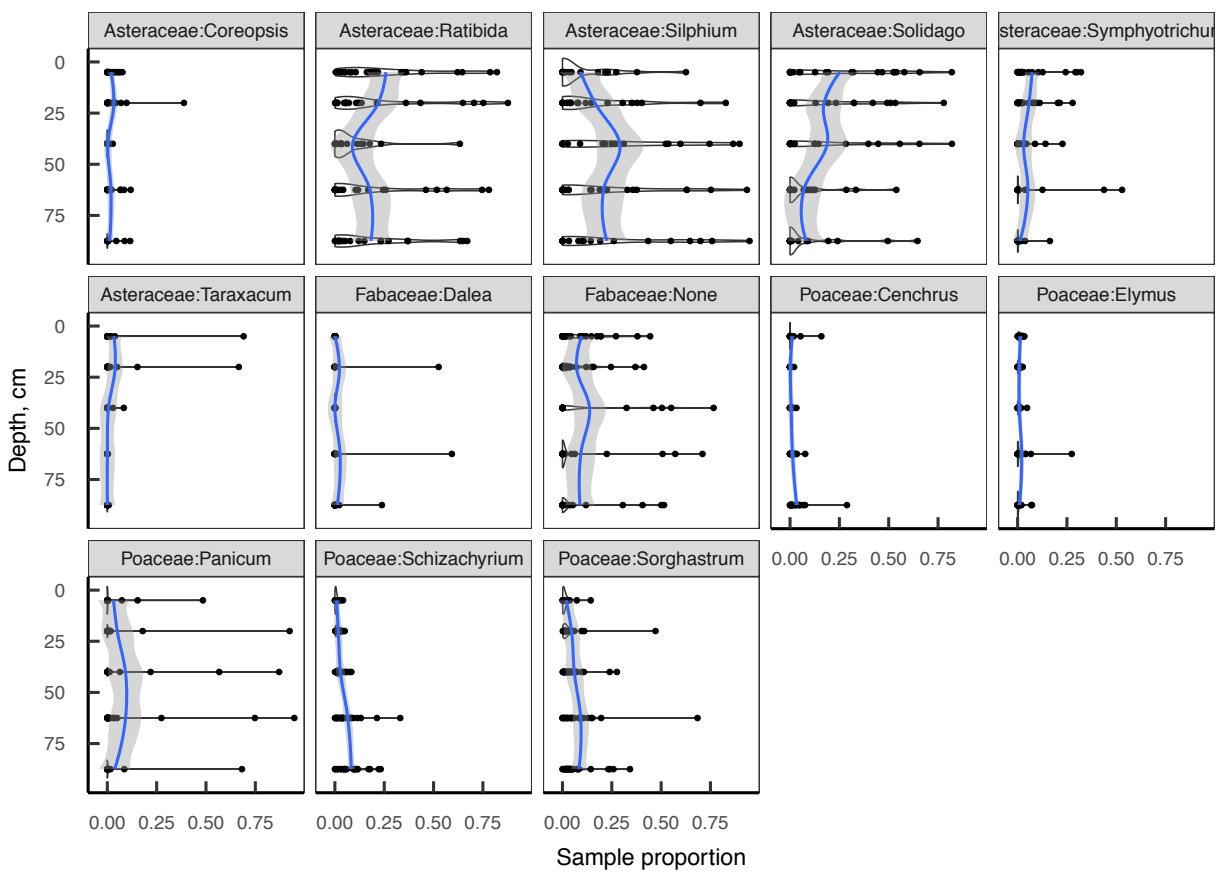


Figure 4.S4: Relative abundance (fraction of reads from each sample) as a function of sample depth for each observed plant genus. Sequences were clustered at 99% similarity and identified to species according to the closest BLAST match against the Genbank nt database. Taxa were then collapsed by genus and groups with a mean abundance less than 1% per sample were removed for plotting.

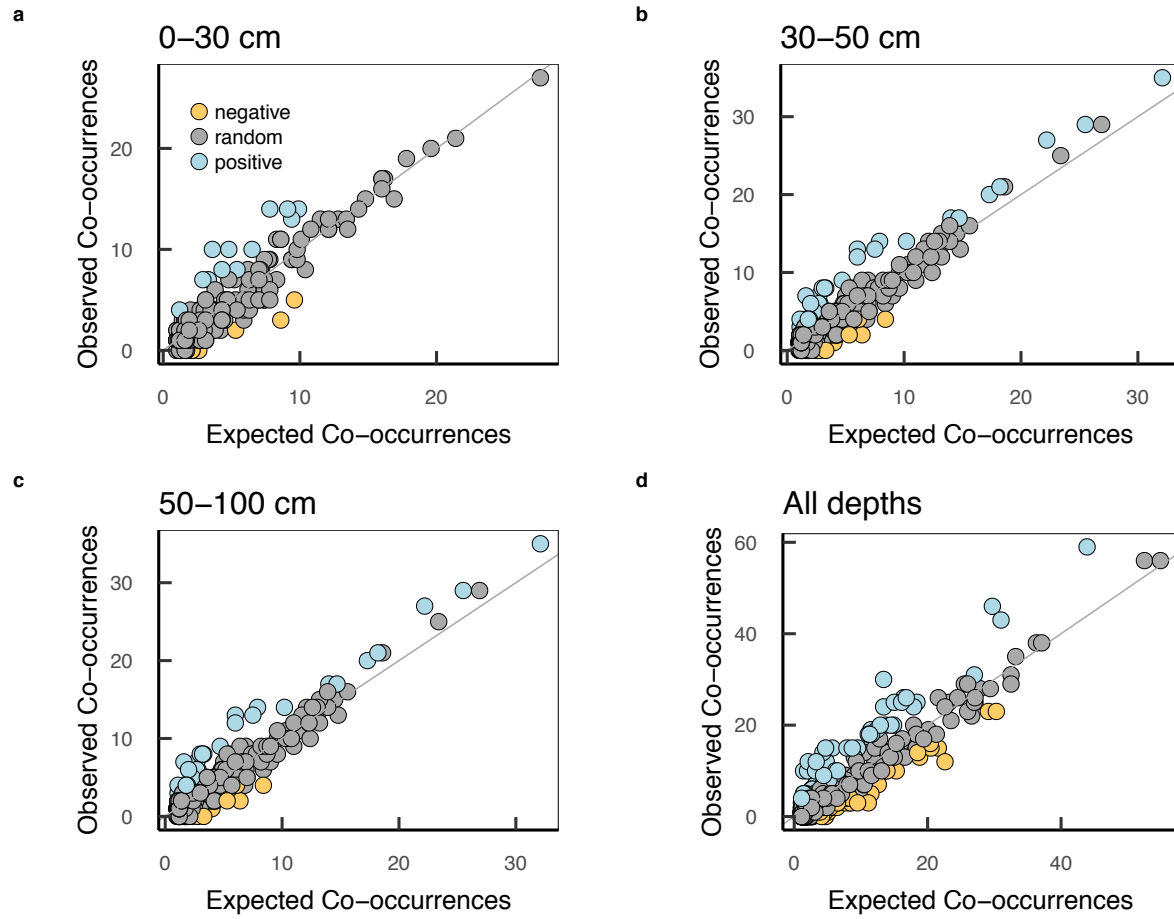


Figure 4.S5: Observed species co-occurrence rates versus the rates expected for independent, randomly distributed species of the same abundance, calculated separately for (a-c) shallow, medium, and deep soil layers, or (d) all samples from all depths. Each point represents one pair of species and the observed co-occurrence rate is the number of root samples with at least 1% of reads attributed to each species in the pair. Colors indicate species pairs whose co-occurrence rate differs significantly ($p < 0.05$) from the null model.

Chapter 5

Conclusion

In this research, I have explored how three possible land use scenarios could affect the carbon balance of the agricultural Midwest. In each chapter I focused on a different aspect of belowground C flow, but I have tried to show how each study contributes toward reducing uncertainty about the C-cycling consequences of management decisions.

The business as usual scenario paints a grim picture: Higher temperatures increased microbial breakdown of soil organic matter, and higher soil C inputs under eCO₂ appeared to prime further heat-related respiratory losses rather than offset them. Modeling the biogeochemical feedbacks of this whole process, I found that higher temperature and CO₂ are likely to lead to profound losses of soil organic matter if continued for decades with conventional tillage and cropping rotations.

The high-intensity bioenergy cropping scenario looks more sustainable: Once established, high-yielding perennial grasses require little tillage, allocate tremendous amounts of C into the soil layers most likely to store them for long timescales, and still also produce an energy crop that can offset fossil fuel emissions. By correcting for an artifact of the minirhizotron imaging method, I produced good agreement between core-based and image-based estimates of root volume, opening the possibility of tracking whole root profiles at much higher temporal resolution than is possible with direct coring.

Prairie grasses, although lower-yielding than *Miscanthus* or switchgrass, also require little management input and would be likely to build soil C and support greatly increased biodiversity—but perhaps no profit—for any landowner who planted them. By high-throughput sequencing of root *ITS* regions, I showed that grasses tend to occur deeper in the soil than forbs,

suggesting a degree of niche partitioning. Since grass roots often show lower decomposition rates than those of forbs, this suggests a possible further enhancement of C storage through enriching the deep soil layers in better-protected C while forbs maintain faster-cycling tissue near the surface.

Although these findings are informative, several key uncertainties remain. Climate change provided the motivating context for this project, but only maize and soybean were measured under climate-change conditions. Since the crops under consideration in the high-yielding scenario were all C4 grasses, I do not expect them to show dramatic CO₂ responses, but water availability under high temperatures may have the potential to limit their growth. Fortunately the same deep rooting habits that make *Miscanthus* and switchgrass attractive C sinks are likely to also help them maintain resilience to limited water supplies; their apparent resilience to the dry summer of 2012 appears to confirm this. The prairie system, with a mix of C4 grasses and C3 forbs and legumes, may respond unpredictably; if the legumes in the prairie mix respond to heat and CO₂ in the same way soybeans do, it is possible that prairie soils too could lose C to a CO₂ priming effect.

An additional uncertainty is hidden in the phrase “once established” above: Perennials may well be more resilient to individual extreme events and be highly profitable once mature, but the grass systems I describe here require a 3-5 year establishment phase to reach maximum yield, and must continue growing for many years beyond that to build any substantial amount of soil C. This implies that any individual landowner who plants perennials is making a many-year commitment and needs assurance against crop failure or policy changes during the lag phase before production begins. Long-term carbon storage will require long-term cooperation from

land owners and policies should be constructed to promote this. I hope this dissertation research has offered some small measure of help toward making those policies.